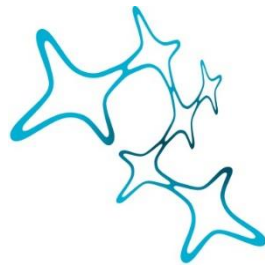

LEARNING IN A SMALL VERTEBRATE:
A NOVEL PARADIGM FOR JUVENILE
ZEBRAFISH TO STUDY CONDITIONED PLACE
AVOIDANCE

Ksenia Yashina



Graduate School of
Systemic Neurosciences

LMU Munich



Dissertation der
Graduate School of Systemic Neurosciences
der Ludwig-Maximilians-Universität München

August 1st, 2018

First Reviewer and Supervisor:

Prof. Dr. Herwig Baier

Max-Planck Institute for Neurobiology

Second Reviewer and Supervisor:

Prof. Dr. Andreas Herz

Department Biologie II, LMU, Germany

External Reviewer:

Prof. Dr. Emre Yaksi

Date of Submission:

August 1st, 2018

Date of Defense:

September 18th, 2018

Abstract

Learning has been extensively studied in many species (including primates, rodents, and insects). In larval and juvenile zebrafish, an established model organism, simple learning paradigms with one or two cues have been developed, with fish responding to classical and operant conditioning. However, more sophisticated paradigms, which would allow the study of more complex forms of learning, are still missing. We aimed to expand the existing set of learning paradigms for larval and juvenile zebrafish by introducing a conditioned place avoidance protocol in a Y-maze.

Fish were conditioned to avoid one of the visually distinct arms of a Y-maze. Mild electric shocks were used as unconditioned aversive stimuli (US). We found that a robust response to conditioning emerges in 3-week-old juvenile zebrafish. The fish required distinct visual cues to develop a conditioned response. Moreover, we showed that fish could use various strategies to avoid the US: pattern avoidance, a preference for a safe pattern, or a preference for the center of the maze.

The described paradigm lays the groundwork for studies of more complex learning abilities of juvenile zebrafish, such as spatial learning. Moreover, the juvenile zebrafish, which allows for non-invasive whole-brain imaging, provides an opportunity to study how different parts of the brain interact during memory formation and retrieval.

Table of contents

List of figures.....v

List of tables..... vii

1 Introduction.....1

1.1 Types of learning 1

1.2 Learning as a subject of experimental research 2

1.3 Neural basis for associative learning and methodological limitations..... 3

1.4 Zebrafish as a model organism for learning 4

1.4.1 Model organism *Danio rerio* 4

1.4.2 Behavioral repertoire of larval and juvenile zebrafish..... 4

1.4.3 Existing studies of learning in larval and juvenile zebrafish 6

2 Methods.....9

2.1 Fish husbandry 9

2.2 Behavioral setup..... 9

2.2.1 Setup 9

2.2.2 Visual stimuli 11

2.2.3 Electrical stimulation 12

2.3 Behavioral tracking..... 12

2.3.1 Calculation of fish position..... 12

2.3.2 Filtering..... 12

2.3.3 Calculation of swim bouts 14

2.3.4 Calculation of heading direction..... 15

2.3.5 Calculation of orientation in the arm 16

2.3.6	Calculation of fish size	16
2.4	Experimental protocols	17
2.5	Modeling	20
2.5.1	Model description	20
2.5.2	No-learning model	22
2.5.3	Model with a learning rule.....	23
2.6	Analysis of conditioning effects	24
2.6.1	Metrics for the CPA paradigm.....	24
2.6.2	Sliding window curves.....	24
2.6.3	Permutation testing	25
2.6.4	Analysis and clustering of shock-triggered swim bouts	27
3	Results	29
3.1	A conditioned place avoidance paradigm for larval and juvenile zebrafish.....	29
3.1.1	Setup and protocol	29
3.1.2	Metrics for quantification of fish performance in the CPA paradigm	32
3.1.3	Optimizing experimental design: assessing preference stability of maze arms and inherent preferences of fish.....	33
3.2	Comparison of responses to conditioning in different age groups	38
3.2.1	Changes in the entry frequency of the shocked arm are significant for 3-week-old fish..	39
3.2.2	Changes in occupancy of the shocked arm are similar in all three age groups.....	41
3.2.3	Pseudo-random walk model explains some, but not all results of CPA	41
3.3	Experimental and modeling results suggest that 3-week-old zebrafish can form aversive memories.....	44
3.3.1	Expanding the behavioral paradigm	44
3.3.2	A no-learning model can explain only some aspects of the CPA results.....	47
3.3.3	Modeling with an added learning component can qualitatively reproduce experimental metrics	48
3.3.4	Differentiating between ‘extinction’ and ‘forgetting’ in CPA paradigm.....	50

3.4	Distinct types of responses of zebrafish to electric shock	55
3.4.1	Characterization of responses to electric shock	56
3.4.2	Response types and their correlation with learning	60
3.5	The role of visual cues in the CPA paradigm	69
3.5.1	Response of fish to CPA paradigm in the absence of visually distinct cues.....	69
3.5.2	Decoupling the maze arm and the visual pattern	72
3.5.3	Alternative strategies to pattern aversion.....	77
4	Discussion.....	83
4.1	Onset of learning in the CPA paradigm	83
4.2	Dynamics of CPA metrics	84
4.3	Effects of conditioning in the Test session	85
4.4	Variability in responses to shocks and shock response types	86
4.5	The role of visual cues in the CPA paradigm	88
4.6	Fish strategies in the CPA paradigm.....	89
5	Outlook.....	90
5.1	Further behavioral experiments	90
5.2	Imaging of a behaving juvenile zebrafish in a Y-maze	90
6	Conclusion	93
7	Appendix.....	95
7.1	Abbreviations	95
7.2	Number of animals used in experiments.....	96

Bibliography	97
Acknowledgements.....	106
Curriculum Vitae	108
Author contributions	111
Eidesstattliche Versicherung / Affidavit	113

List of figures

Figure 1. Y-maze dimensions and placement.	10
Figure 2. Schematic for the spread of light in different mediums.	10
Figure 3. Calculation of swim bouts from displacement curves.....	15
Figure 4. Schematic for calculation of heading direction.	16
Figure 5. Probability density function for the Gamma distribution used in modeling.	21
Figure 6. Schema of the pseudo-random walk model, used to simulate experimental results.	22
Figure 7. Histogram of the distribution of permutation scores for a toy dataset.	27
Figure 8. Schematic drawing of the setup.....	29
Figure 9. Schematic description of the CPA protocol.	30
Figure 10. Examples of individual fish trajectories in different sessions of the CPA protocol....	31
Figure 11. An example of the calculation of CPA metrics.	32
Figure 12. An example of sliding window analysis for a single fish.....	33
Figure 13. Sliding window curves for control experiments.....	34
Figure 14. Occupancy of maze arms grouped by the associated visual pattern.	35
Figure 15. Positioning of the mazes in the experimental room.	36
Figure 16. Intrinsic biases in the setup or in innate fish behavior.	37
Figure 17. Distribution of fish body size across different ages.	38
Figure 18. Changes in arm entry frequencies across different age groups.	40
Figure 19. Changes in arm occupancies across different age groups.	41
Figure 20. Schematic of the “no-learning” model.	42
Figure 21. Sliding window curves for simulated trajectories of the fish in no-learning conditions.	43
Figure 22. Examples of individual trajectories for fish that responded to conditioning by staying in the center of the maze.....	45
Figure 23. Changes in CPA metrics in conditioning and test sessions.....	46
Figure 24. Changes in CPA metrics for simulated trajectories of the fish in no-learning conditions, including a test session.....	48
Figure 25. Changes in CPA metrics for simulated trajectories of the fish with an added learning component.....	49

Figure 26. Changes in CPA metrics in experiments with a 5-minute delay before the test session.	51
Figure 27. Changes in CPA metrics in experiments with a 10-minute delay before the test session.....	53
Figure 28. Variability in performance in the CPA paradigm.....	56
Figure 29. Typical responses to electric shocks of a fish.	57
Figure 30. Comparison of distributions of swim bout amplitudes: spontaneous vs. triggered by shocks.	58
Figure 31. Schema for calculation of fish orientation in the maze arm.....	59
Figure 32. Strength of shock responses depends on the orientation of the fish in the electric field.	60
Figure 33. Separation of shock responses into types.	61
Figure 34. Features of identified response types.	63
Figure 35. A toy example for calculation of conditioning efficiency after different swim bout types in a 10-minute time interval.	64
Figure 36. The shocked arm is avoided more strongly after swim bouts with high amplitude than after swim bouts of other response types.....	66
Figure 37. Effects of high-amplitude swim bouts on the occupancy/entry frequency of the shocked arm last up to 50 minutes.....	67
Figure 38. Changes in CPA metrics in experiments with identical visual patterns.....	71
Figure 39. Changes in CPA metrics in experiments with pattern rotation (cw/ccw) in the test session.....	73
Figure 40. Changes in CPA metrics in experiments with the rotation of patterns (cw/ccw) in the test session (colors correspond to the patterns before the rotation).....	75
Figure 41. Examples of fish trajectories before and after the rotation.....	76
Figure 42. Changes in CPA metrics in control experiments for the replacement of the shocked pattern.	78
Figure 43. Changes in CPA metrics in experiments in which the shocked pattern was replaced in the test session.	80
Figure 44. Individual examples of fish trajectories with successful avoidance of the shocked arm after the replacement of the shocked pattern in the test session.	81

List of tables

Table 1. Control protocol.....	17
Table 2. Age comparison protocol.....	17
Table 3. Protocol with a test session.....	18
Table 4. Protocol with a delay and a test session.....	18
Table 5. Protocol with identical patterns.	18
Table 6. Control protocol for replacement of shocked pattern: switch to gray.	19
Table 7. Control protocol for replacement of shocked pattern: switch to a new pattern.....	19
Table 8. Protocol for replacement of shocked pattern.	19
Table 9. Protocol with pattern rotation.	20
Table 10. An example for the calculations of experimental and permutation scores.	26
Table 11. Occupancy of maze arms, grouped by patterns, in control experiments.	35
Table 12. Occupancy of arms in two mazes, grouped by absolute position in the experimental room, in control experiments.....	37
Table 13. Entry frequency in the last 10 minutes of the conditioning session for different age groups.	39
Table 14. Arm entry frequency and arm occupancy in the experiments with a test session.	47
Table 15. Arm entry frequency and arm occupancy in experiments with a 5-minute delay before the test session.	52
Table 16. Arm entry frequency and arm occupancy in experiments with a 10-minute delay before the test session.	54
Table 17. Occupancy and entry frequency of the shocked arm in the 10-minute interval immediately after a shock-triggered bout for different swim bout types.	62
Table 18. Post-hoc pairwise comparisons of the occupancy and entry frequency of the shocked arm immediately after the shock for different response types.....	65
Table 19. Arm entry frequency and arm occupancy in the experiments with identical patterns..	70
Table 20. Arm entry frequency and arm occupancy in the experiments with pattern rotation.....	72
Table 21. Arm entry frequency and arm occupancy in experiments with pattern rotation (metrics for the test session are calculated in relation to the originally shocked arm).	74

Table 22. Arm entry frequency and arm occupancy in the experiments with the replacement of
the shocked pattern. 79

1 Introduction

1.1 Types of learning

The ability to learn allows animals to stop relying on chance in their interaction with the environment, and instead to start using past experiences and planning to increase their survival rate. There are two main categories of learning: non-associative and associative learning. Non-associative learning in particular leads to an adaptation of behavior due to exposure to a repeated stimulus, and is not caused by sensory adaptation or fatigue. In fact, this type of learning does not create an association of the stimulus or behavior with any particular cue. Examples of non-associative learning are habituation (during which the behavioral response to a repeated stimulus gradually diminishes) and sensitization (the behavioral response to a repeated stimulus is gradually enhanced). Associative learning, on the other hand, is a powerful and versatile type of learning, which allows an animal to build a connection between a pair of events, and to predict one from the other (Moore, 2004; Roberts, Bill, & Glanzman, 2013). Well studied paradigms of associative learning include classical conditioning and operant conditioning.

Classical conditioning involves the pairing of an biologically relevant unconditioned stimulus (US), such as the smell of food or an electric shock, with a conditioned stimulus (CS), which is initially a neutral stimulus, such as the sound of a bell or a flash of light (Pavlov, Gantt, Volborth, & Cannon, 1928). A US causes an unconditioned response, which is represented by a reflex (e.g. salivation or an escape response). During the conditioning, the CS and US are presented to an animal simultaneously or one after the other (e.g. the sound of the bell precedes the appearance of food or the flash of light precedes the electric shock). After the association between the US and the CS is learned by the animal, the previously neutral CS now causes a conditioned response even in the absence of a US (the sound of a bell causes salivation, a flash of light leads to an escape response).

Operant conditioning involves an animal learning to associate a behavior, such as pressing a lever, with a particular outcome, such as reward or punishment (Skinner, 1938). This type of conditioning

differs from the classical type in the fact that the conditioning stimulus reinforces a non-reflexive behavioral output (so-called operants).

1.2 Learning as a subject of experimental research

There is a long tradition of studying different types of learning via the use of model organisms in controlled experimental conditions. Studies of classical and operant conditioning have focused on various features of learning: its acquisition, extinction (relearning of the neutrality of the CS), rapid reacquisition of the conditioned response after the extinction upon presentation of a single US, blocking (a competition between two CS for forming an association with the US), etc. (Todd, Vurbic, & Bouton, 2014).

A simple, yet effective experimental set-up for studying associative learning is an operant conditioning chamber (the so-called ‘Skinner box’, Skinner, 1938). In the Skinner box, the chamber is shielded from outside distractions by light- and soundproof barriers. The necessary elements present in the box are the sources of the US (in case of the classical conditioning) or the readouts of the operant behavior (such as levers, in case of the operant conditioning), and the sources of the CS (devices for delivery of rewards/punishments). The crucial feature of such a setup is the minimal amount of participating elements, allowing for the control of biases, and for presentation and manipulation of the cues.

Other commonly used setups for studying learning include Y/T-mazes, plus-mazes, and radial mazes (Olton, 1979). In these set-ups, the number of behavioral options for the animal is increased but still limited and controlled for, thus allowing studies of more sophisticated learning behaviors (including more cues or more behavioral steps), such as learning of turn sequences and spatial learning.

A popular paradigm in associative learning research is the conditioned place preference/aversion (CPP/CPA), which involves classical conditioning (Mucha, Van Der Kooy, O’Shaughnessy, & Buceniaks, 1982). In this paradigm, the animal is introduced to a chamber with two or more compartments. The animal first explores the chamber during a habituation phase. During the conditioning phase, the animal is placed into one of the compartments, which is paired either with a reward (in conditioned place preference) or a punishment (in conditioned place aversion). The

animal learns to associate the cues of the conditioned compartment with the positive or negative experience presented. In the test phase, the animal is allowed to move freely around all compartments of the chamber, and the amount of preference/aversion of the conditioned compartment indicates how successful the conditioning was.

1.3 Neural basis for associative learning and methodological limitations

Over the years, attempts have been made to find neuronal correlates for associative learning. Mammals remain one of the main model organisms used in this research. The dopaminergic and serotonergic systems of the brain have been implicated in reward and punishment processing during conditioning (Bauer, 2015; Schultz, Dayan, & Montague, 1997). Several brain areas are believed to serve as a neural substrate for associative learning, including the hippocampus, amygdala and the cerebellum (Duvarci & Pare, 2014; Freeman, 2015; Giustino & Maren, 2015). Yet the overall understanding of how learned behavior, starting from the sensory input and ending in motor output, is coded in brain circuits is still missing. This is partly due to the limitations of the existing methods for recording of mammalian brain activity. Methods such as electrophysiological recordings or calcium imaging provide high-resolution recordings of the activity of single neurons. However, due to the size and anatomy of the mammalian brain, only a small fraction of the neurons can be recorded simultaneously despite the recent advancements in the number of simultaneously recorded neurons (Jun et al., 2017). In addition, complicated surgical procedures are necessary to access parts of the mammalian brain for recordings. In fact, deeper brain areas often require even more elaborate preparations (such as the insertion of a microprism (Low, Gu, & Tank, 2014)).

These challenges in the recordings of the mammalian brain could be possibly overcome in other model organisms, as non-mammalian species also possess the capacity for associative learning (Lopez, Bingman, Rodriguez, Gomez, & Salas, 2000; Skinner, 1948; Tully & Quinn, 1985 among others).

1.4 Zebrafish as a model organism for learning

1.4.1 Model organism *Danio rerio*

An established model organism that has attracted recent interest is the zebrafish (*Danio rerio*). Adult zebrafish are known to be capable of performing complicated cognitive tasks, including associative learning, social interactions, and spatial learning (Aoki, Tsuboi, & Okamoto, 2015; Kalueff et al., 2013; Kenney, Scott, Josselyn, & Frankland, 2017; Miller & Gerlai, 2012). Zebrafish are vertebrates, and share homology of many brain regions with mammals despite a large evolutionary distance (Wullimann & Mueller, 2004). Zebrafish are easy to breed and maintain in captivity, and their relatively small size allows for high-throughput behavioral assays. Zebrafish larvae are small and transparent, and their size, combined with this transparency, allows for non-invasive imaging of neuronal activity of the entire brain. There exists a large number of genetically modified lines, which allow unparalleled access to targeted brain areas. This permits the use of cutting edge methods such as labeling and recording, optogenetic manipulations, and laser ablations. Recent improvements in imaging methodology (for example, the genetically encoded calcium indicator GCaMP6 (T.-W. Chen et al., 2013)) allow for high signal-to-noise ratio and near single-spike resolution in calcium imaging recordings. New techniques such as volumetric imaging (dal Maschio, Donovan, Helmbrecht, & Baier, 2017) or light-sheet imaging (Vladimirov et al., 2014) permit recordings from several brain regions simultaneously, as well as whole-brain imaging with cellular resolution in awake animals. Taking these technical and biological advantages into account, the study of learning in zebrafish could shed light on how different brain regions act together during the learning process.

While an impressive body of behavioral studies has accumulated over the decades of learning research in mammals, little is known about the learning abilities of the larval and juvenile zebrafish, which are commonly used for imaging of neuronal activity (imaging being possible due to transparency of the animals at this developmental stage).

1.4.2 Behavioral repertoire of larval and juvenile zebrafish

Zebrafish undergo a quick development from an egg to a larva during the first 5 days of development (Kimmel, Ballard, Kimmel, Ullmann, & Schilling, 1995). At 5 days post fertilization

(dpf) the larvae hatch and can swim freely. Larvae move in easily identifiable discrete bouts, which allow reliable behavioral tracking and classification of movement types using supervised (Jouary & Sumbre, 2016; Mirat, Sternberg, Severi, & Wyart, 2013) and unsupervised classification algorithms (Marques, Lackner, Félix, & Orger, 2018).

Larval zebrafish exhibit a range of visually guided behaviors, most of which are elicited by fairly simple types of stimulation:

- Differences in luminance elicit phototactic behavior, in which larvae change their turning probabilities to steer towards lighter areas (Burgess, Schoch, & Granato, 2010; X. Chen & Engert, 2014; Guggiana-Nilo & Engert, 2016);
- Continuous translational motion of visual stimuli triggers the optomotor response (OMR), during which the fish start swimming in the direction of the perceived motion (Orger, Smear, Anstis, & Baier, 2000);
- Rotational motion triggers the optokinetic response (OKR), causing the fish to turn their eyes together with the perceived motion and stabilize the moving image on the retina (Easter & Nicola, 1996; Kubo et al., 2014);
- Fast looming objects cause the larvae to perform an escape response – a fast stereotyped movement, initiated with a so-called C-bend, followed by a series of powerful swim bouts to move away from the looming object (Dunn et al., 2016; Temizer, Donovan, Baier, & Semmelhack, 2015);
- Small moving objects attract the larvae and elicit a prey capture response, which includes a sequence of stereotyped movements: convergence of the eyes, followed by approach swims, and culminating in a capture strike (Bianco, Kampff, & Engert, 2011; Patterson, Abraham, MacIver, & McLean, 2013; Semmelhack et al., 2014).

Apart from these simple behaviors, non-associative types of learning in larval zebrafish have been described: larvae show a gradual reduction (habituation) in response to repeated visual and acoustic stimuli (Roberts et al., 2011; Wolman, Jain, Liss, & Granato, 2011). Yet zebrafish at this age are still developing, and it remains unclear if they are capable of more sophisticated forms of learning.

After hatching the larvae grow and further develop over the next weeks, until they reach the transformation into the juvenile zebrafish at approximately 3-4 weeks post fertilization (Parichy, Elizondo, Mills, Gordon, & Engeszer, 2009). Being at the intermediate stage of development, juvenile zebrafish of 3 weeks post fertilization are still transparent and relatively small, which makes imaging possible. At the same time, zebrafish of this developmental stage have been shown to develop more sophisticated behaviors. For example, social behavior develops where groups of two or more juvenile zebrafish show social attraction, which manifests as decreased inter-animal distance (Dreosti, Lopes, Kampff, & Wilson, 2015; Hinz & de Polavieja, 2017). Other studies established the existence of abilities for associative learning in larval and juvenile zebrafish (Aizenberg & Schuman, 2011; Matsuda, Yoshida, Kawakami, Hibi, & Shimizu, 2017; Valente, Huang, Portugues, & Engert, 2012).

1.4.3 Existing studies of learning in larval and juvenile zebrafish

Classical fear conditioning was demonstrated in larval and juvenile zebrafish (Aizenberg & Schuman, 2011; Matsuda et al., 2017). Larval zebrafish were conditioned to associate a touch on the tail (US) with a flash of light (CS). Naïve fish respond to the touch with increased tail movement. After the conditioning the flash of light alone could evoke increased tail movement, indicating successful conditioning. In a different paradigm, juvenile zebrafish were conditioned to associate an electric shock (US) with a dark flash (CS). The fish responded to the US with bradycardia – decreased heart rate. After the conditioning the initially neutral CS started causing bradycardia even in the absence of electric shocks. In both studies, calcium imaging in cerebellum revealed that the CS and the US evoked neuronal activity of cerebellum. The activity of CS-responsive cerebellar granule cells was increased at the end of the conditioning compared to the responses in the beginning of the conditioning. This activity was then gradually abolished as extinction took place.

Operant conditioning was demonstrated in juvenile zebrafish (Valente et al., 2012). In brief, a 2-compartment arena was used, marked with distinct visual cues. The study used pairs of cues (a conditioned pattern CS+ and a neutral pattern CS-). Three different pairs were used: white and red backgrounds, gray and checkerboard patterns, and curvilinear blue shapes and a blue grid. The conditioning was carried out using electric shocks (US) to elicit avoidance of the compartment

with CS+. Both cues were presented to the fish during the conditioning phase. The electric shock was administered only when the fish entered the compartment with the CS+. The animals showed a robust response to the operant conditioning starting from 3 weeks of age. The fish learned to associate their behavior with the outcome (punishment), and started to avoid entering the compartment with the CS+, thus successfully undergoing operant conditioning.

In the described operant conditioning paradigm the animals were offered two visual cues, and thus the behavior of the fish was reduced to a binary choice task: stay in compartment A / stay in compartment B. The fish were conditioned to associate a visual pattern with an electric shock, but it is not clear if the fish could use more sophisticated environmental cues, were they available. Thus, even though this operant conditioning paradigm offers an elegant and simple way to study associative learning, its simplicity limits the amount of possible manipulations with which to challenge the animal.

In natural conditions, the zebrafish could be capable of using multiple cues and strategies to avoid a dangerous or noxious part of the environment. However, a natural scene offers a broad mix of cues, making it hard to manipulate and control which cues are accessible to the fish. To test if various learning strategies exist in a zebrafish, a controlled setup with more than two cues is required. In such a setup the aptitude for operant conditioning can serve as a tool for investigation of how the fish interact with their environment, what features of the environment they can learn, and eventually, whether the fish can combine information from multiple cues to form spatial memories.

The described studies show that juvenile zebrafish can be an appropriate model organism for future studies of learning in behavior and its neural basis. It is therefore highly interesting to study the abilities of the juvenile zebrafish to learn in complex environments.

The aim of the present PhD study was to investigate the behavioral response of larval and juvenile zebrafish to conditioning in a more complex yet controlled environment. A Y-maze, a popular tool used in memory research in rodents, was chosen as a behavioral chamber. The Y-maze contains more cues and allows for more manipulations of the visual cues when compared to the 2-compartmental arena. In particular, in the Y-maze the zebrafish is able to explore the three arm

compartments and a central compartment. To test if zebrafish are capable of extracting and memorizing salient features of their environment, a conditioned place avoidance paradigm was used. In this paradigm, the animal is conditioned to avoid one of the visually distinct arms of the Y-maze by pairing this arm with a noxious stimulus (an electric shock). The expected response of the zebrafish in the case of successful conditioning – and hence learning – would be the avoidance of the conditioned arm. Various manipulations of the cues in the maze (e.g. rotation of the visual cues presented in the arms of the Y-maze) can then be used to distinguish which environmental cues were important for the fish during the conditioning.

These considerations led to following main objectives of this thesis:

- (1) What is the earliest developmental stage at which zebrafish can undergo conditioning under the CPA paradigm?
- (2) How important are visual cues in the CPA paradigm?
- (3) Are there different strategies that the fish can use to learn to avoid an aversive location in the maze?

2 Methods

2.1 Fish husbandry

Wild-type zebrafish of strain TL were maintained at 28 degrees on a 14h-10h light-dark cycle. Embryos were obtained by spawning three adult fish pairs simultaneously. Embryos were raised in Danieau's buffer (17 mM NaCl, 2 mM KCl, 0.12 mM MgSO₂, 1.8 mM Ca(NO₃)₂, 1.5 mM HEPES) for the first 7 days of development. At 7 dpf the larvae were transferred to 3.5l tanks with fish system water (approx. 30 animals per tank). From 5 dpf to 20 dpf they were fed twice a day with live Rotifers and dry algae powder (Tetra Aufzuchtsfutter). From day 20 onwards, the diet was smoothly changed to a combination of freshly hatched artemia and Gemma micro dry food (Skretting). Animals were taken out of the fish facility and into the behavior room directly before the start of each experiment.

All animal procedures were conducted in accordance with the institutional guidelines of the Max Planck Society and the local government (Regierung von Oberbayern, animal license 55.2-1-54-2532-108-2016).

2.2 Behavioral setup

2.2.1 Setup

The setup was custom built in the lab. The walls and bottom of the Y-maze were laser-cut out of cast acrylic. The maze arms had a 1:1 width-to-length ratio, with a length of 30 mm; the walls were 10 mm high (Fig. 1). Each arm opened to the triangular center of the maze. Ends of the arms were rounded (observations of the fish showed that they tend to spend a lot of time in the corners, data not shown).

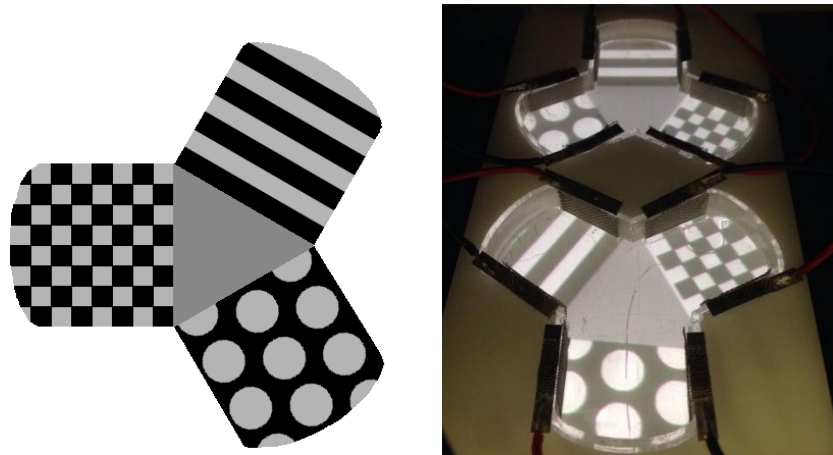


Figure 1. Y-maze dimensions and placement.

Shape of the maze with patterns (left) and a photo of the set-up with projected patterns and inserted electrodes, ready for experiments (right).

There were two identically built mazes used in the experiments in parallel, allowing the testing of two fish simultaneously, and therefore increasing the throughput. Each maze had a piece of diffusive paper underneath for back projection of the visual stimuli. Both the mazes and the diffusive paper were placed into a water basin, in order to remove the additional air layer between the screen and the fish. This was done to reduce light refraction, as the refractive indices of water and plastic are rather similar, while the refractive index of air is different and can cause distortions of the projected image (Fig. 2).

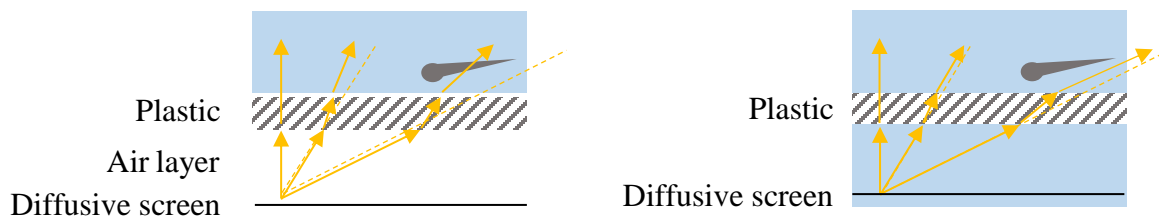


Figure 2. Schematic for the spread of light in different mediums.

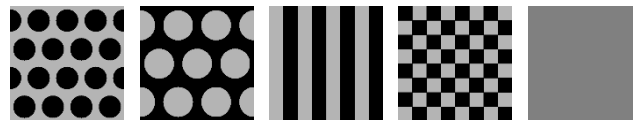
Left: from the diffusive paper to the fish through 3 layers (air, plastic and water), as shown on the left, or 2 layers (water, plastic), as shown on the right. Notice that aberrations in the light path are smaller in the case of two layers. Refractive index of water $n_{\text{water}} = 1.333$, plastic $n_{\text{plastic}} = 1.495$, air $n_{\text{air}} = 1.0003$.

The scene was illuminated from below with a custom-built IR LED array. Both mazes were positioned under a high-speed camera (Ximea USB3.0, model MQ013MG-ON), in such a way that the walls did not produce a vertical shadow (i.e. fish could be observed at any point of an experiment). The camera had an IR filter to filter out transmitted visible light. The setup was surrounded with black, non-transparent walls to shield the fish from distracting visual cues in the room.

2.2.2 Visual stimuli

Visual stimuli were projected onto the diffusive paper with an LED-projector (LG) via a cold mirror (see Fig. 8 in Results). The mirror was positioned at 45° , in a way to let the IR light from below pass through, and to reflect the light from the projector onto the diffusive screen. Stimuli were projected under the arms of the maze. The central area always had a uniform gray color (RGB = (135, 135, 135)), which was lighter than the gray in the arms to ensure that there was a contrast border at the entrance to the arms. The projected stimuli included:

- Black dots on light gray background
- Light gray dots on black background
- Black and light gray stripes
- Checkered pattern of black and light gray colors
- Uniform gray (RGB = (128, 128, 128))



The light gray color was used instead of white to lower the brightness of the arena (high brightness levels could increase stress levels of the fish, from observations of the fish, data not shown). The patterns were designed in such a way that the light-to-dark area ratio was 1:1. This was done to prevent differences in luminance between the stimuli, as larval zebrafish exhibit phototactic behavior (Burgess & Granato, 2007; Orger et al., 2000). Light gray RGB values were (180, 180, 180), black RGB values were (0, 0, 0).

2.2.3 Electrical stimulation

Each arm contained a pair of electrodes, which were located at the sidewalls. The electrodes were made out of steel mesh (wire diameter 0.2 mm, aperture 0.5 mm) and covered the whole of the sidewall. The electrodes were connected to a constant current stimulator (Digitimer DS3).

Electrical stimulation was applied at 1 Hz in the periods between the entry and the exit of the fish from the conditioned arm. Electric pulses lasted between 50 and 100 ms, depending on the experiment. Pulse amplitude was 0.7 mA (the value was chosen to elicit visible responses to shocks in all animals, data not shown). The water used in the experiments was obtained from the fish facility (pH 7.5, temperature 28°C, conductivity 650 μ S).

2.3 Behavioral tracking

All tracking was performed using custom-written scripts in Python.

2.3.1 Calculation of fish position

Black-and-white images were recorded at 60 fps. The position of the fish was identified using background subtraction in real-time. This time-dependent background value was calculated as a running average of the last 20 seconds of the recording. Background was subtracted from the current frame, the result was filtered with a Gaussian filter with a 5x5 pixel kernel to eliminate point pixel noise, and then binary thresholded. The fish was identified as the contour with the largest area on the thresholded image. Fish position was calculated as the center of mass of the corresponding contour.

2.3.2 Filtering

The identified position was corrected using a Kalman filter to reduce the noise in the recordings. The filter was implemented in Python. For simplicity of calculations the fish motion was modeled with constant speed.

Filter algorithm for updating position:

- (1) Prediction of the state X and error covariance matrix P based on the motion model

$$X^{predict} = F \cdot X^{current}$$

$$P^{predict} = F \cdot P^{current} \cdot F^T + Q$$

- (2) Calculation of the error between predicted and observed positions

$$y = (x^{observed}, y^{observed}) - H \cdot X^{predict}$$

- (3) Calculation of the filter gain K , which determines how much the calculated error influences the predicted state

$$S = H \cdot P^{predict} \cdot H^T + R$$

$$K = P^{predict} \cdot H^T \cdot S^{-1}$$

- (4) Update of the current state and the uncertainty covariance matrix using the calculated gain

$$X^{new} = X^{predict} + K \cdot y$$

$$P^{new} = (I - K \cdot H) \cdot P^{predict}, \text{ where } I \text{ is the identity matrix}$$

Parameters for the Kalman filter:

- (1) $X = (x, y, v_x, v_y)^T$ – state vector, containing current x and y coordinates and current velocity projections v_x and v_y

- (2) P – a 4x4 error covariance matrix

- (3) $F = \begin{pmatrix} 1 & 0 & 0.1 & 0 \\ 0 & 1 & 0 & 0.1 \\ 0 & 0 & 1 & 0 \\ 0 & 0 & 0 & 1 \end{pmatrix}$ – transition function from the previous state into the current state,

corresponding to a movement with constant speed ($X^{new} = F \cdot X$):

$$x^{new} = x + 0.1v_x$$

$$y^{new} = y + 0.1v_y$$

$$v_x^{new} = v_x$$

$$v_y^{new} = v_y$$

The multiplier 0.1 corresponds to a discrete time step for the update of the state vector.

- (4) $H = \begin{pmatrix} 1 & 0 & 0 & 0 \\ 0 & 1 & 0 & 0 \end{pmatrix}$ – measurement function to translate the current state into the coordinates

$$(x, y = H \cdot X)$$

- (5) S – a 2x2 residual covariance matrix
- (6) Q – a 4x4 covariance matrix for the motion noise
- (7) R – a 2x2 covariance matrix for the measurement noise

There were two sources of noise: a larger error in the position due to the detection of a different moving object (type 1), and a smaller error due to the noise in the video recording (type 2). Two sets of parameters for the Kalman filter were used to address each type of error. The sets differed in the balance between covariance matrices for the motion noise and for the measurement noise. First, in case of a large error (when the newly identified position was further than 15 pixels away from the previous position), filter parameters were tuned to be conservative and ‘distrust’ the new measurements, thus preventing extreme changes in the position (measurement error was considered much larger than motion error). Second, in case of small errors, filter allowed updates in the fish position based on the new measurements, while reducing the jitter in the position due to noise in the video recording. Noise along x- and y-coordinates was assumed to be independent, thus matrices Q and R were diagonal. For larger errors (type 1), values in the covariance matrix for the measurement noise were much larger than values for the motion noise. For smaller errors (type 2), values for the measurement and the motion noise were of the same order of magnitude.

2.3.3 Calculation of swim bouts

Swim bouts were estimated from the time series of fish positions in the maze. First, the displacement was calculated as the Euclidean distance between positions at adjacent time points. The displacement was then filtered using a finite impulse response (FIR) filter with a low-pass kernel to eliminate high-frequency noise (Mitra, 2001). The kernel was designed using the Parks–McClellan algorithm (McClellan & Parks, 1973). The cutoff frequency was equal to 4Hz. Scipy library implementations of filter and kernel design algorithm were used. Swim bouts were identified by setting a threshold on the amplitude of the filtered curve (see Fig. 3). The threshold was set manually to minimize the error between automatically identified swim bouts and manually identified bouts from video recordings (data not shown). The bout size was calculated by integrating the area under the displacement curve.

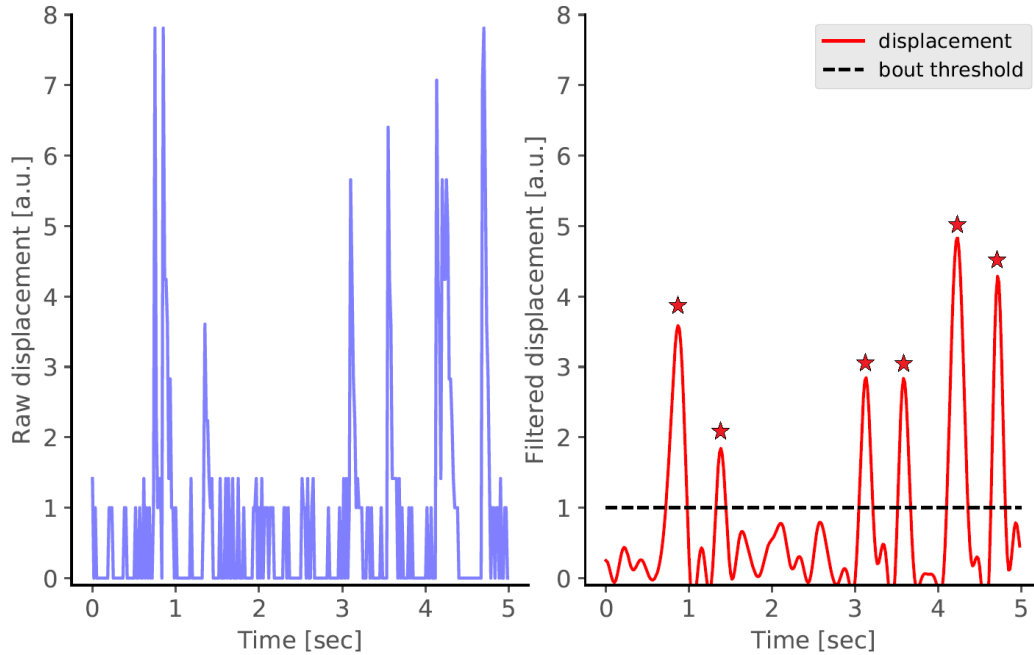


Figure 3. Calculation of swim bouts from displacement curves.

Example of fish displacement in a part of an experiment before (left) and after (right) filtering. Stars indicate identified swim bouts.

2.3.4 Calculation of heading direction

Heading direction was calculated after the experiment by analyzing the recorded videos. A heading direction vector of the fish was calculated for each frame of the video.

First, a contour of the fish was identified in a manner similar to the calculation during the experiment (see Methods 3.1). In particular, the fish contour can be approximated by an elongated triangle, with the base of the triangle at the head. The terminal point of the heading vector was located at the center of mass of the contour (which roughly corresponded to the head of the fish). The initial point of the vector was located at the furthestmost point of the contour from the center of mass (which corresponded to the tail tip of the fish). The heading direction was calculated as the angular coordinate of the heading vector in a polar coordinate system, whose polar axis was parallel to the horizontal edge of the image (Fig. 4).

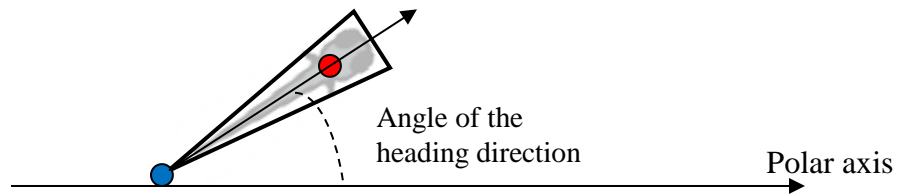


Figure 4. Schematic for calculation of heading direction.

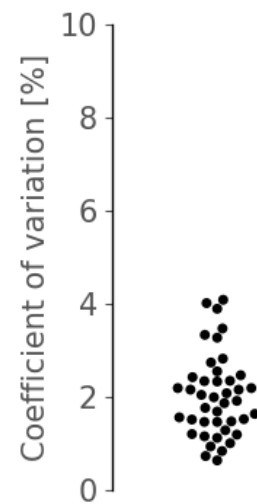
Schema of the calculation of the heading direction. The black arrow shows the heading direction vector on top of the fish contour. The initial point of the vector is in blue at the tail tip of the fish; the terminal point of the vector is in red and at the center of mass of the contour.

2.3.5 Calculation of orientation in the arm

The orientation of the fish in the arm was calculated as the difference between the heading direction of the fish and the orientation of the arm (see Fig. 31 in the Results). The orientation of the arm was defined by the arm vector, whose initial point was located at the maze center, and whose terminal point was located at the arm center. The direction of the arm vector was identified by the angular coordinate of the arm vector in a polar coordinate system, whose polar axis was parallel to the horizontal edge of the image.

2.3.6 Calculation of fish size

Fish size was calculated as the Euclidean distance between the tip of the head and the tip of the tail, whose positions were manually picked by analyzing recorded videos. To reduce the human error, the length was identified 5 times for every fish based on randomly picked frames of the video. Afterwards the final length was obtained by averaging the five handpicked lengths. To estimate the accuracy of this procedure, coefficient of variation (CV) of fish size was calculated for every fish by dividing the standard deviation of manually measured fish lengths by the mean of those lengths. CVs were calculated for a random sample of all experimentally tested fish ($n = 42$). Obtained values did not exceed 5%.



2.4 Experimental protocols

Every experimental protocol consisted of one or more experimental sessions. The sessions followed each other without an interruption, and each session could be characterized by its duration, the patterns that were projected into the maze, and the ON/OFF status of the electric stimulation.

In each protocol, every fish was tested individually. For protocols with electric stimulation, the experiment was terminated if the fish remained in the shocked arm for longer than one minute. This was done to prevent excessive stress for the animals. Such fish were also excluded from the analysis (“overstayers” in Appendix 1).

In addition, fish that stayed in the center of the maze for longer than 60% of the duration of the conditioning session were excluded from the analysis (“center” in Appendix 1). These fish responded to conditioning by avoiding all of the arms, independent of the distinct visual cues, and did not contribute to distinguishing what types of visual strategies fish might use in the CPA paradigm.

See Appendix 1 for detailed numbers of the animals used for each protocol.

The protocol for control of inherent fish biases and stability of maze arm preference included one session (Results Chapter 3.1).

Table 1. Control protocol.

Session	Duration [min]	Patterns	Shock
CONTROL	120	3 patterns (‘checkered’, ‘stripes’, ‘white dots’)	No

The protocol for age comparison included two sessions (Results Chapter 3.2).

Table 2. Age comparison protocol.

Session	Duration [min]	Patterns	Shock
HABITUATION	30	3 patterns (‘checkered’, ‘stripes’, ‘white dots’)	No
CONDITIONING	60	Same patterns in same locations	Yes

The protocol for testing learning effects after the end of conditioning included three sessions (Results Chapter 3.3).

Table 3. Protocol with a test session.

Session	Duration [min]	Patterns	Shock
HABITUATION	30	3 patterns ('checkered', 'stripes', 'white dots')	No
CONDITIONING	60	Same patterns in same locations	Yes
TEST	30	Same patterns in same locations	No

The protocol for testing time dynamics of memory fading included four sessions (Results Chapter 3.3).

Table 4. Protocol with a delay and a test session.

Session	Duration [min]	Patterns	Shock
HABITUATION	30	3 patterns ('checkered', 'stripes', 'white dots')	No
CONDITIONING	60	Same patterns in same locations	Yes
GRAY	5 or 10	Uniform gray in all arms	No
TEST	30	Original patterns in original locations	No

The protocol for testing the importance of distinct visual cues in the CPA paradigm included three sessions (Results Chapter 3.5).

Table 5. Protocol with identical patterns.

Session	Duration [min]	Patterns	Shock
HABITUATION	30	Identical patterns in all arms ('black dots')	No
CONDITIONING	60	Same patterns in same locations	Yes
TEST	30	Same patterns in same locations	No

The protocol for control of how aversive the switch of preferred pattern to uniform gray is for the fish included two sessions (Results Chapter 3.5).

Table 6. Control protocol for replacement of shocked pattern: switch to gray.

Session	Duration [min]	Patterns	Shock
HABITUATION	30	3 patterns ('checkered', 'stripes', 'white dots')	No
GRAY	30	Same patterns in same locations, except the pattern of the preferred arm switched to uniform gray	No

The protocol for control of how aversive the switch of preferred pattern to a new pattern is for the fish included two sessions (Results Chapter 3.5).

Table 7. Control protocol for replacement of shocked pattern: switch to a new pattern.

Session	Duration [min]	Patterns	Shock
HABITUATION	30	3 patterns ('checkered', 'stripes', 'white dots')	No
DOTS	30	Same patterns in same locations, except the pattern of the preferred arm switched to 'black dots'	No

The protocol for replacement of shocked pattern in the test session included three sessions (Results Chapter 3.5).

Table 8. Protocol for replacement of shocked pattern.

Session	Duration [min]	Patterns	Shock
HABITUATION	30	3 patterns ('checkered', 'stripes', 'white dots')	No
CONDITIONING	60	Same patterns in same locations	Yes
DOTS	30	Same patterns in same locations, except the pattern of the preferred arm switched to 'black dots'	No

The protocol with rotation of the patterns in the test session included three sessions (Results Chapter 3.5).

Table 9. Protocol with pattern rotation.

Session	Duration [min]	Patterns	Shock
HABITUATION	30	3 patterns ('checkered', 'stripes', 'white dots')	No
CONDITIONING	60	Same patterns in same locations	Yes
ROTATE	30	Same patterns rotated by 120° cw or ccw (randomly chosen)	No

2.5 Modeling

A model was used to investigate how reactions to shocks, independent of learning, could influence the occupancy and entry frequency of the shocked arm – two metrics used to quantify the learning effects.

2.5.1 Model description

In the model, the maze was reduced to a Y-maze, whose three arms were one-dimensional (1D) linear tracks. Each 1D arm had a length (parameter L) and a coordinate axis associated with it, with the arm opening located at 0, and the arm end located at distance L from the origin. The center of the maze was modeled as a separate 1D compartment of length L_{center} .

The simulated agent moved along the arm axis in discrete steps. Each step had a direction ('left' towards the arm opening, and 'right' towards the arm end) and a size S . The step direction was chosen randomly at each simulation step. The step size S was drawn from a distribution based on the experimentally observed distribution of swim bout sizes (see Fig. 30, blue histogram). Experimental values were fitted to a Gamma distribution with shape parameter value 1.79 and scale parameter 0.062. The mean of the observed distribution, calculated as a product of shape and scale parameters, was equal to 1.1 mm, and length of maze arm was equal to 30 mm. Thus the average swim bout size constituted a fraction of $\frac{1.1}{30} = 0.037$ of the maze arm length. The scale of the Gamma distribution, used for modeling, was chosen so that the distribution mean was equal to $0.037 \cdot L$, where L was the length of the arm in the modeled maze (Fig. 5).

$$f(x, a) = \frac{x^{a-1} \exp(-x)}{\Gamma(a)}, \quad \text{where } \Gamma(z) = \int_0^{\infty} x^{z-1} e^{-x} dx \quad (1)$$

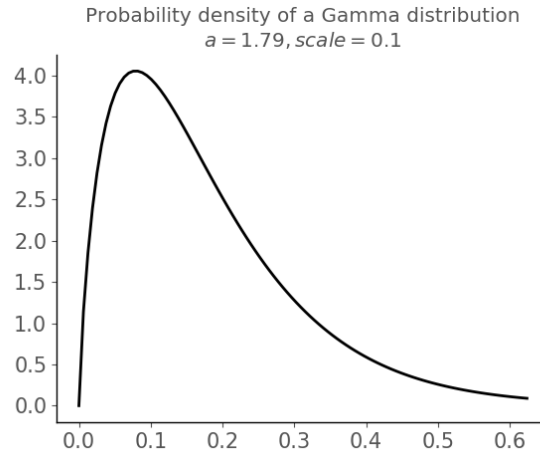


Figure 5. Probability density function for the Gamma distribution used in modeling.

Shape parameter $a = 1.79$, scale parameter = 0.1 for $L = 5$. Mean of the distribution = $0.037 \cdot 5 = 0.185$; scale = $0.185/a = 0.185/1.79 = 0.1$.

If the simulated agent moved to the left of the arm opening, it exited its current arm and entered the central compartment. On the other side, the arm's end was 'sticky': when the simulated agent moved to the right of the arm end, it stopped at the arm end until the next step of the simulation. Both boundaries of the central compartment were treated equally: if the simulated agent stepped over either the left or the right boundary of the central compartment, it entered an arm. Each arm had a probability of entry associated with it, with all probabilities summing to one (see Fig. 6).

The effects of the electric shocks could be simulated in one of the arms. The size of every step made in the 'shocked' arm was multiplied by a parameter $\alpha \geq 1$, to simulate the increased swim bout amplitude in response to electric shocks. The α -value in the central compartment of the simulated maze remained always equal to 1.

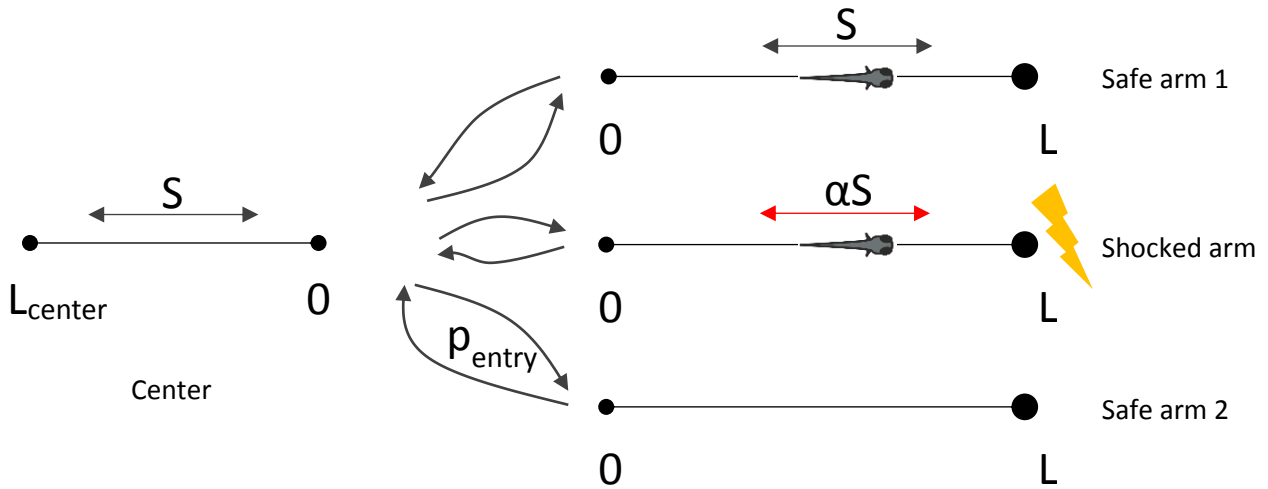


Figure 6. Schema of the pseudo-random walk model, used to simulate experimental results.

Three arms of the simulated maze (right) have length L . Fish moves in each of the arms with a step S or $\alpha \cdot S$ (in case of the ‘shocked arm’). From the left end of the arm (arm opening) the fish enters the ‘center’ (left). The fish enters back into the arms with a probability p_{entry} , specified for each arm.

2.5.2 No-learning model

The “no-learning” model was used to investigate if the increased speed in the shocked arm alone could explain the changes in learning metrics during conditioning (arm occupancy and arm entry frequency, see Results Chapters 3.2 and 3.3).

An experiment was simulated with 2 or 3 sessions. Each session lasted n steps. In the starting ‘habituation’ session, the step size of the simulated agent in all arms was drawn from the same distribution. At the end of the ‘habituation’ session, the arm with the highest occupancy was selected as the ‘shocked’ arm for the next ‘conditioning’ session (occupancy was higher in the arm due to stochastic reasons). In the ‘conditioning’ session, the step size of the simulated agent in the ‘shocked’ arm was multiplied by the parameter α to simulate increased swim bout amplitude during the shocks. In the third (‘test’) session, step sizes in all of the arms were again drawn from the same distribution. Probabilities of entry into any of the arms were equal to $\frac{1}{3}$ in all sessions.

All simulations were run using custom-written scripts in Python.

Parameter set used for simulations in Chapter 3.2:

$L = 5$; $L_{\text{center}} = 1.5$; $\text{scale} = 0.1$; $\alpha = 2$; $n_{\text{habituation}} = 5,000$ steps; $n_{\text{conditioning}} = 10,000$ steps.

Parameter set used for simulations in Chapter 3.3:

$L = 5$; $L_{\text{center}} = 1.5$; $\text{scale} = 0.1$; $\alpha = [1, 2, 3, 4]$; $n_{\text{habituation}} = 5,000$ steps; $n_{\text{conditioning}} = 10,000$ steps; $n_{\text{test}} = 5,000$ steps.

2.5.3 Model with a learning rule

A learning component was added to the model to investigate if the decrease in learning metrics, i.e. the entry frequency of the shocked arm during the conditioning and test sessions, and the occupancy of the shocked arm during the test session, could be reproduced (see Results Chapter 3.3).

In the learning model, the probability of entry into the arms of the simulated maze was changed from a constant to a variable parameter. The learning rule consisted of decreasing the probability of entry into the shocked arm every time an entry into the shocked arm happened during the ‘conditioning’ session. The rule corresponded to an exponential decay of the probability of entry, with a learning rate β with a floor of 0.1 (a non-zero value was chosen because in the experiments the probability of entry never reduced to 0, Equation 2). The probabilities of entry into the other two arms increased correspondingly, to keep the sum of all probabilities equal to one (Equations 3 and 4).

$$\Delta p_{\text{entry}}^{\text{shock}} = \beta \cdot (0.1 - p_{\text{entry}}^{\text{shock}}) \quad (2)$$

$$\Delta p_{\text{entry}}^{\text{non-shock}} = -\frac{1}{2} \cdot \Delta p_{\text{entry}}^{\text{shock}} \quad (3)$$

$$\sum_{\text{all arms}} p_{\text{entry}} = 1 \quad (4)$$

Relearning that the conditioned arm was safe again was simulated by relaxation of the probability of entry into the shocked arm back to the $\frac{1}{3}$ level during the test session (Equation 5). The probability was increased every time an entry into the ‘conditioned’ arm happened. The probabilities of entry into the other two arms were decreased correspondingly (Equation 6 and 7)

$$\Delta p_{entry}^{shock} = \beta \cdot \left(\frac{1}{3} - p_{entry}^{shock} \right) \quad (5)$$

$$\Delta p_{entry}^{non-shock} = -\frac{1}{2} \cdot \Delta p_{entry}^{shock} \quad (6)$$

$$\sum_{all\ arms} p_{entry} = 1 \quad (7)$$

The learning rate β used in Chapter 3.3 was equal to 0.05.

2.6 Analysis of conditioning effects

All analysis was performed using custom-written scripts in Python.

2.6.1 Metrics for the CPA paradigm

Behavior in the CPA paradigm was assessed with two metrics: occupancy of the arms and entry frequency of the arms (Fig. 11 in Results). Occupancy of a particular arm was calculated by dividing the time spent in that arm by the total amount of time spent in all of the arms. Occupancy was additionally calculated for the central compartment of the maze. Entry frequency of a particular arm was calculated by dividing the number of times that the fish entered into that arm by the total amount of entries the fish performed into all of the arms. The two metrics could be calculated for the whole time of an experiment as well as for a part of an experiment (in a corresponding time window).

2.6.2 Sliding window curves

Dynamics of CPA metrics in an experiment were visualized using sliding window curves. Window size was chosen to be 10 minutes long, with a 1-minute sliding step, i.e. two adjacent windows had a 9-minute overlap (except a 5-minute time window with a 30-second step for Fig. 26 and 27 in Results). Every point on the sliding window curve represents the occupancy/entry frequency in a single time window.

Sliding windows on the border between two sessions include fish trajectories from both sessions (sessions can have different experimental conditions, i.e. ON/OFF stimulation); vertical dashed lines were drawn around each border to include all such windows with mixed conditions.

For some fish, the number of arm entries within a 10-minute time window could be very small or zero (e.g. because the fish froze for a part of the conditioning session). If the number of entries was less than three, the fish could not have visited all of the arms, and the entry frequency was not a useful metric. Entry frequency for such time windows was not calculated, and the corresponding points on individual sliding window curves were missing. These time windows were not included in the averages across individual fish, and they were not included in the statistical testing either.

2.6.3 Permutation testing

Permutation testing was used to assess the significance of differences between the occupancy/entry frequency of the shocked arm and the other two arms of the maze. For each experimental protocol, a permutation test was performed for the last 10 minutes of the conditioning session (to estimate the significance of the reactions to shocks during the conditioning) and for the first 10 minutes of the test session (to estimate the effects of the conditioning after the electric stimulation was switched off). Occupancies/entry frequencies of each arm for each fish were calculated in these time windows. Then, for each fish separately, the arms were randomly relabeled, so that the occupancy/entry frequency values were reassigned to different arms. Such relabeling (permutation) was performed $n = 10^7$ times.

A score was calculated for the experimental values and for each permutation as the difference between the mean occupancy/entry frequency of the shocked arm and the average of mean occupancies/entry frequencies of the other two arms (Equation 8 for the occupancy score, $Score_O$, and Equation 9 for the entry frequency score, $Score_E$).

$$Score_O = \langle Occupancy_{shock} \rangle - \frac{1}{2} (\langle Occupancy_{safe1} \rangle + \langle Occupancy_{safe2} \rangle) \quad (8)$$

$$Score_E = \langle Entry_freq_{shock} \rangle - \frac{1}{2} (\langle Entry_freq_{safe1} \rangle + \langle Entry_freq_{safe2} \rangle) \quad (9)$$

Scores obtained from all permutations constitute a distribution of score values for the null hypothesis, i.e. that all arms are interchangeable for the fish, and therefore that there is no

significant difference between the occupancy/entry frequency of the shocked arm and the other two arms. The experimental score lies somewhere in this distribution. The significance value of the experimental score is assessed by calculating the fraction of the score values in the distribution which are equal or lower than the experimental score value (Equation 10).

$$p_{value} = P(\text{Score} \leq \text{Score}^{exp}) \quad (10)$$

This procedure can be illustrated with a toy example. The toy dataset contains arm occupancies from six individual fish. The experimental score, Score^{exp} , can be calculated from the average occupancies of all the arms using Equation 8. After that, occupancy values are permuted for each fish, and for every permutation a permutation score, Score^{perm} , can be calculated (Table 10).

Table 10. An example for the calculations of experimental and permutation scores.

Left: toy dataset of ‘experimental’ arm occupancy values. Right: dataset after permutation of occupancy values. Each row of the table contains arm occupancies of individual fish. Average occupancy is calculated for each column. Score is calculated using Equation 8.

Before permutation				After permutation			
	Shocked arm	Safe arm 1	Safe arm 2		Shocked arm	Safe arm 1	Safe arm 2
Arm occupancy of individual fish	0.15	0.33	0.52	Arm occupancy of individual fish	0.33	0.15	0.52
	0.2	0.35	0.45		0.2	0.45	0.35
	0.1	0.46	0.44		0.44	0.1	0.46
	0.3	0.4	0.3		0.3	0.4	0.3
	0.8	0.1	0.1		0.1	0.8	0.1
	0.1	0.47	0.43		0.43	0.47	0.1
Average occupancy	0.28	0.35	0.37	Average occupancy	0.3	0.39	0.31
$Score^{exp} = 0.28 - \frac{0.35 + 0.37}{2} = -0.08$				$Score^{perm} = 0.3 - \frac{0.39 + 0.31}{2} = -0.05$			

These permutations are repeated $n = 10^6$ times, and a distribution of permutation scores is obtained (Fig. 7).

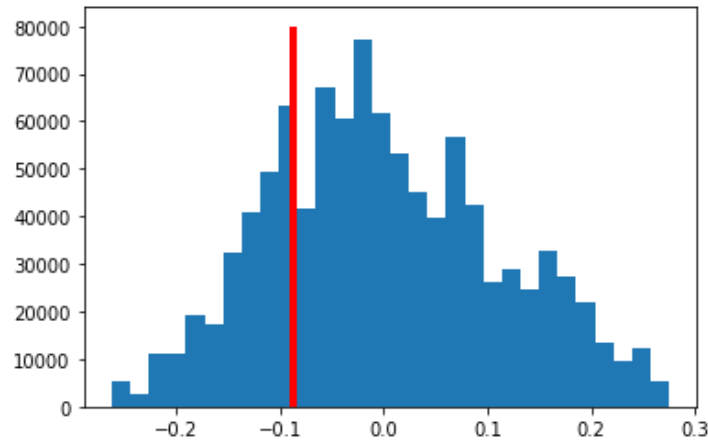


Figure 7. Histogram of the distribution of permutation scores for a toy dataset.

Red line shows the position of the experimental score in the distribution. $n = 10^6$ permutations.

Finally, the p -value of the experimental score is calculated by dividing the number of permutation scores less-than or equal to the experimental score by the total number of permutations (Equation 10). This gives the p -value of 0.23, suggesting that we should accept the null-hypothesis, i.e. that arm occupancies do not differ significantly in this toy dataset.

Sometimes, in the cases of very strong effects of conditioning, none of the permutations produced an effect stronger than experimental value. In such cases the estimated p -value was equal to 0, and was marked with b.l.s.t = beyond the limit of the statistical test.

2.6.4 Analysis and clustering of shock-triggered swim bouts

The dataset for shock swim bouts was obtained from the conditioning sessions of 53 fish. It contained responses to 16,151 shocks. For every shock, fish coordinates were extracted for the 20-second interval starting at the shock onset. Every coordinate sequence was then transformed into a displacement, calculated as the Euclidean distance between coordinates from adjacent time points.

Every displacement curve was smoothed using univariate splines. For every displacement, three parameters were calculated: an amplitude (maximal value), onset time (a time point when the first derivative of the displacement curve exceeded the value of 0.3), and rise time (the difference between peak time and onset time). Displacements whose amplitudes were lower than a threshold of 5 were considered non-responses; the rest were considered swim bouts. The orientation of the fish in the shocked arm at the time of shock onset was determined for every displacement curve (the orientation was calculated for the time of shock onset, as described in Methods section 3.5).

Hierarchical clustering with Ward's method was performed on a reduced dataset, in which non-responses were excluded (11,766 non-responses). The final dataset was represented by a 4,385-by-3 matrix (3 parameters for each identified swim bout: amplitude, onset time and rise time; orientation in the arm was not included as a parameter for the clustering). Ward's method minimizes variance within the formed clusters. The cluster tree was cut at a level to produce five clusters. Every cluster was considered to represent a separate response type.

Comparison of the learning effects between different response types was performed using one-way ANOVA, followed by post-hoc t-test group comparisons with a Bonferroni correction. Four response types were compared amongst each other (6 pairs), the fifth response type contained 'spontaneous' swim bouts (noise) and was discarded from the analysis. The corrected significance level was equal to $\frac{0.05}{6} = 0.008$. The learning effects were estimated by calculating the occupancy/entry frequency of the shocked arm in the next 10 minutes after every shock response of a particular type (Fig. 36 and 37 in Results).

3 Results

3.1 A conditioned place avoidance paradigm for larval and juvenile zebrafish

3.1.1 Setup and protocol

Two Y-mazes were positioned next to each other, making it possible to test two fish at the same time. Each arm of the maze displayed a distinct visual pattern, which was projected from below using an LED-projector. Every arm of the maze contained two steel-mesh electrodes, covering the sidewalls of the arm. The electrodes were connected to a constant current stimulator, which could provide pulses of direct electric current (see Methods). The maze was recorded from above using a high-speed camera (Fig. 8).

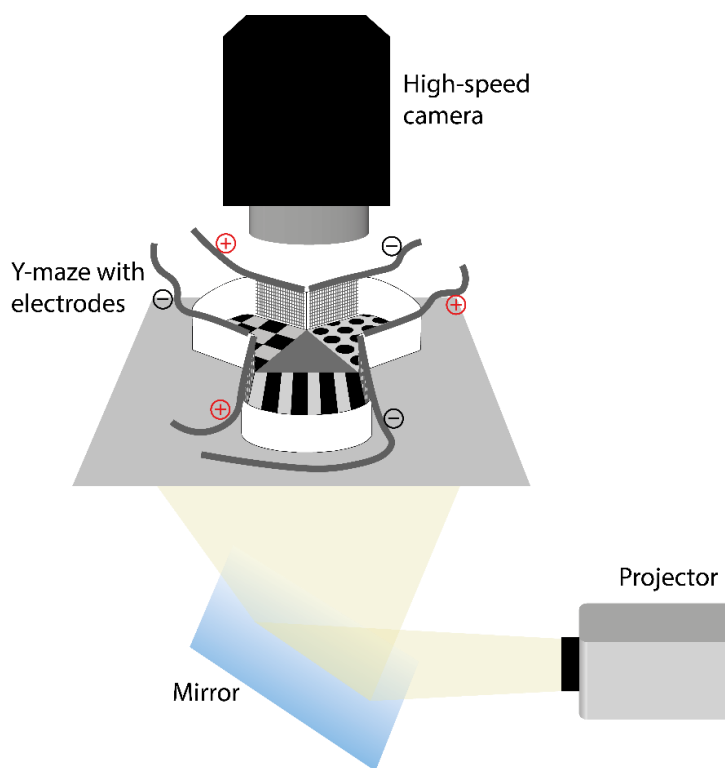


Figure 8. Schematic drawing of the setup.

Visual patterns are projected from below. Each arm contains a pair of steel-mesh electrodes.

A typical conditioning experiment consisted of three sessions (Fig. 9). In the first session, termed habituation, the fish was introduced into the center of the maze using a pipette and allowed to explore the Y-maze for 30 minutes. Following the habituation period, the fish's preferred arm was defined as the arm where it spent the most time (see Chapter 3.1.2 for of calculation). The conditioning session followed immediately after the habituation session and lasted for 60 minutes. During the conditioning session, the fish received mild electric shock pulses with a frequency of 1 Hz while in the preferred arm, as defined in the previous session. Finally, the third session, a test session, lasted for 30 minutes. Electrical pulses were not administered during the test session. This final session was used to examine whether a memory of an aversive location in the maze was formed and how long this memory lasted (see Fig. 10 for individual examples of fish trajectories in the three sessions of the protocol). Importantly, visual stimuli in the test session could be manipulated (e.g. rotation of the visual patterns) to investigate what types of cues were necessary for the memory to form.

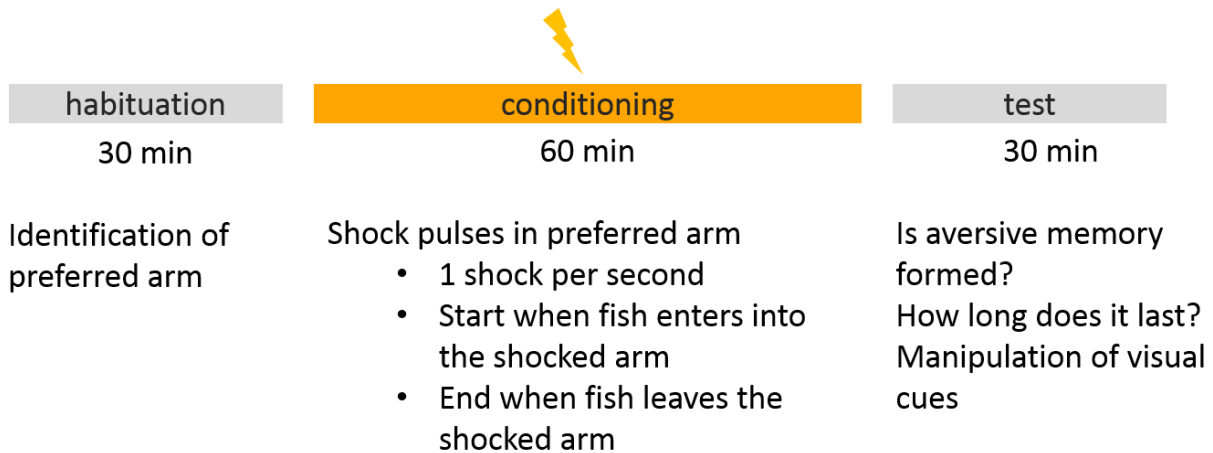


Figure 9. Schematic description of the CPA protocol.

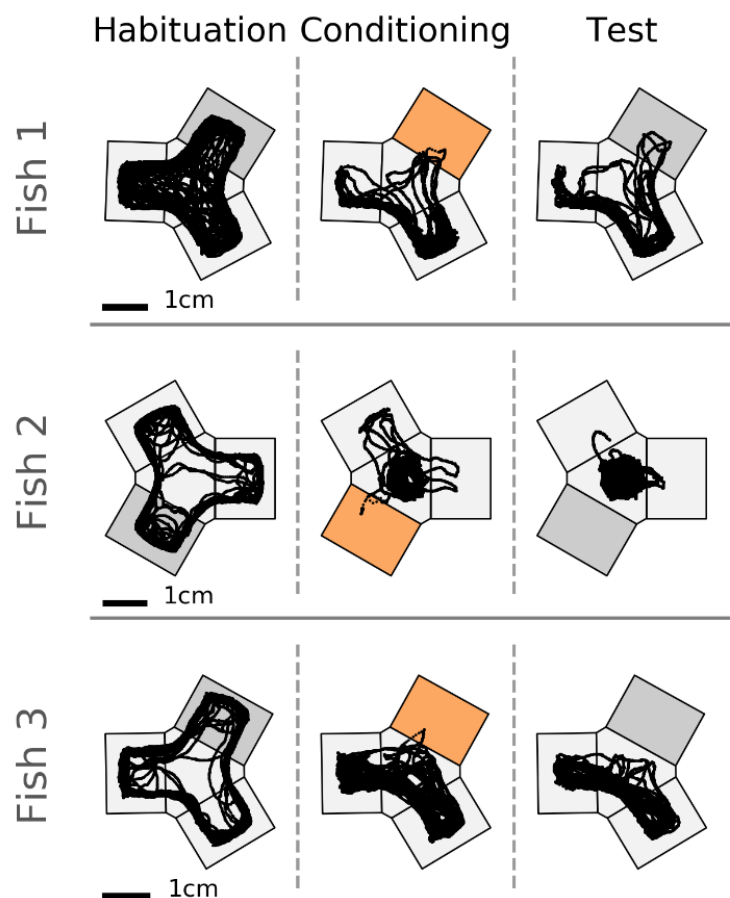


Figure 10. Examples of individual fish trajectories in different sessions of the CPA protocol. The preferred arm in the habituation session is shown in dark gray, in the conditioning session in orange (when electric shocks were presented), and in the test session in dark gray again (when electric shocks had been stopped).

Execution of the protocol was fully automated: the position of the fish was tracked in real-time using a custom-designed computer vision algorithm (see Methods); transitions between protocol sessions and the timing of the electric shocks were controlled by custom-written software, and did not require the experimenter's presence. This minimized the amount of distractions for the animal during an experiment.

3.1.2 Metrics for quantification of fish performance in the CPA paradigm

Two metrics were developed to estimate the performance of the fish in the CPA paradigm: arm occupancy and arm entry frequency. Arm occupancy was calculated by dividing the time spent in a maze arm during a 10-minute time window by the length of the time window (Fig. 11, top). Arm entry frequency was calculated by dividing the number of entries into a maze arm by the total number of entries to all maze arms during the time window (Fig. 11, bottom).

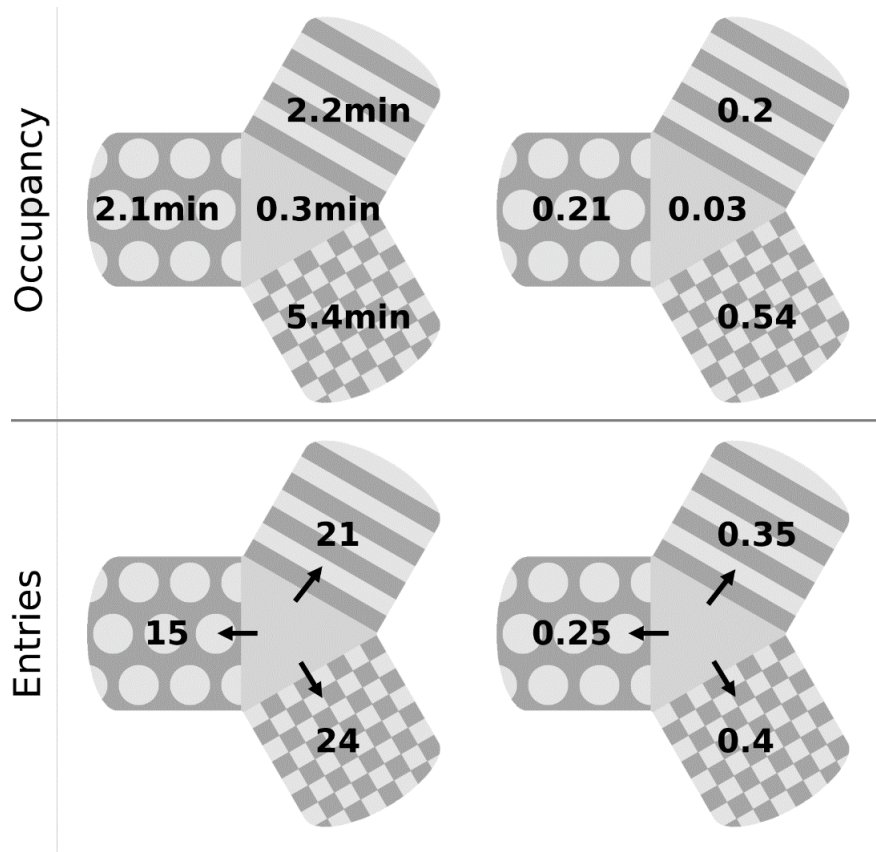


Figure 11. An example of the calculation of CPA metrics.

Top: arm occupancy. Bottom: arm entry frequency. Absolute values are on the left, normalized values are on the right.

These metrics were calculated throughout the course of the experiment by using a sliding time window. The resulting sliding window curve shows the evolution of preference/avoidance for individual arms in the Y maze during the experiment (Fig. 12).

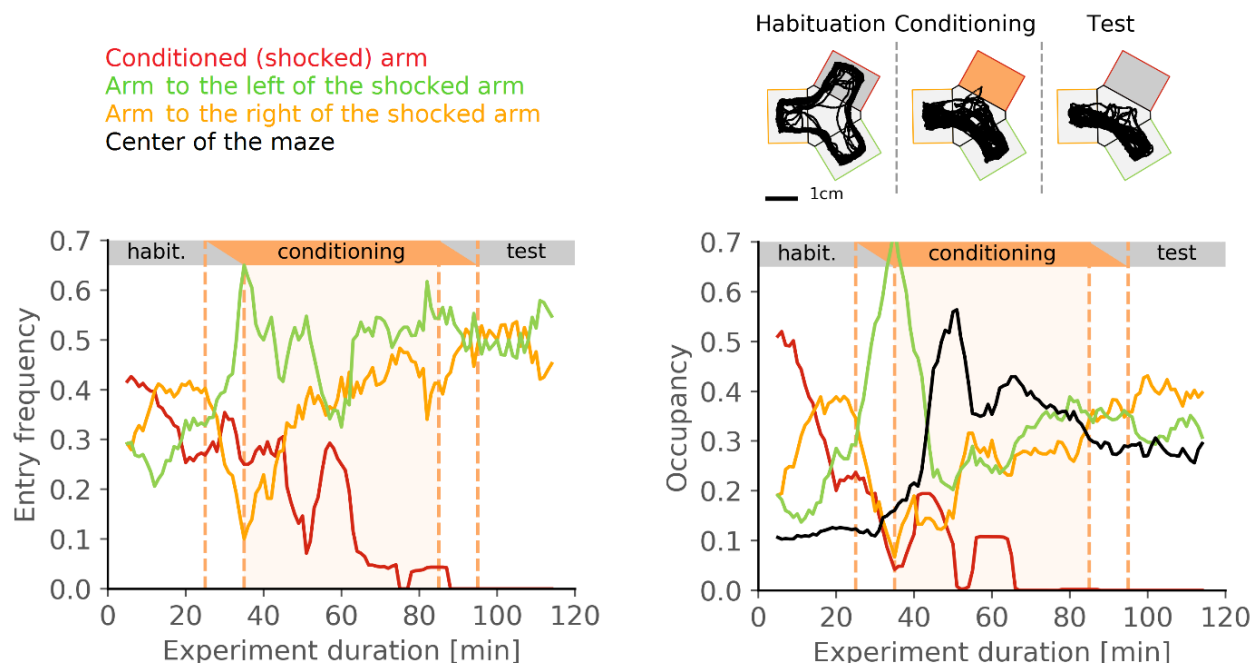


Figure 12. An example of sliding window analysis for a single fish.

Top right: the trajectory of the fish in the CPA sessions. Bottom: sliding window curves for entry frequency and occupancy of the arms. Colors of the sliding window curves correspond to the legend in top left. Vertical dashed lines mark the transition periods during which the sliding window contained information from two sessions. The sliding window was 10 minutes long, with a sliding step of 1 minute. Fish age was 24 dpf.

3.1.3 Optimizing experimental design: assessing preference stability of maze arms and inherent preferences of fish

Before starting the conditioning phase of the CPA paradigm, possible confounds in the experimental setup were investigated.

Firstly, arm preference, established during the first 30 minutes of the experiment, was tested for stability on the time scale compatible with the full length of the experiment (2 hours). An unstable preference would mean occupancy and/or entry frequency of the preferred arm can change during the experiment regardless of conditioning, therefore confounding the results. Both occupancy and entry frequency of the preferred arm were stable on average (Fig. 13). This suggests that, if in the

conditioning experiments the occupancy and/or the entry frequency of the shocked arm decreased, it would be due to the conditioning effects and not due to innate variation in fish preferences.

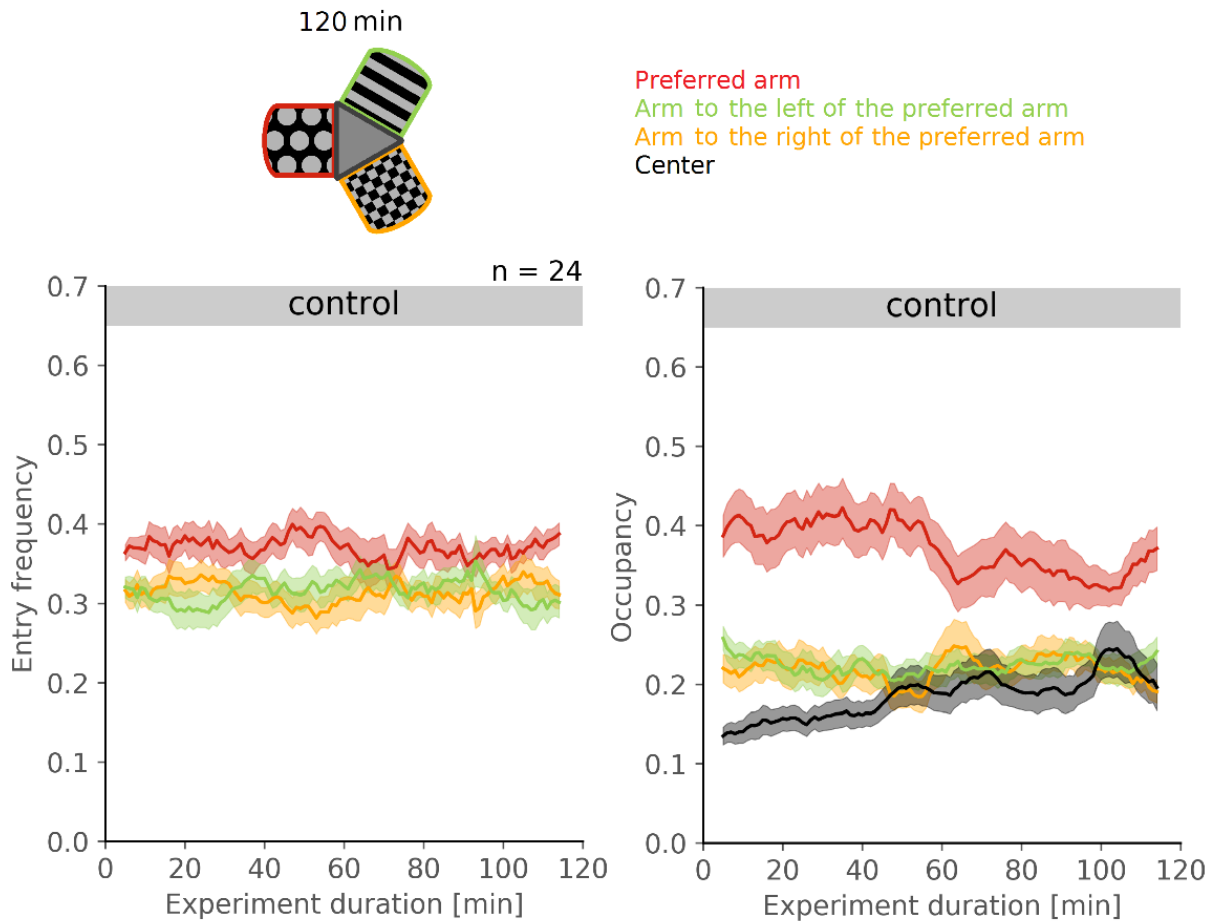





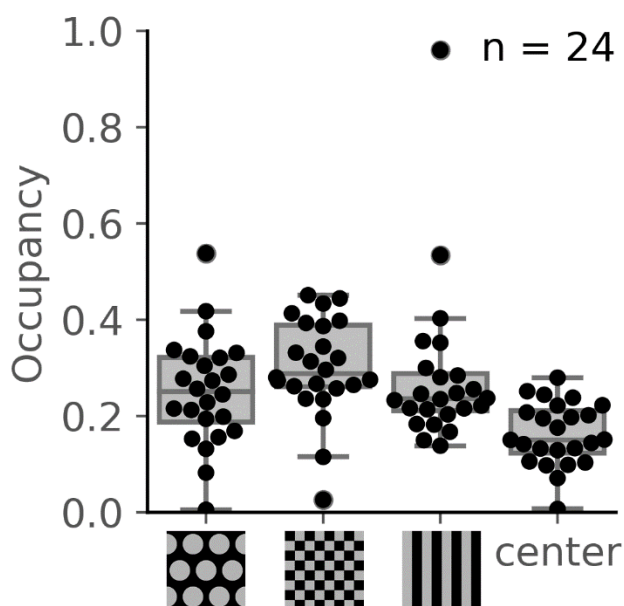
Figure 13. Sliding window curves for control experiments.

Arm preference is stable throughout the 2-hour experiment. The preferred arm was defined in the first 30 minutes of the experiment. Solid lines show arm occupancies averaged across individual fish. Ribbons show s.e.m. Colors correspond to the legend in the top right. Positions of the visual patterns in the schema in the top left are given as examples but were alternated for each fish. Fish age was between 22 and 23 dpf. $n = 24$.

Secondly, any innate preference for the visual patterns that were used to distinguish the arms of the maze was tested. No significant difference in occupancies of the arms grouped by associated pattern were found, thus visual patterns should not cause any bias in the results of the conditioning (Fig. 14, Table 11). In all experiments the significance level was chosen to be 0.05.

Table 11. Occupancy of maze arms, grouped by patterns, in control experiments.Mean \pm s.e.m.

				n	One-way ANOVA	
					F	<i>p</i> -value
Occupancy	0.25 \pm 0.02	0.31 \pm 0.02	0.28 \pm 0.03	24	0.87	0.42

**Figure 14. Occupancy of maze arms grouped by the associated visual pattern.**

There was no significant innate preference for any of the patterns. Occupancy was calculated over the 2-hour time period of the experiment. Box plots show the median and quartiles; whiskers show 1.5 multiples of the inner quartile range (values outside the whisker range are considered as outliers). One-way ANOVA $F = 0.87$, p -value = 0.42, $n = 24$.

Finally, the relation between the arm occupancies and absolute ‘geographic’ positions of the maze arms in the room was analyzed. As two mazes were used in parallel the positions of both mazes were examined separately (Fig. 15).

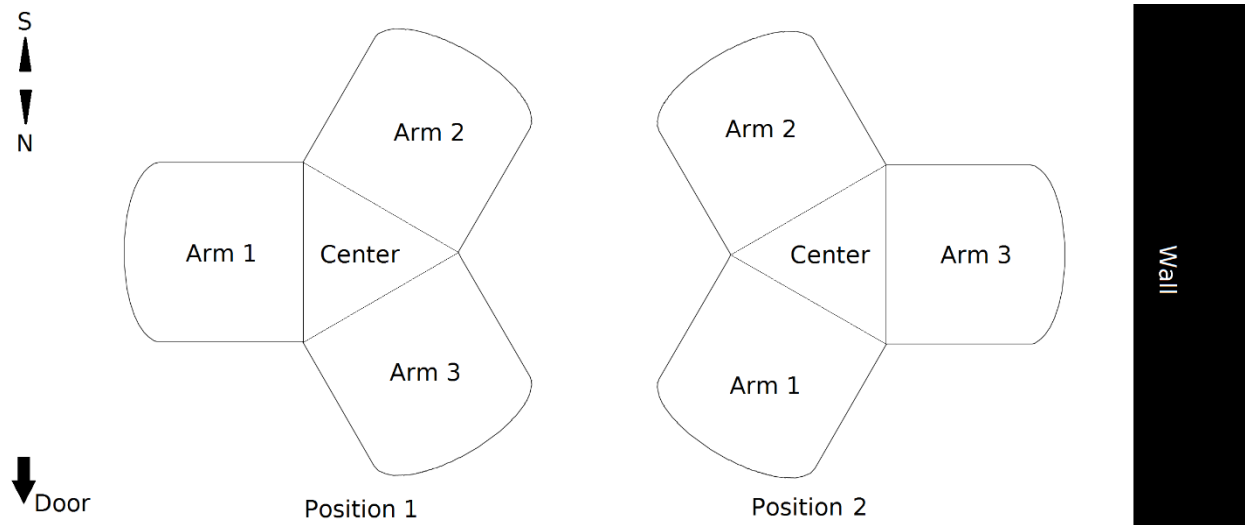


Figure 15. Positioning of the mazes in the experimental room.

Top left corner shows the North/South directional axis.

A significant bias in arm occupancies of the maze in Position 1, but not in Position 2, was observed (Fig. 16, Table 12).

The bias was independent of the visual patterns displayed or the initial position of the fish in the maze. Moreover, the mazes were radially symmetric, and were exchanged between Position 1 and Position 2, excluding the influence of a defect or similar cue within the mazes themselves. The presence of this bias suggested that some non-visual, and yet unexplained, cues influenced the behavior of the fish. To investigate whether this non-visual bias could play a role in the conditioning phase of the CPA paradigm, experiments were performed in which all visual patterns in the arms of the maze were identical, thus depriving the fish of distinct visual cues. If the fish were able to use non-visual cues, the absence of visually distinct patterns should not influence their performance. Alternatively, if the fish could not undergo conditioning in the absence of distinct visual cues, it would mean that the non-visual bias is not a confounding factor in the experiments. Results of these tests are described in Chapter 3.5.

Table 12. Occupancy of arms in two mazes, grouped by absolute position in the experimental room, in control experiments.

Mean \pm s.e.m.

	Arm 1	Arm 2	Arm 3	n	One-way ANOVA	
					F	<i>p</i> -value
Maze 1	0.19 \pm 0.01	0.26 \pm 0.02	0.36 \pm 0.02	12	14.35	3e-05
Maze 2	0.30 \pm 0.04	0.22 \pm 0.02	0.32 \pm 0.06	12	1.47	0.24

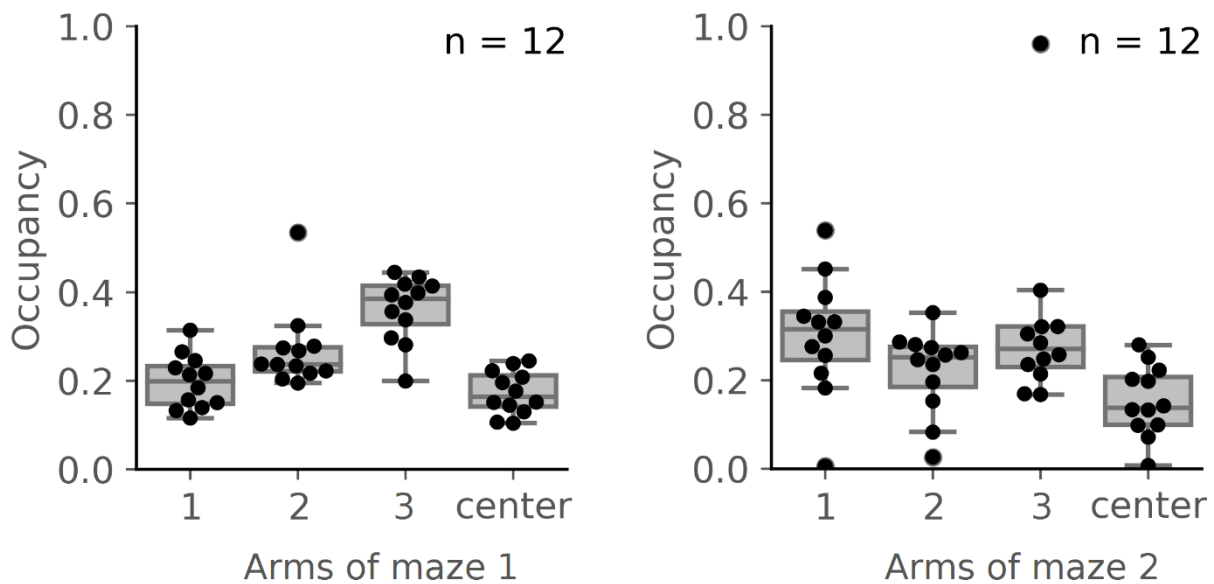


Figure 16. Intrinsic biases in the setup or in innate fish behavior.

Left: there is a significant difference in arm preference in the maze placed in position 1. Right: there is no significant arm preference for arms in maze in position 2. Box plots are same as before. One-way ANOVA: Maze 1 $F = 14.25$, $p\text{-value} = 3e-05$, $n = 12$; Maze 2 $F = 1.47$, $p\text{-value} = 0.24$, $n = 12$.

The protocol used for age comparison consisted of two experimental sessions: a habituation session for 30 minutes, and a conditioning session for 60 minutes. Age groups were assessed for robust and significant changes in the entry frequency and/or occupancy of the shocked arm. The significance of the changes in both metrics was quantified using permutation testing (see Methods).

3.2.1 Changes in the entry frequency of the shocked arm are significant for 3-week-old fish

Changes in entry frequencies of the shocked maze arm between different age groups were compared (see Table 13 for details). 1wo fish did not show any significant changes in the entry frequency of the shocked arm throughout the experiment (Fig. 18, left). 2wo fish showed highly variable responses, with half of the fish showing a high level of freezing/little movement by the end of the conditioning session: for the fish that froze the entry frequency could not be calculated (total number of entries was lower than three per a time window of 10 minutes, see Methods). The entry frequency of the shocked arm was still not significantly lower than of the other two arms (Fig. 18, middle). In contrast, the entry frequency of the shocked arm of 3wo fish was significantly lower than the entry frequencies to the other two arms by the end of the conditioning session (Fig. 18, right).

Table 13. Entry frequency in the last 10 minutes of the conditioning session for different age groups.

Mean \pm s.e.m.

	Shocked arm	Safe arm on the left	Safe arm on the right	n	Permutation test p -value
1wo fish	0.29 \pm 0.03	0.31 \pm 0.04	0.40 \pm 0.04	14	0.17
2wo fish	0.17 \pm 0.06	0.56 \pm 0.10	0.27 \pm 0.08	10	0.10
3wo fish	0.19 \pm 0.04	0.33 \pm 0.05	0.48 \pm 0.06	16	0.02

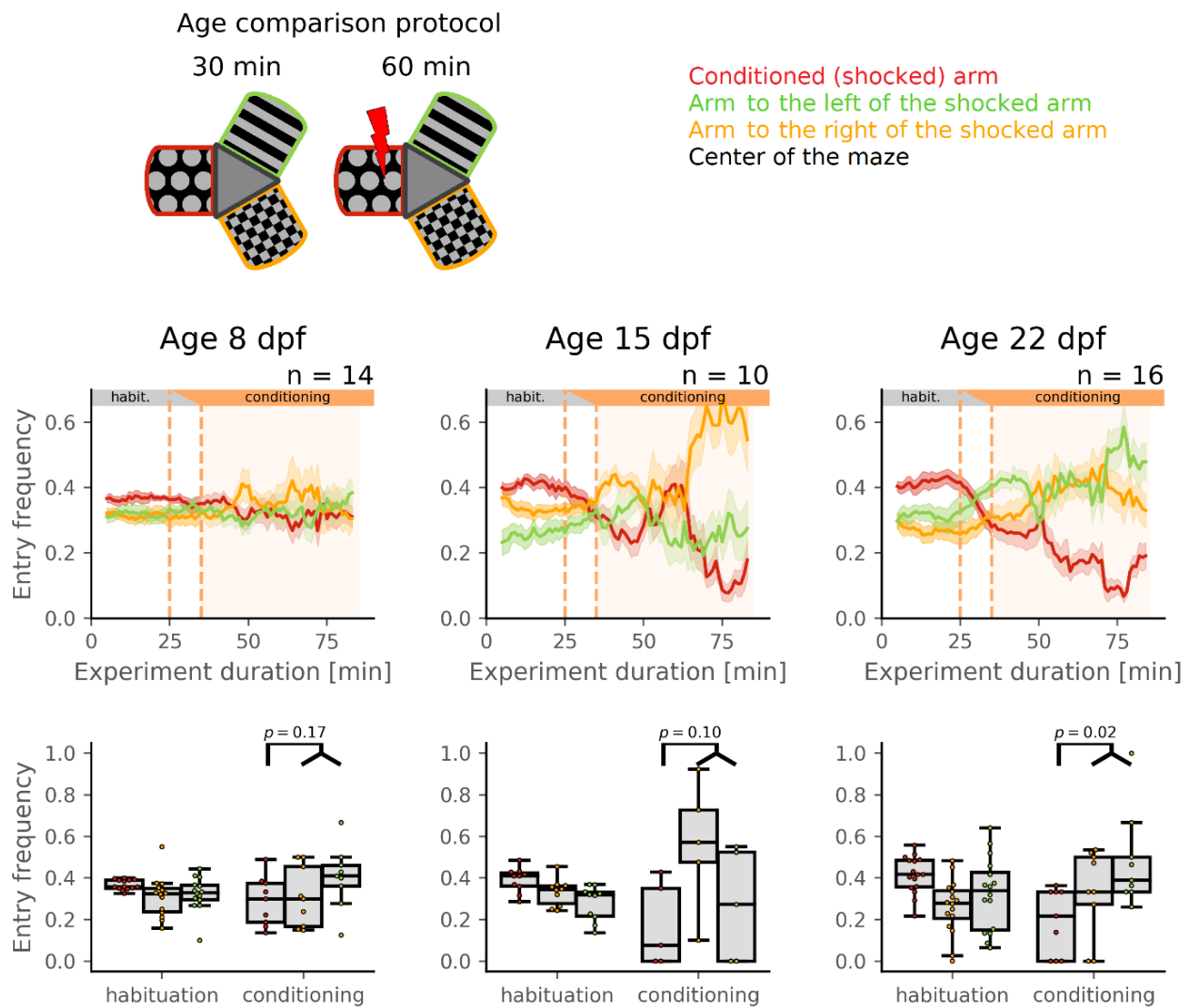


Figure 18. Changes in arm entry frequencies across different age groups.

Top row: schema of the protocol and color legend. Middle row: sliding window curves for arm entry frequency for each age group, averaged across conditioning individual fish, mean \pm s.e.m. Bottom row: quantification of conditioning effects for the last 10 minutes of the habituation session and the last 10 minutes of the conditioning session; individual values are shown in circles. Colors correspond to arms of the maze. Box plots are same as before. The group with 3wo fish shows a significant decrease in the entry frequency of the shocked arm by the end of the conditioning session. Permutation test for last 10 minutes of conditioning: 8 dpf group $n = 14$, p -value = 0.17; 15 dpf group $n = 10$, p -value = 0.1; 22 dpf group $n = 16$, p -value = 0.02.

3.2.2 Changes in occupancy of the shocked arm are similar in all three age groups

Next, changes in the occupancies of the shocked arm between different age groups were compared. In contrast to the results observed in entry frequency, the occupancy of the shocked arm was dramatically reduced at the end of the conditioning for all three age groups (Fig. 19).

Two explanations are appropriate for these results. Either that learning in the CPA paradigm manifests differently in the two metrics or, alternatively, that fish react to shocks by performing swim bouts of increased amplitude (see also Chapter 3.4). Such a reaction could lead to a faster escape from the shocked arm even in the absence of any memory, and consequently to a lower occupancy of the shocked arm. To test this hypothesis, I developed a pseudo-random walk model, in which the simulated fish did not show any learning, but reacted to electric shocks by increasing the amplitude of its swim bouts (see Methods, No-learning model).

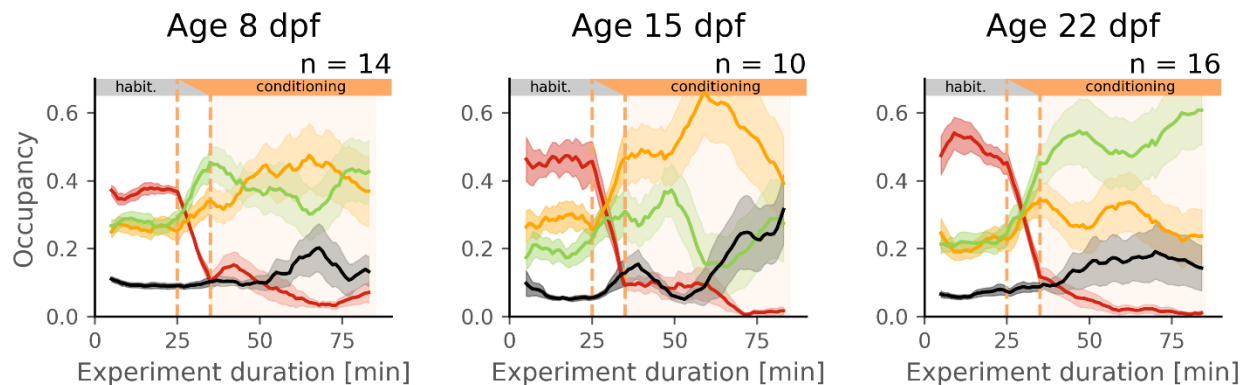


Figure 19. Changes in arm occupancies across different age groups.

The occupancy of the shocked arm dramatically decreases in all age groups. Colors are same as in Figure 18.

3.2.3 Pseudo-random walk model explains some, but not all results of CPA

In order to test if the observed decrease in the occupancy of the shocked arm can be explained by reactions to shocks alone (with no learning involved), an experimental simulation was run using a “no-learning” model. The simulated maze consisted of three arms and a central compartment (Fig. 20). The simulated fish moved in the maze with a step of size S . It could exit from any arm into

the central compartment, and from the central compartment it could enter any of the arms with equal probability $p_{\text{entry}} = \frac{1}{3}$. During the simulated ‘conditioning’ session, the fish moved faster in the shocked arm of the maze than in the other two arms to mimic reactions to electric shock. The speed in the shocked arm was increased by multiplying the ‘normal’ step size by a factor α .

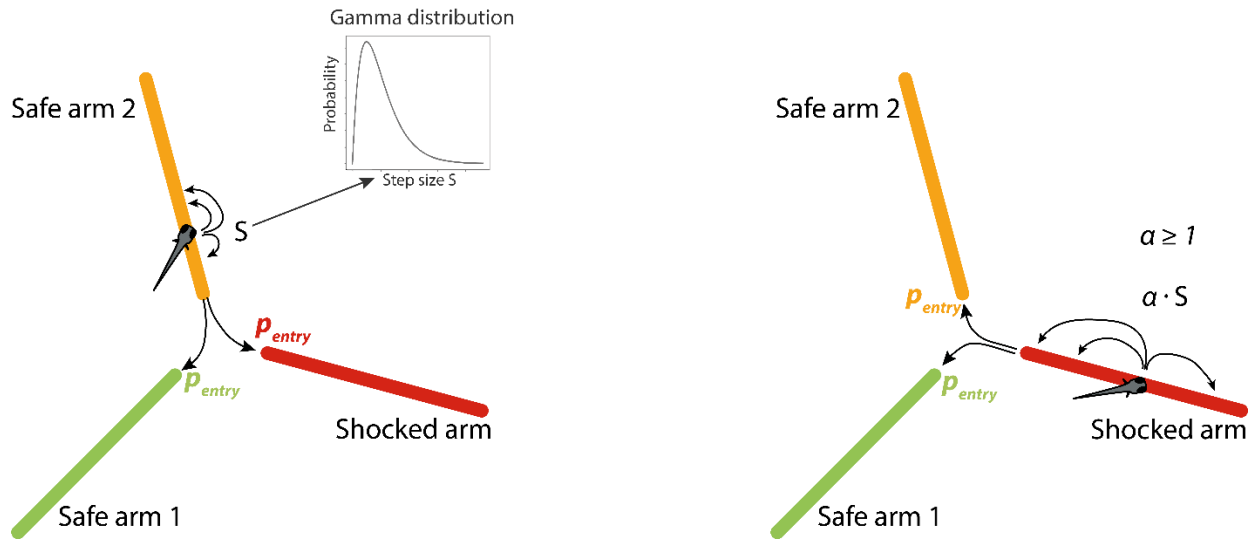


Figure 20. Schematic of the “no-learning” model.

Left: the fish moves in the non-shocked arm of the maze with discrete steps of size S , step size S is drawn from a Gamma distribution (inset, see Methods). Right: the fish moves with larger steps in the ‘shocked’ arm (red, here step size is $\alpha \cdot S$, $\alpha \geq 1$); all arms have the same probability of entry (p_{entry}).

Results of the simulation indicate that the occupancy of the ‘shocked’ arm can indeed decrease as a simple consequence of increased swim speed in the shocked arm (Fig. 21). However, the entry frequency of the shocked arm does not decrease dramatically in the simulation. These results suggest that only the entry frequency dynamics are useful as a metric for the selection of the age group during conditioning sessions: lowered occupancy of the shocked arm may simply be an artifact of the fish’s response to electric shock.

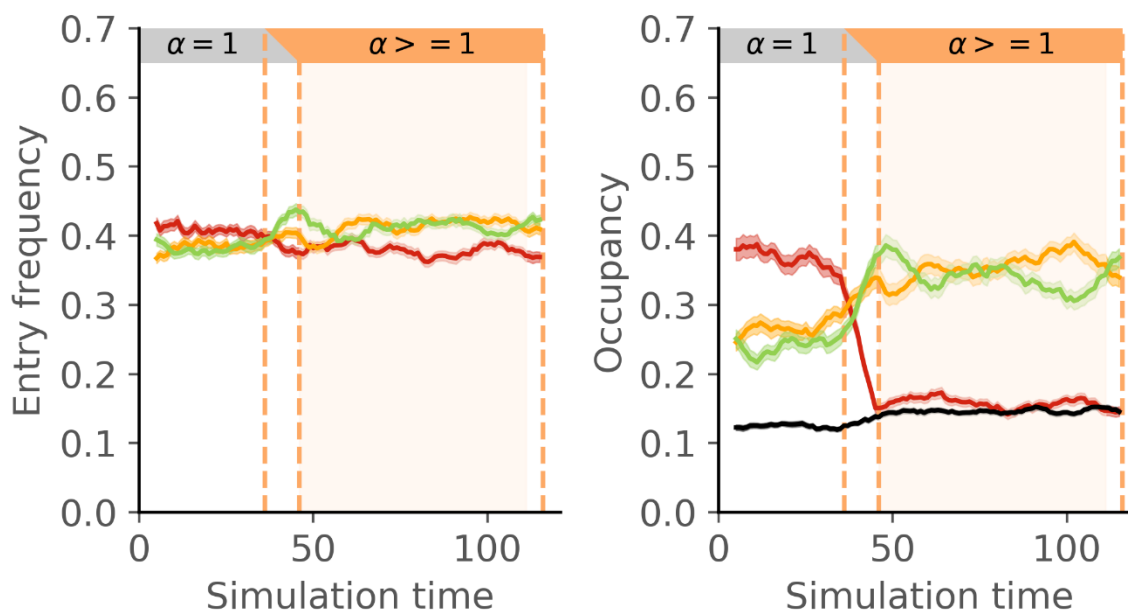


Figure 21. Sliding window curves for simulated trajectories of the fish in no-learning conditions.

Left: entry frequency of the shocked arm does not decrease greatly in the simulation. Right: occupancy of the shocked arm decreases dramatically in the simulation due to the increased speed of the fish's swim bouts in the shocked arm. Color scheme corresponds to the model schematic in Figure 20. Parameters: 15,000 simulation steps (5,000 steps for 'habituation', 10,000 steps for 'conditioning'), sample size = 100 simulations, speed factor $\alpha = 2$.

Based on the changes of entry frequencies of the shocked arm, it can be concluded that zebrafish start showing a robust response to conditioning starting from the age of 3 weeks. Thus, 3wo fish were used in all further experiments.

3.3 Experimental and modeling results suggest that 3-week-old zebrafish can form aversive memories

3wo fish showed a robust response to conditioning. In particular, they showed a decrease in the occupancy of the shocked arm, which was an indication of their responsiveness to aversive stimuli. Additionally, the fish showed a decrease in entry frequency of the shocked arm, which could not be explained by increased swim speed in response to shock application alone, and suggested that the fish were learning to avoid the conditioned arm.

Further experiments with 3wo zebrafish were needed to investigate if the aversion of the shocked arm had any lasting effects after the conditioning period.

3.3.1 Expanding the behavioral paradigm

To further investigate performance of 3wo fish in the CPA paradigm, the protocol was extended to include a 30-minute test session after the conditioning, during which visual patterns stayed the same but no electric shocks were administered (Fig. 23, top left).

In these and further experiments a subgroup of fish learned to stay in the central compartment of the maze as a result of conditioning (Fig. 22). In this type of response the fish learned to avoid all arms, independent of visually distinct patterns. Occupancies of all arms were low for such fish, and entries into the arms were rare. Such fish skewed the distributions of CPA metrics, and were excluded from the analysis (in these and further experiments). The criterion used for the exclusion was the occupancy of the central compartment: all excluded fish stayed in the central compartment for 60% of the conditioning time or longer. The number of excluded fish in each experiment can be found in Appendix 1.

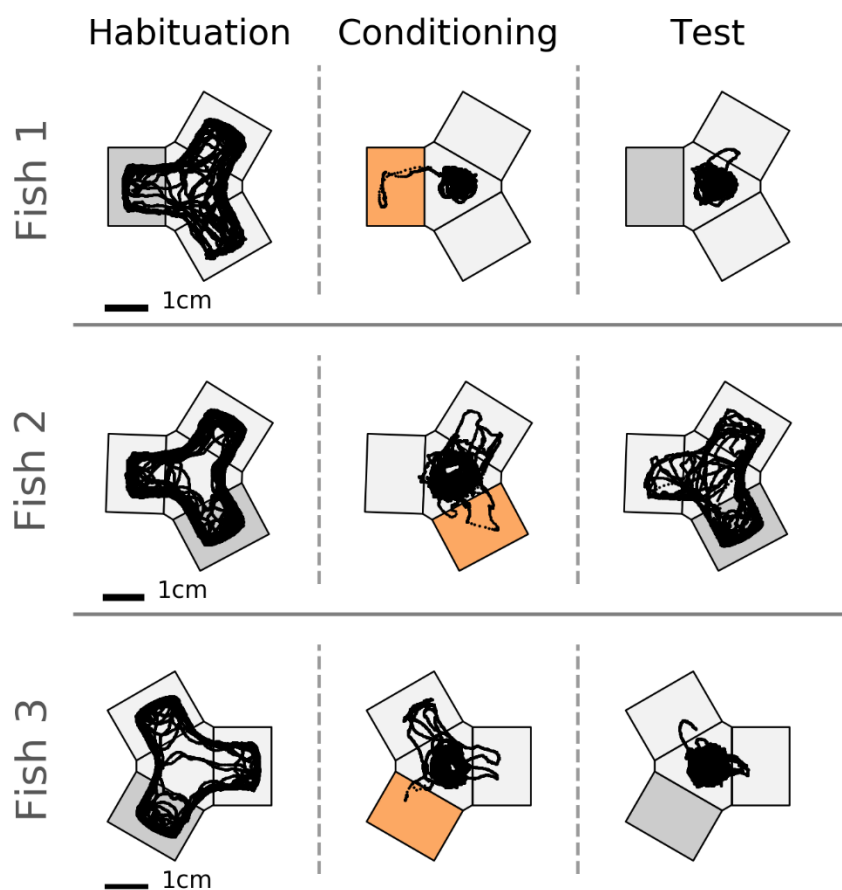


Figure 22. Examples of individual trajectories for fish that responded to conditioning by staying in the center of the maze.

The preferred arm in the habituation session is shown in dark gray, in the conditioning session in orange (when electric shocks were presented), and in the test session in dark gray again (when electric shocks were stopped).

Results of conditioning for the remaining fish ($n = 42$) are shown in Figure 23. Sliding window curves show that both entry frequency and occupancy of the shocked arm were significantly reduced by the end of the conditioning. Moreover, both metrics stayed significantly reduced during the first 10 minutes of the test session (Fig. 23, bottom, Table 14).

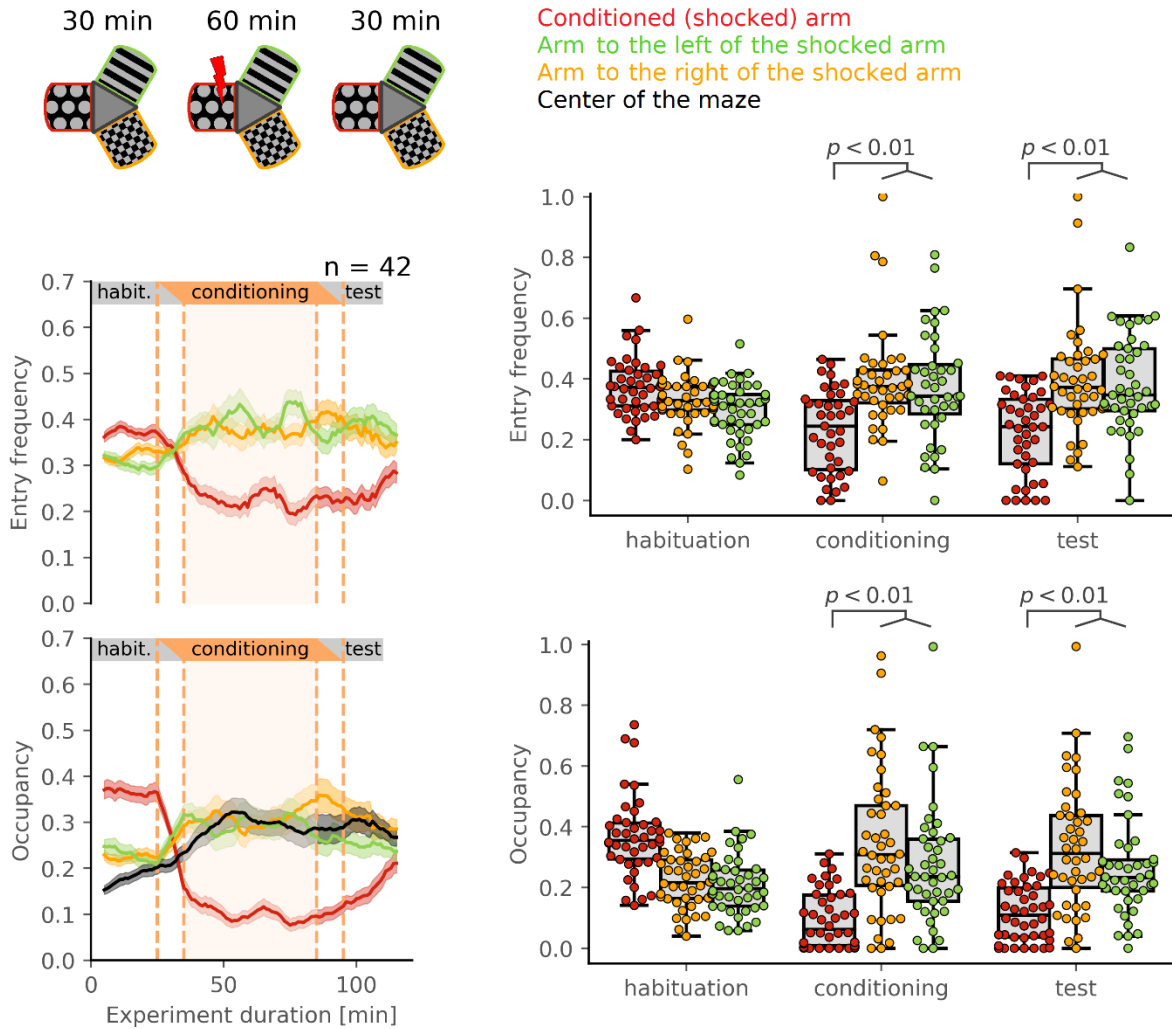


Figure 23. Changes in CPA metrics in conditioning and test sessions.

Top row: a schema of the protocol, with the shocked arm shown in red; here visual pattern locations serve as an example, but they varied across trials for different fish. Left: sliding window curves for entry frequency and occupancy of the shocked arm, colors and plots are same as before. Right: entry frequency and occupancy of the shocked arm stay significantly lower at the end of the conditioning and the beginning of the test session, box plots are same as before. Fish age was between 21 and 25 dpf. Permutation test for the last 10 minutes of conditioning: entry frequency p -value = $7e-06$, occupancy p -value = 0 (beyond the limit of the statistical test, see Methods); permutation test for the first 10 minutes of test: entry frequency p -value = $1e-06$, occupancy p -value = 0 (beyond the limit of the statistical test). n = 42.

Table 14. Arm entry frequency and arm occupancy in the experiments with a test session.Mean \pm s.e.m. b.l.s.t. = beyond the limit of the statistical test (see permutation test in Methods).

	Shocked arm	Safe arm on the left	Safe arm on the right	n	Permutation test p -value
Last 10 minutes of the conditioning session					
Entry freq.	0.23 \pm 0.02	0.39 \pm 0.02	0.37 \pm 0.03	42	7e-06
Occupancy	0.09 \pm 0.01	0.34 \pm 0.03	0.27 \pm 0.03	42	b.l.s.t. (0.0)
First 10 minutes of the test session					
Entry freq.	0.22 \pm 0.02	0.39 \pm 0.03	0.38 \pm 0.02	42	1e-06
Occupancy	0.12 \pm 0.01	0.33 \pm 0.03	0.26 \pm 0.02	42	b.l.s.t. (0.0)

3.3.2 A no-learning model can explain only some aspects of the CPA results

Modeling in Chapter 3.2 showed that the lower occupancy of the shocked arm during the conditioning session can be explained by reactions to shocks, which were unrelated to learning. To check if the lowered occupancy in the test session could be an artifact of the lowered occupancy observed at the end of the conditioning session, the simulation under the no-learning condition was run again, now including the ‘test’ session. The amplitude of the responses to shocks was tested for a possible effect on the results. Specifically, different values of the speed factor α were tested, with higher α -values corresponding to stronger reactions to shocks. Higher α -values produced larger decreases in the occupancy of the shocked arm during the conditioning session, as could be expected. However, sliding window curves show that the lower occupancy of the shocked arm in the beginning of the test session cannot be reproduced by the model (Fig. 24), independent of any chosen α -value tested.

These results suggest that lowered occupancy of the shocked arm during the test session could be an indicator of learning, together with the lowered entry frequency during the conditioning and test sessions.

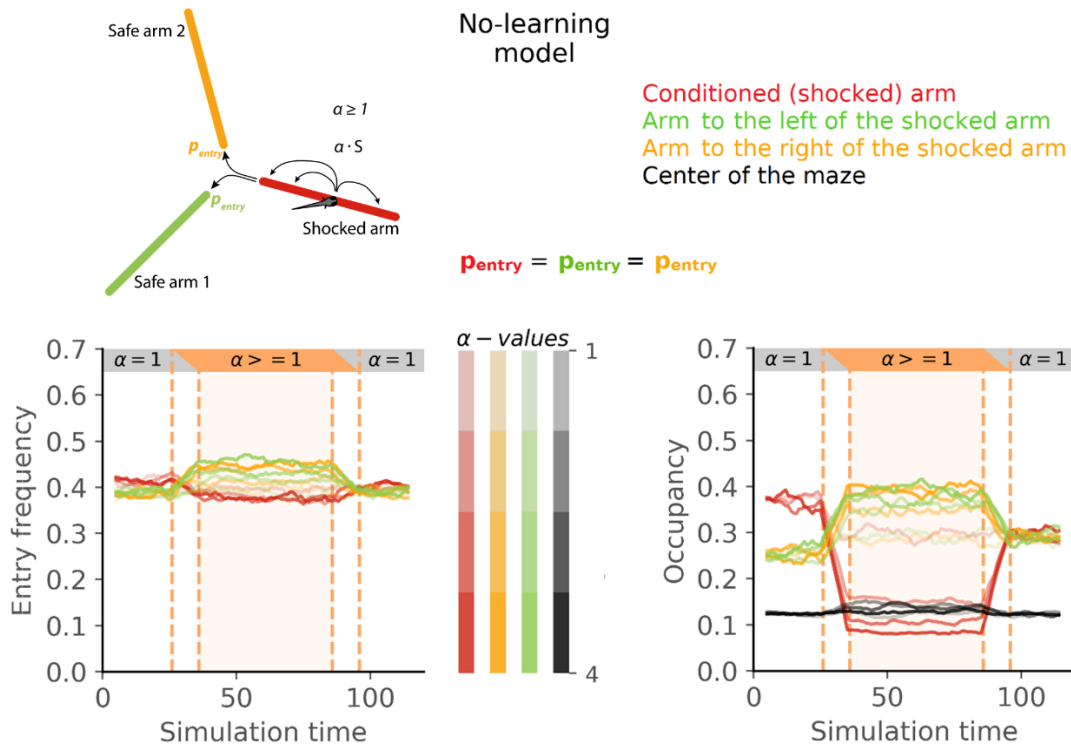


Figure 24. Changes in CPA metrics for simulated trajectories of the fish in no-learning conditions, including a test session.

Top row: model schema and color legend. Bottom row: sliding window curves for entry frequency (left) and occupancy (right) of the simulated arms. Each curve corresponds to the mean of the metric in the corresponding arm across the simulations with a particular α -value. More saturated colors correspond to simulations with higher α -values. Parameters: 20,000 simulation steps (5,000 steps for ‘habituation’, 10,000 steps for ‘conditioning’, 5,000 steps for ‘test’), sample size = 100 simulations, speed factor $\alpha = [1, 2, 3, 4]$.

3.3.3 Modeling with an added learning component can qualitatively reproduce experimental metrics

Modeling with no-learning conditions revealed that the lowered entry frequency of the shocked arm in the conditioning and the test sessions, as well as the lowered occupancy of the shocked arm in the test session, could not be reproduced. To test if these results might be explained by a learning component a learning rule was added to the model in an attempt to match the experimental curves.

The learning rule consisted of setting the probability of entry into the shocked arm as a variable instead of a constant, as it was in the “no-learning” model. Initially, the probability of entry into any arm was the same, i.e. equal to $\frac{1}{3}$. Every entry into the shocked arm during the ‘conditioning’ session caused a decrease in the probability for the next entry into the shocked arm. Every entry into the previously shocked arm during the ‘test’ session caused an increase in the entry probability towards the initial value of $\frac{1}{3}$ (simulating a “relearning” that the previously shocked arm was now free of shock, see Methods). Results of the simulation reproduced the decrease in entry frequency of the shocked arm during the conditioning, and the decrease in occupancy and entry frequency of the shocked arm at the beginning of the test session (Fig. 25).

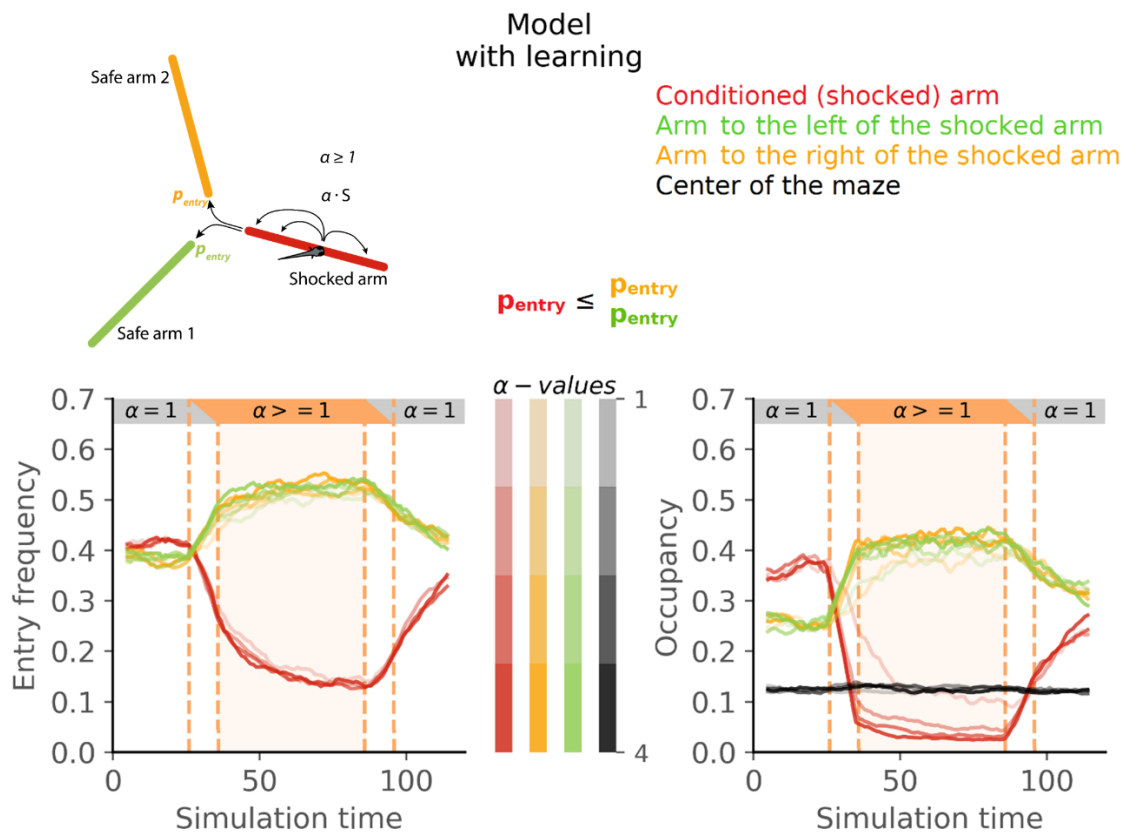


Figure 25. Changes in CPA metrics for simulated trajectories of the fish with an added learning component.

Plots are same as in Fig. 24. More saturated colors correspond to simulations with higher α -values. Parameters: 20,000 simulation steps (5,000 steps for ‘habituation’, 10,000 steps for ‘conditioning’, 5,000 steps for ‘test’), sample size = 100 simulations, speed factor $\alpha = [1, 2, 3, 4]$.

3.3.4 Differentiating between ‘extinction’ and ‘forgetting’ in CPA paradigm

Chapter 3.3.1 demonstrated that aversive response, formed during the conditioning session of the CPA paradigm, persists beyond the cessation of shock application, continuing on average for the first 15 minutes of the test session. Two explanations for the loss of the aversive response in the test session present themselves: forgetting (passive loss) or extinction (in which the fish actively relearns that the previously aversive arm is now safe). To distinguish between these two scenarios a fourth session – a delay between conditioning and test sessions – was introduced, during which visual patterns were replaced with a uniform gray in all arms.

If the fish were experiencing forgetting, the memory would fade as a function of time, independent of the presence of the patterns. When the patterns were redisplayed in their original locations during the test session, the memory would be gone if sufficient time had passed from the end of the conditioning session.

Instead, if the fish experienced extinction, then during the absence of the patterns extinction would be delayed, and after the patterns returned the fish should perform as if the gap was not present, given the memory is intact. This effect should be independent of the gap length.

As the conditioned response was maintained for 15 minutes in the test session, two intermediate durations for the delay session (5 minutes and 10 minutes) were chosen.

During the 5-minute delay, entry frequency and occupancy of the shocked arm returned to chance level (seen as a ‘bump’ in the sliding window curves at the 95th minute of the experiment, Fig. 26, Table 15). Entry frequency and occupancy of the shocked arm decreased again when the patterns were redisplayed in the test session (Fig. 26, Table 15).

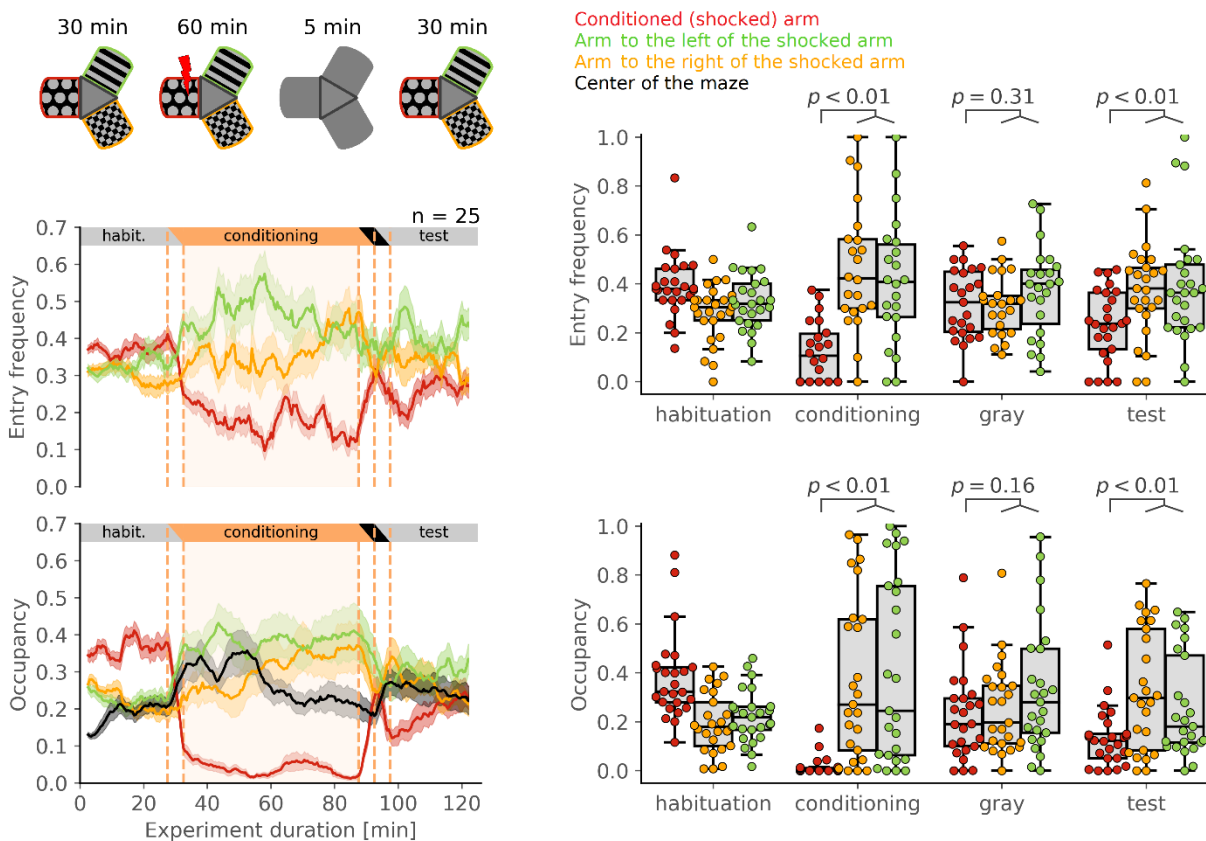


Figure 26. Changes in CPA metrics in experiments with a 5-minute delay before the test session.

The black bar at the top of sliding window plots indicates the delay session. Notice the ‘bump’ in the red sliding window curve at the 95th minute of the experiment, corresponding to the ‘delay’ session when the visual patterns were replaced with a uniform gray screen: both metrics of the shocked arm return to chance level. When the patterns were re-presented in the test session, the metrics for the shocked arm decreased again for the next 10 minutes. In this plot a 5-minute sliding window with a 30-second step was used to avoid ‘smoothing-out’ the short 5-minute ‘delay’ session. Box plots are the same as before. Fish age was between 20 and 24 dpf. Permutation test for 5 minutes of delay: entry frequency p -value = 0.31, occupancy p -value = 0.16; permutation test for the first 5 minutes of test: entry frequency p -value = 0.004, occupancy p -value = 0.001. $n = 25$.

Table 15. Arm entry frequency and arm occupancy in experiments with a 5-minute delay before the test session.

Mean \pm s.e.m.

	Shocked arm	Safe arm on the left	Safe arm on the right	n	Permutation test p -value
5 minutes of the delay session (all arms with gray background)					
Entry freq.	0.32 \pm 0.03	0.31 \pm 0.02	0.37 \pm 0.04	25	0.31
Occupancy	0.23 \pm 0.04	0.25 \pm 0.04	0.33 \pm 0.05	25	0.16
First 5 minutes of the test session					
Entry freq.	0.23 \pm 0.03	0.37 \pm 0.04	0.39 \pm 0.05	25	0.004
Occupancy	0.13 \pm 0.02	0.33 \pm 0.05	0.26 \pm 0.04	25	0.001

During the 10-minute delay, entry frequency of the shocked arm also returned to chance level, while occupancy moved closer to chance level (97th minute of the experiment, Fig 27, Table 16). Both occupancy and entry frequency of the shocked arm decreased again in the test session, when the visual patterns were displayed again. However, the effects were smaller and the metrics were closer to chance level than in experiments performed with the 5-minute delay (Fig. 27, Table 16).

This analysis indicates that passive forgetting occurs during the delay session. The effect of conditioning, still strong after the 5-minute delay session, became weaker after the 10-minute delay session, independent of the presence of visual patterns. However, extinction of the conditioned response cannot be excluded by these results, as extinction and passive forgetting could be happening concomitantly.

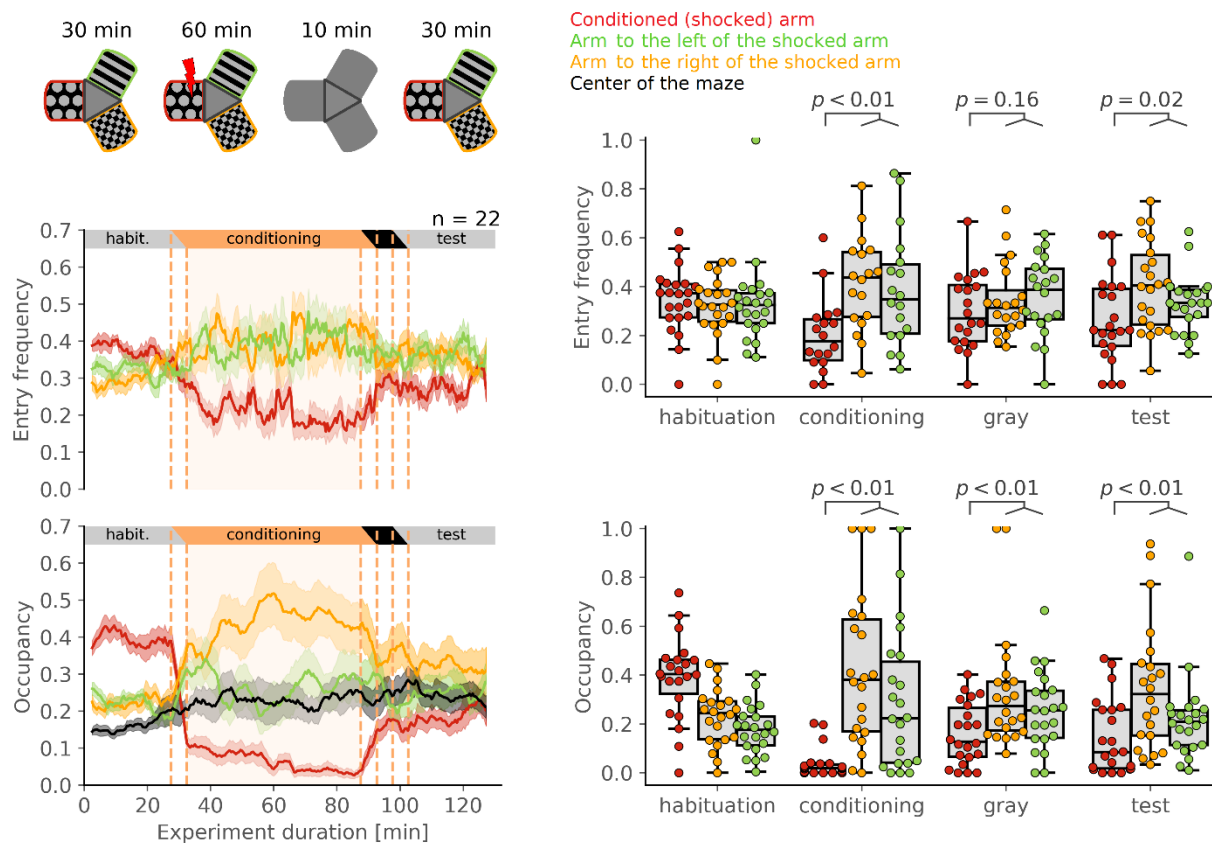


Figure 27. Changes in CPA metrics in experiments with a 10-minute delay before the test session.

The black bar at the top of sliding window plots indicates the delay session. In this plot a 5-minute sliding window with a 30-second sliding step was used to avoid ‘smoothing-out’ the short 10-minute ‘delay’ session effect. Panels are similar to the ones in Fig. 26. Fish age was between 19 and 24 dpf. Permutation test for 5 minutes from delay session: entry frequency p -value = 0.16, occupancy p -value = 0.03; permutation test for the first 5 minutes of test: entry frequency p -value = 0.02, occupancy p -value = 0.009. $n = 22$.

Table 16. Arm entry frequency and arm occupancy in experiments with a 10-minute delay before the test session.Mean \pm s.e.m.

	Shocked arm	Safe arm on the left	Safe arm on the right	n	Permutation test <i>p</i> -value
5 minutes from the middle of the delay session (all arms with gray background)					
Entry freq.	0.30 \pm 0.03	0.34 \pm 0.05	0.36 \pm 0.03	22	0.16
Occupancy	0.16 \pm 0.01	0.33 \pm 0.03	0.25 \pm 0.02	22	0.003
First 5 minutes of the test session					
Entry freq.	0.26 \pm 0.03	0.40 \pm 0.06	0.33 \pm 0.04	22	0.02
Occupancy	0.15 \pm 0.02	0.35 \pm 0.05	0.22 \pm 0.04	22	0.009

Based on the results in the Chapter 3.3, it can be concluded that 3-week-old zebrafish are capable of forming an aversive memory in our Y-maze paradigm. The memory lasts at least 10 minutes after the end of conditioning, during which the fish gradually forget the aversive location.

3.4 Distinct types of responses of zebrafish to electric shock

In the experiments described in Chapters 3.2 and 3.3, a great variability in responses to conditioning by electric shocks was observed. This variability was present between different fish as well as within an individual's performance. Some fish reacted to shocks strongly by avoiding the shocked maze arm consistently during conditioning and test sessions (Fig. 28, left), while other fish did not exhibit lowered occupancy of the shocked arm even during the conditioning session (in contrast to predictions by modeling in Chapters 3.2 and 3.3, Fig. 28, middle). Some fish responded to the shocks for a part of the conditioning session and then stopped (Fig. 28, right). In addition, fish reacted to shocks with different swim bout amplitudes even though the intensity of the electric shock was always the same. This raised the question of whether different responses to shocks could be linked to variability in performance observed throughout the behavioral paradigm.

It has been previously shown that mild electric shocks cause stereotyped escape-like responses in fish (Tabor et al., 2014). The same study observed other response types of higher variability, when stronger electric pulses were applied. This response diversity matched observations in the experiments described in this dissertation, and called for a further investigation of response variability and its connection to aversive learning.

Thus, individual responses of fish to individual shock pulses were analyzed for specific reactions to shock that correlated with learning.

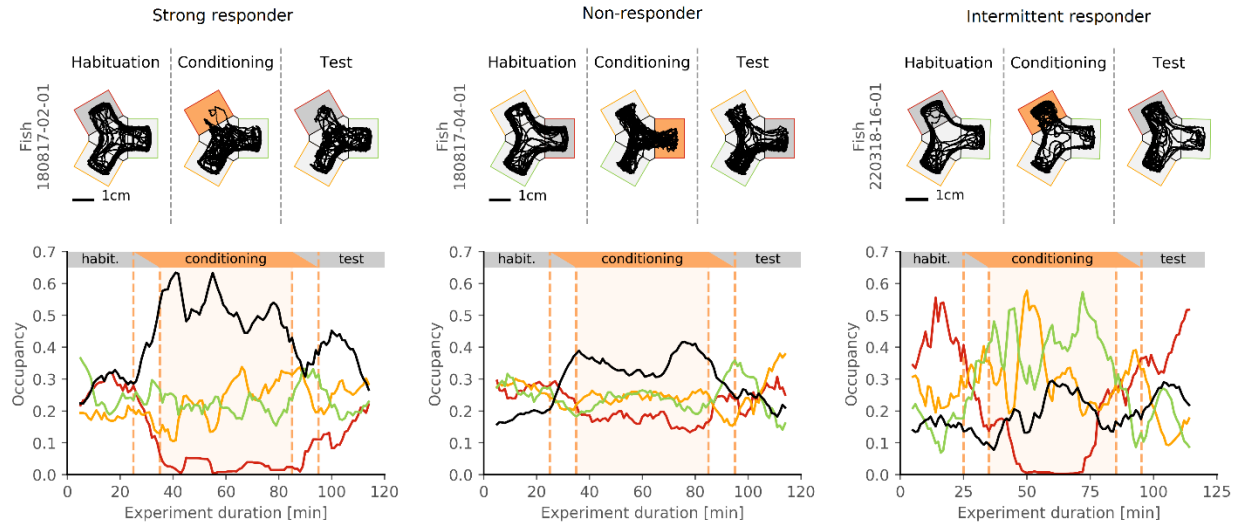


Figure 28. Variability in performance in the CPA paradigm.

Left column: a fish that responded strongly to shocks during conditioning and test sessions (‘strong responder’, age 19 dpf). Middle column: a ‘non-responder’ fish, the occupancy of the shocked arm did not decrease during conditioning (age 19 dpf). Right column: a fish that responded to shocks only in the first half of the conditioning session (‘intermittent responder’, age 24 dpf). Each column shows the fish trajectory at the top and the corresponding sliding window curve for maze arm occupancies at the bottom. The trajectories show the last 10 minutes of habituation, the last 10 minutes of conditioning, and the first 10 minutes of test.

3.4.1 Characterization of responses to electric shock

Fish typically spent 5.8 ± 8.3 seconds in the shocked arm (mean \pm SD), during which they received an electric shock every second (data from fish with age between 20 and 26 dpf). Electric shocks triggered swim bouts, and each bout could be represented by a displacement curve (Fig. 29). Shock duration varied between 50 and 100 ms, depending on the experiment.

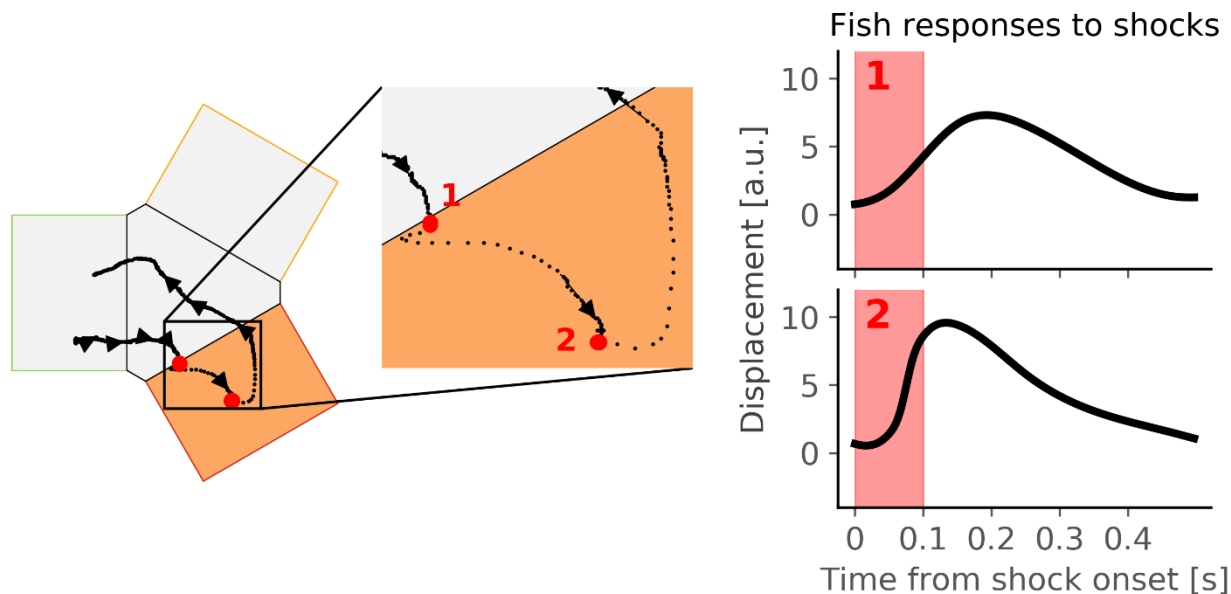


Figure 29. Typical responses to electric shocks of a fish.

Left: fish trajectory with an entry into the shocked arm. Arrows indicate the movement direction of the fish; the fish experienced two electric shocks before leaving the shocked arm. The time points when the fish received electric shocks are shown with red circles. Right: displacement curves during the shock-triggered swim bouts, corresponding to the trajectory on the left. Red vertical bars indicate the duration of the electric pulse (100 ms). Fish age was 26 dpf.

Swim bout occurrences were inferred from the displacement curves of the fish by using a combination of smoothing and low-pass filtering (see Methods). Swim bout sizes were estimated by calculating the area under the displacement curves. Swim bouts triggered by electric shocks were larger on average than bouts observed during spontaneous swimming (Fig. 30).

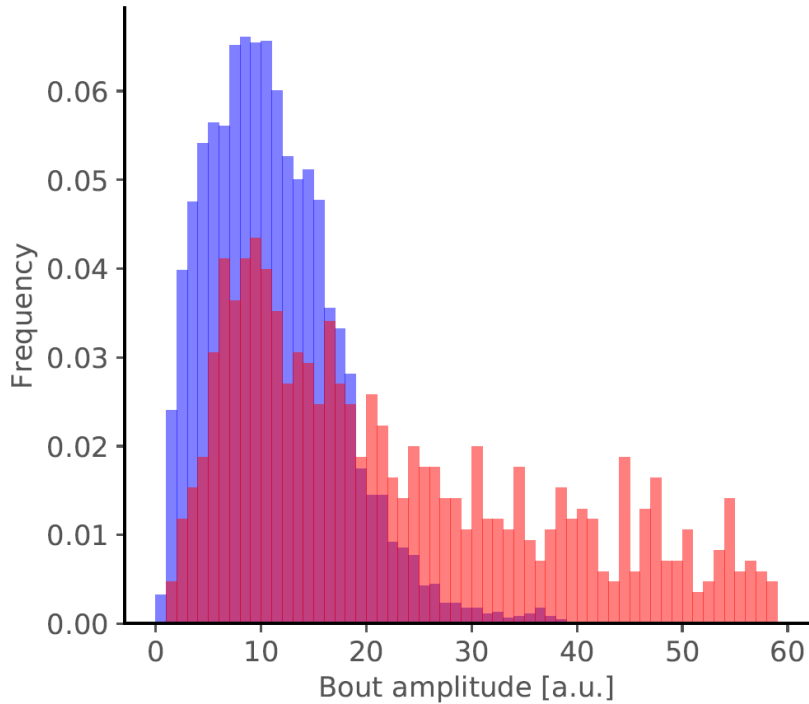


Figure 30. Comparison of distributions of swim bout amplitudes: spontaneous vs. triggered by shocks.

Distribution for spontaneous swim bout amplitudes is shown in blue; for shock-triggered swim bouts – in red. The distribution of amplitudes of shock-triggered swim bouts is skewed to higher values. Fish age was between 20 and 26 dpf.

It has been observed that fish react to electric shocks more strongly when their body axis is oriented parallel to the electric field (Tabor et al., 2014). In the experiments described in this dissertation the electric field ran from one sidewall of the maze arm to the other sidewall. Fish were oriented parallel to the electric field when facing the sidewalls of the arms (90° or 270° orientation), and perpendicular to the electric field when facing the arm ends or arm openings (0° or 180° orientation, Fig. 31).

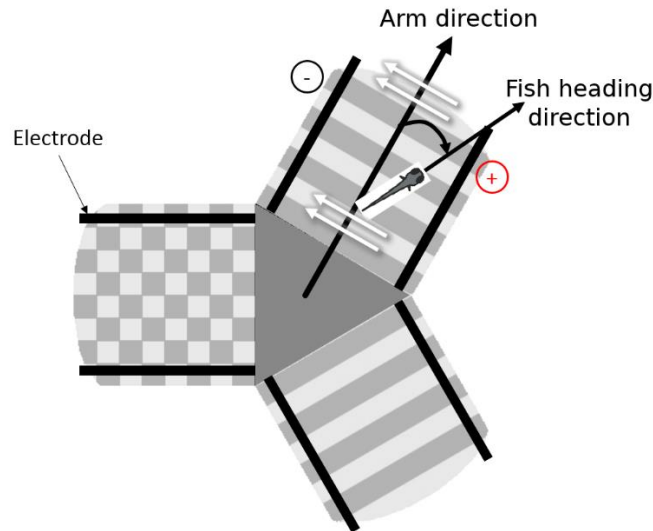


Figure 31. Schema for calculation of fish orientation in the maze arm.

Electrodes were located at the sidewalls of the arms. The electric field ran from one sidewall to the other; the direction is depicted with white arrows. Fish orientation was calculated as the angle between arm direction and fish heading direction.

Amplitudes of shock-triggered swim bouts were significantly higher when fish were oriented parallel to the electric field (i.e. towards the electrodes), in agreement with previous observations (Fig. 32 left and middle, compare black to gray, t-test p -value = $3 \cdot 10^{-10}$). Moreover, reactions to electric shocks in orientation towards the cathode were stronger than in orientation to the anode (Fig. 32 middle, compare black bars, t-test p -value = 0.004). In addition, fish reacted stronger when oriented into the arm than when oriented out of the arm (Fig. 32 middle, compare gray bars, t-test p -value = 0.003).

Sometimes electric shocks did not elicit any response from a fish (a non-response), suggesting that those shocks could be not effective for conditioning. In the cases of perpendicular orientation to the electric field, the proportion of non-responses to response swim bouts was much higher than for parallel orientation (Fig. 32 right, compare the two black and two gray bars). This could explain why the total number of shocks for perpendicular orientation was much higher than for parallel orientation (Fig. 32 right, compare gray to black): stronger reactions in parallel orientation led to a change in the fish's orientation; non-responses in perpendicular orientation allowed the fish to stay longer in the same orientation and thus produce more non-responses.

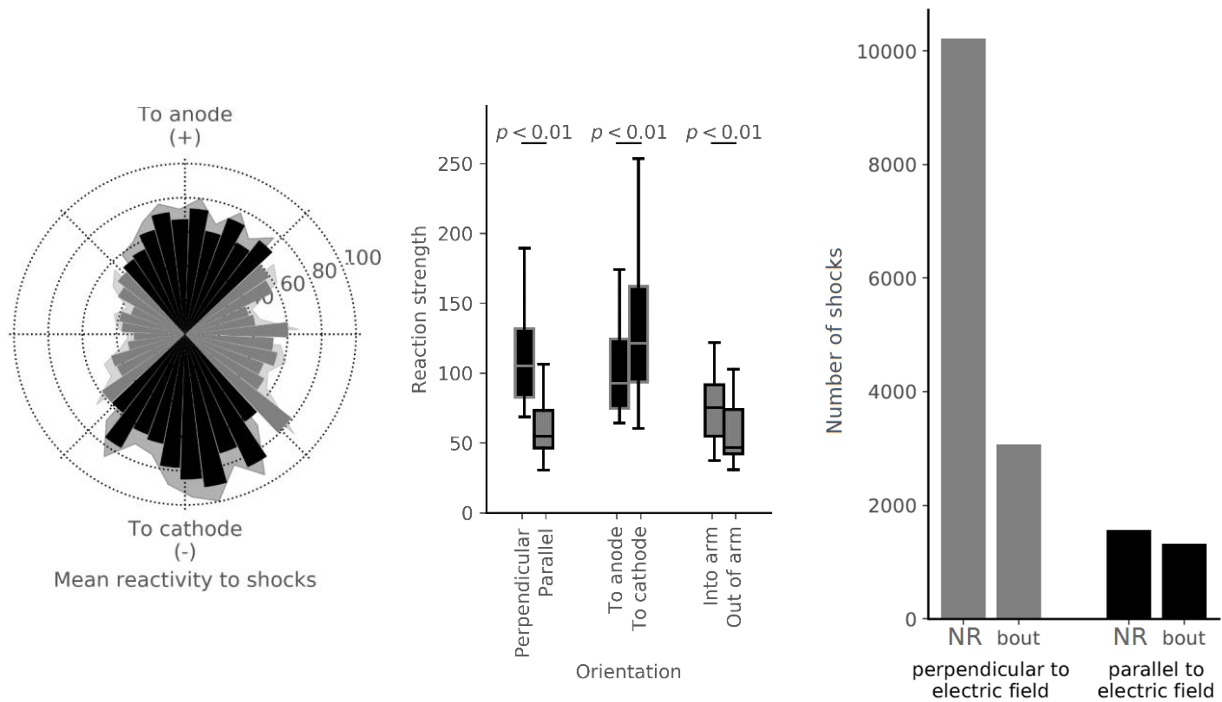


Figure 32. Strength of shock responses depends on the orientation of the fish in the electric field.

Left: amplitude of shock-triggered swim bouts as a function of fish orientation in the electric field. The bars in the polar plot show mean + s.e.m. of shock-triggered swim bout amplitude for each polar bin. Middle: quantification of differences in reaction strength dependent on orientation of the fish. T-test: parallel vs perpendicular p -value = $3e-10$; anode vs cathode p -value = 0.004; into the arm vs out of the arm p -value = 0.003. Boxplots are the same as earlier. Right: numbers of non-responses (NR) and shock-triggered responses (bout) for parallel and perpendicular orientations in the electric field. The proportion of non-responses to bouts for a perpendicular orientation is much higher than for parallel orientation. Parallel orientation is shown in black, covering angles in intervals $[45^\circ, 135^\circ]$ and $[225^\circ, 315^\circ]$. Fish age was between 20 and 26 dpf.

3.4.2 Response types and their correlation with learning

Plotting all responses to shocks ($n = 4,385$ for shock-triggered swim bouts, non-responses were excluded ($n = 11,766$)) revealed structure in the response dynamics: there were different amplitudes, onset times, and rise times in swim bouts occurring in response to electric shock presentation (Fig. 33). Responses were separated into different types by performing hierarchical clustering (see Methods). Five response types were further characterized.

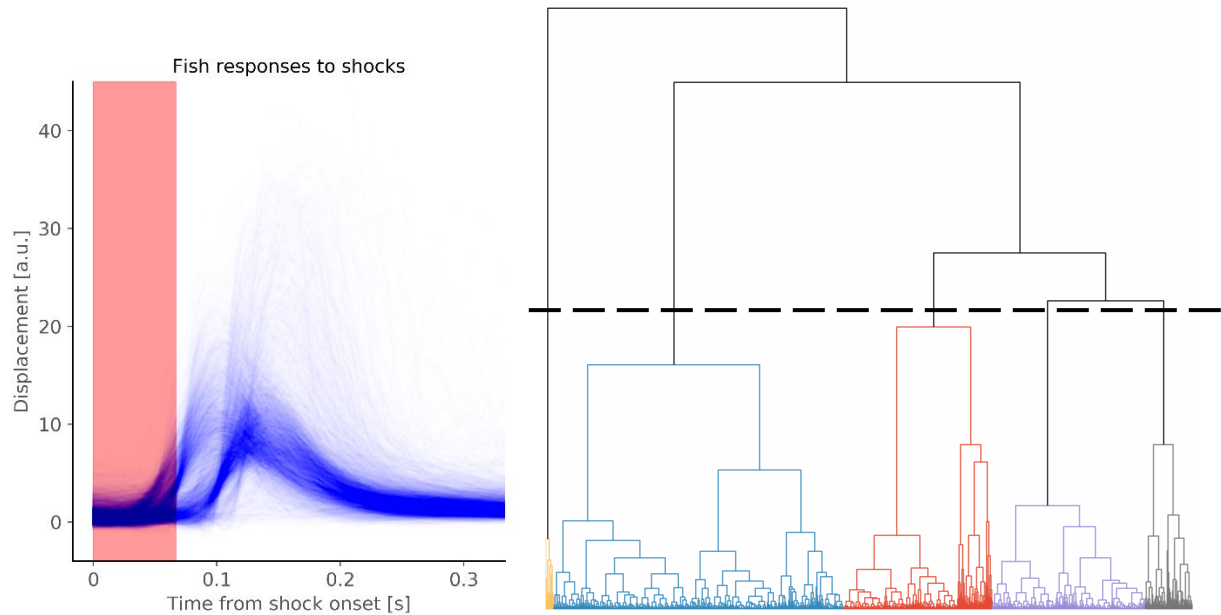


Figure 33. Separation of shock responses into types.

Left: variety of amplitudes and time dynamics of individual responses to electric shocks, plotted as displacement over time. The red vertical bar indicates the duration of the electric pulse. Right: clustering tree with the cut-off line for the clusters. Fish age was between 20 and 26 dpf.

The first large ‘long rise time’ group of responses consisted of low-amplitude (LA) swim bouts, which had a comparatively long rise time and duration ($n = 1,004$, Fig. 34, top row, red). These responses were triggered when the fish was oriented mostly towards the negatively charged electrode (the cathode).

The second large ‘early onset’ group of responses consisted of LA swim bouts with a shorter duration and rise time than group 1 ($n = 1,966$, Fig. 34, second row, blue). These swim bouts were triggered by shock onset, almost exclusively when the fish was oriented towards the positively charged electrode (the anode).

The third ‘late onset’ group consisted of LA swim bouts, which were triggered by shock offset ($n = 1,035$). This response type was very similar to the second group in the rise time of the response. However, in contrast to the second group, these responses were triggered when the fish was oriented towards the cathode (Fig. 34, third row, violet).

The fourth ‘high amplitude’ group consisted of high amplitude (HA) swim bouts, triggered by shock offset ($n = 320$, Fig. 34, fourth row, gray). These swim bouts occurred when the fish was oriented towards the cathode. This group contained a smaller number of swim bouts compared to the first three groups.

Finally, the fifth ‘noise’ group contained very few swim bouts, with bouts resembling noise ($n = 60$). These swim bouts were probably occurring independently of the shocks and may represent spontaneous movements (Fig. 34, bottom row, yellow). These bouts were excluded from further analysis.

In order to test if the efficiency of conditioning correlated with the response types, the CPA metrics (arm occupancy and arm entry frequency), evaluated immediately after the shocks, were examined for correlations with the type of shock response. For every response type, the 10-minute time interval after each individual shock was evaluated and the occupancy/entry frequency of the shocked arm in these time intervals for each response type calculated. Finally, averaged metrics for each response type were compared to each other (Fig. 35).

To exclude fish that froze, only time intervals during which at least three arm transitions happened were included in analysis. Occupancy and entry frequency of the shocked arm differed significantly between the swim bout types (Table 17).

Table 17. Occupancy and entry frequency of the shocked arm in the 10-minute interval immediately after a shock-triggered bout for different swim bout types.

Mean \pm SD.

	Bout type 1	Bout type 2	Bout type 3	Bout type 4	One-way ANOVA	
					F	<i>p</i> -value
Occupancy	0.18 \pm 0.14	0.17 \pm 0.14	0.18 \pm 0.14	0.13 \pm 0.15	11.29	2e-07
Entry freq.	0.28 \pm 0.12	0.29 \pm 0.12	0.29 \pm 0.11	0.24 \pm 0.13	19.49	2e-12

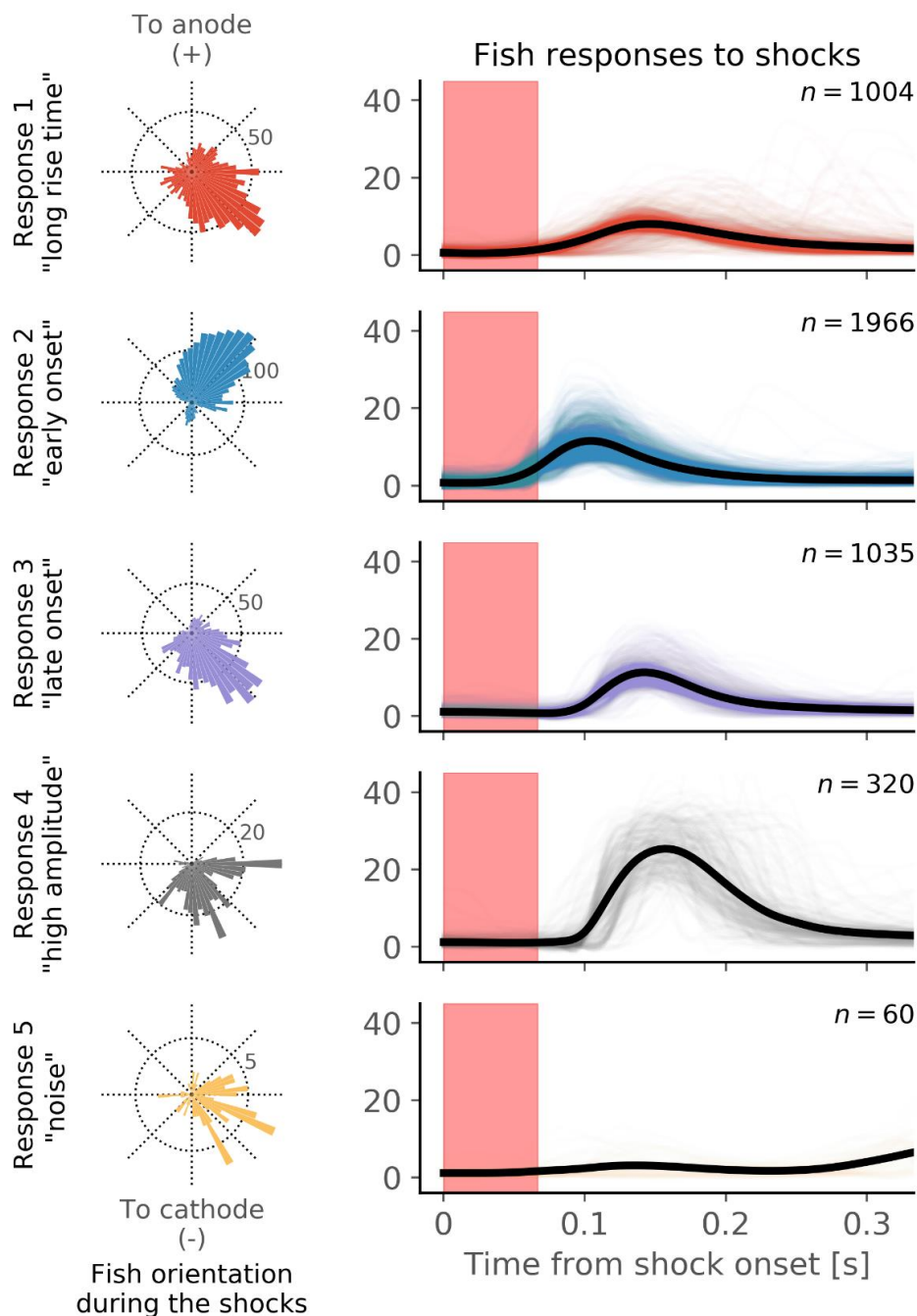


Figure 34. Features of identified response types.

Left: number of swim bout occurrences as a function of orientation of the fish in the electric field. The scaling of the radial axis is indicated by the number at 45°. Right: displacement of the fish as a function of time (i.e. 'bout shape'). Individual swim bout shapes are plotted in a transparent color, while the average for the swim bout type is plotted with a thick black line. Red vertical bar indicates the duration of the electric pulse. Fish age was between 20 and 26 dpf.

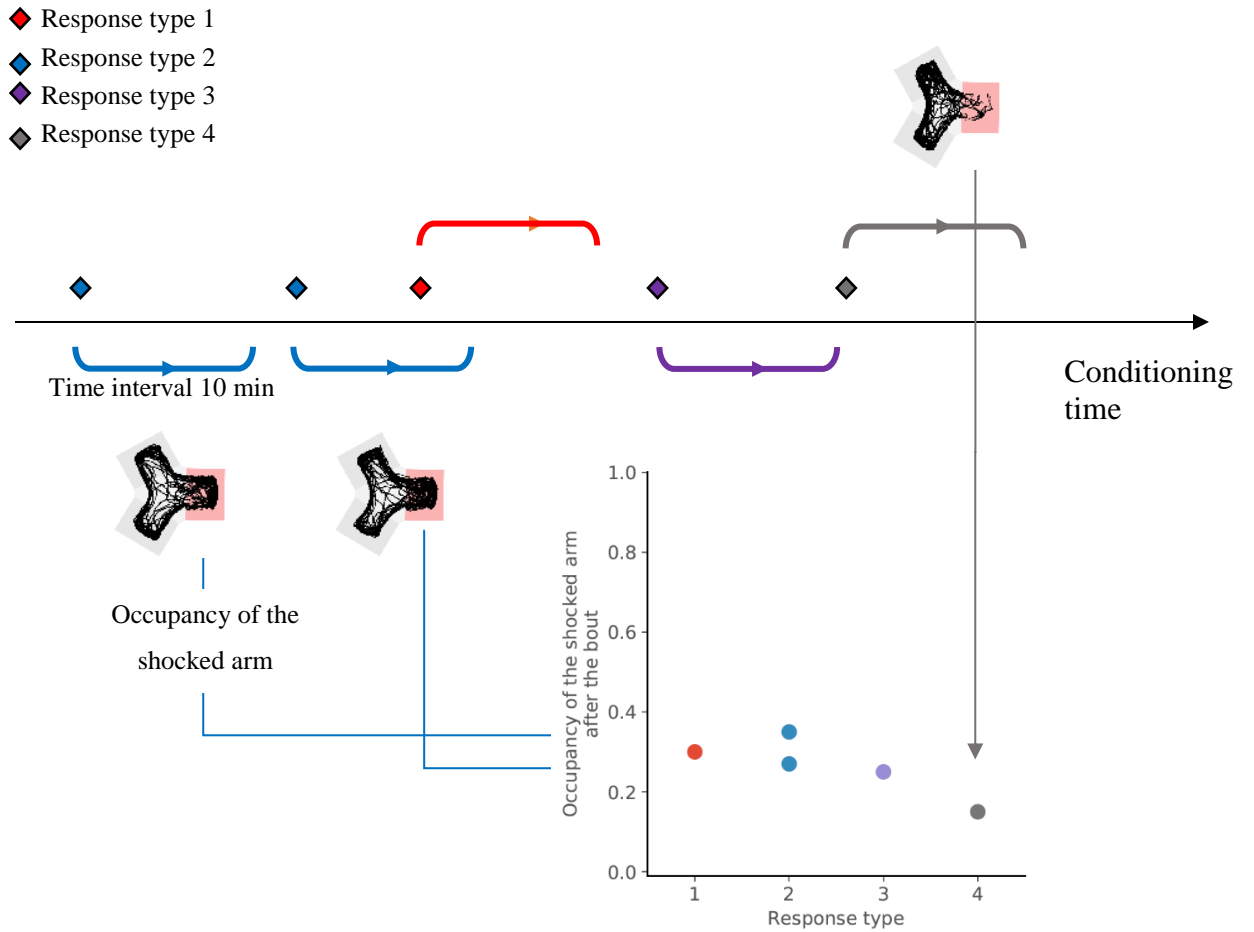


Figure 35. A toy example for calculation of conditioning efficiency after different swim bout types in a 10-minute time interval.

Top axis: an example sequence of shock-triggered swim bouts, indicated with diamonds; different colors correspond to different swim bout types; curved line after each swim bout corresponds to a 10-minute time interval immediately after the swim bout, during which the occupancy/entry frequency of the shocked arm is considered. Bottom: the metrics are grouped by response type and averaged.

Post-hoc pairwise comparison with a Bonferroni correction revealed that both occupancy and entry frequency of the shocked arm was significantly lower in the 10-minute interval after the shock administration for response type 4 (HA responses, Fig. 36, Table 18). Moreover, this result did not change for other time intervals (up to 50 minutes long, Fig. 37).

The lower occupancy of the shocked arm after the HA swim bouts can be explained by the fact the HA swim bouts make it more likely that the fish leaves the shocked arm quicker and ends up in a different arm of the maze. However, the lower entry frequency of the shocked arm after the HA swim bouts cannot be explained this way. Based on the properties of the response types it can be concluded that HA swim bouts were correlated with an increased aversive response.

Table 18. Post-hoc pairwise comparisons of the occupancy and entry frequency of the shocked arm immediately after the shock for different response types.

Each cell contains an uncorrected t-test p -value for a pair of response types. There were six comparisons, so results were considered significant at level $0.05/6 = 0.008$ and lower. Significant p -values after correction are shown in red.

Occupancy of the shocked arm					Entry frequency of the shocked arm				
Response type	1	2	3	4	Response type	1	2	3	4
1		0.38	0.45	9e-07	1		0.06	0.02	6e-08
2			0.07	8e-07	2			0.46	3e-12
3				2e-08	3				2e-12
4					4				

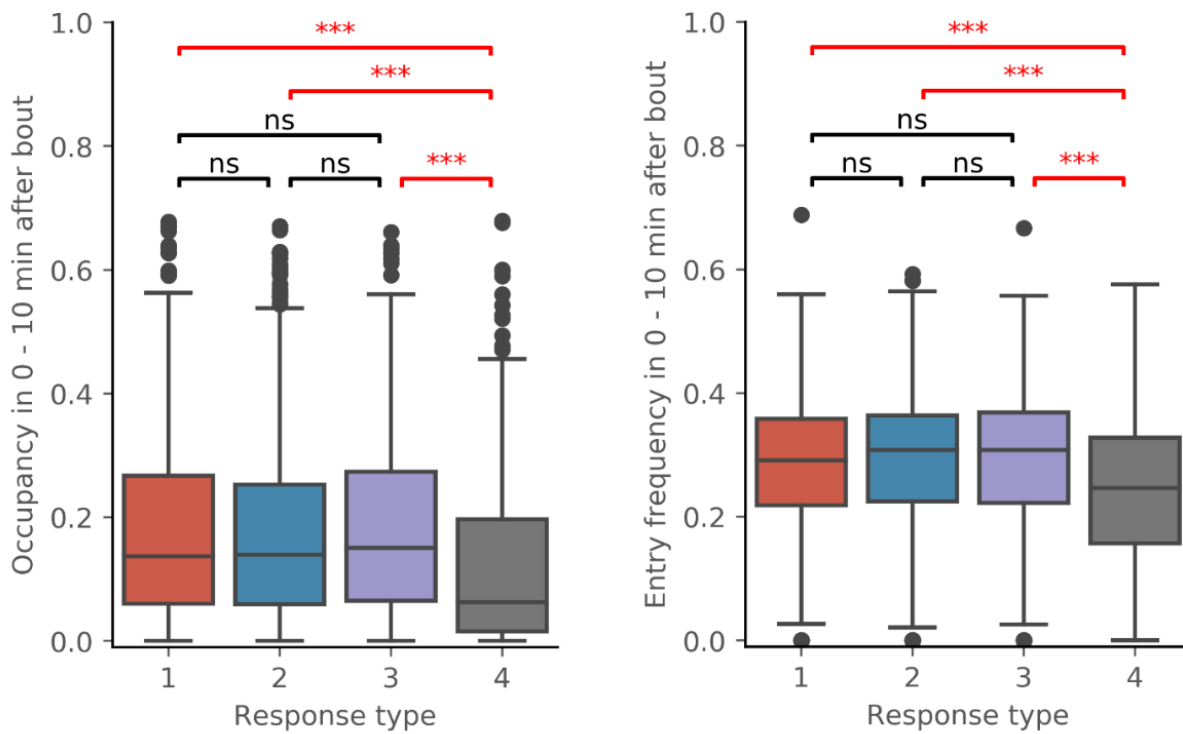


Figure 36. The shocked arm is avoided more strongly after swim bouts with high amplitude than after swim bouts of other response types.

Left: occupancy of the shocked arm in the interval [0, 10] minutes after the swim bout; Right: entry frequency of the shocked arm in the interval [0, 10] minutes after the swim bout. Colors correspond to Fig. 33 and 34. Boxplots are the same as earlier. Fish age was between 20 and 26 dpf. Post-hoc pairwise t-test with Bonferroni correction: difference in occupancy of the shocked arm for response type 4 against response types 1, 2, and 3 has p -value of $9e-07$, $8e-07$, and $2e-08$; difference in entry frequency of the shocked arm for response type 4 against response types 1, 2, and 3 has p -value of $6e-08$, $3e-12$, and $2e-12$. ns – not significant, *** - p -value < 0.01

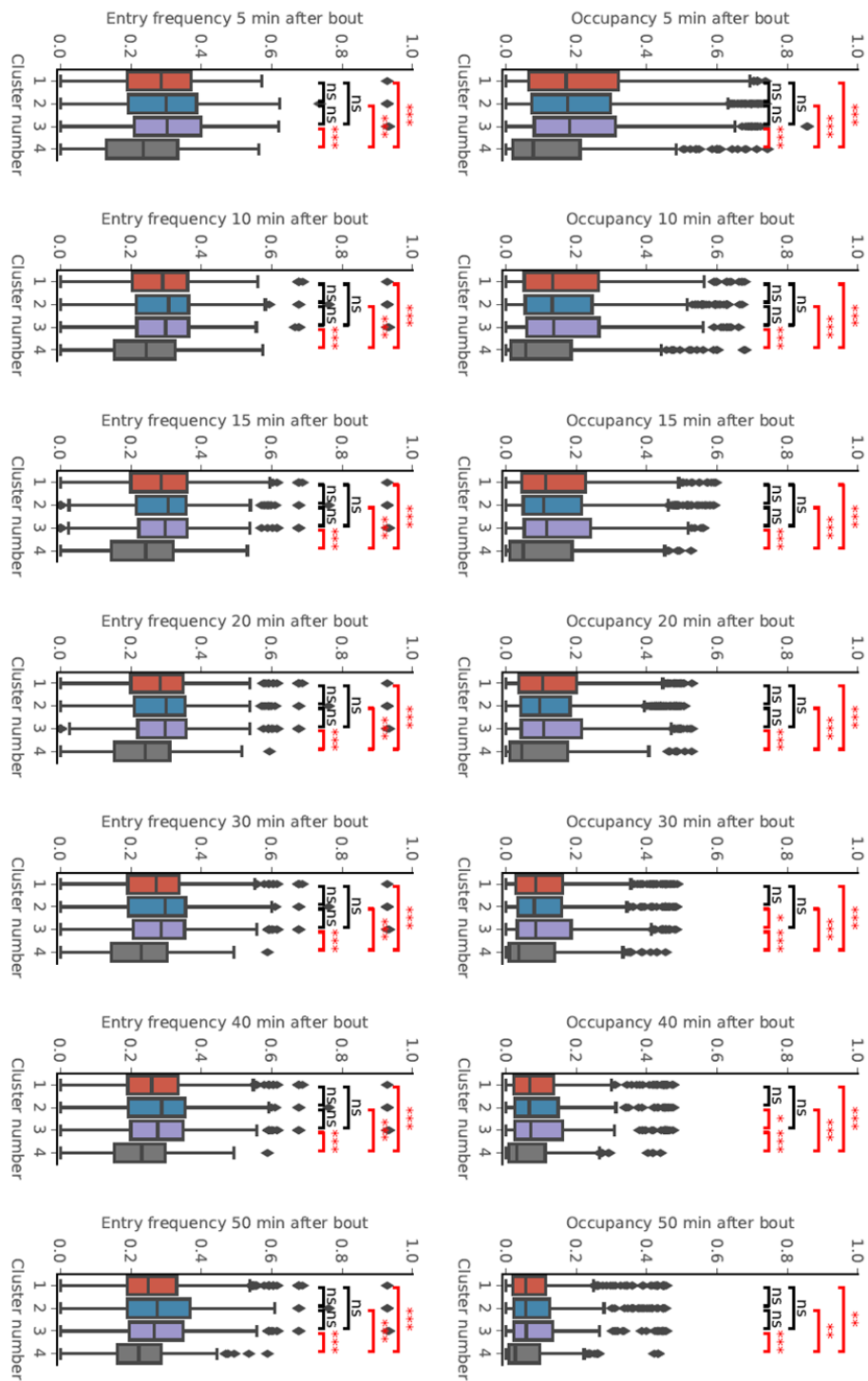


Figure 37. Effects of high-amplitude swim bouts on the occupancy/entry frequency of the shocked arm last up to 50 minutes.

Time intervals of 5, 10, 15, 20, 30, 40, and 50 minutes after the shock-triggered swim bout are used.

Fish age was between 20 and 26 dpf.

The results in Chapter 3.4 strongly suggest that fish show a diverse range of responses to electric shocks. Shock responsiveness differed with the orientation of the fish in the electric field. Moreover, the HA response type can be linked to the efficient conditioning of the fish.

3.5 The role of visual cues in the CPA paradigm

In Chapter 3.3 it was established that fish can learn to avoid a specific arm in a Y-maze when three distinct visual patterns are displayed in each arm. However, these experiments did not allow for a differentiation between all cues that the fish could use to orient in the maze. Possible cues could involve visual, odor-based (e.g. fish could release a stress odor into the water to mark the aversive arm), or yet unidentified in-maze cues (see biases in Chapter 3.1.3). To check if the visual cues are necessary for the fish in the CPA paradigm, additional experiments were performed in which the fish were deprived of distinct visual cues in the arms of the maze.

In the experiments from the earlier chapters the maze arm and the pattern were not discriminated (i.e. the visual cue and the location were treated as one). To decouple the visual pattern from the location, a series of experiments were performed with rotation of the visual patterns in the test session.

If the fish indeed used visual cues in the CPA, this could be explained by different strategies: a simple associative pairing of a pattern with the aversive cue; learning a safe pattern; learning a more complicated relationship between the patterns. An additional learning strategy was already mentioned in Chapter 3.3: staying in the obvious safe compartment, i.e. the center of the maze. As this strategy does not involve learning of visual cues, it was not considered in this chapter. Fish that stayed in the maze center for 60% of the conditioning time or longer were excluded from the experiments. To discriminate between pattern aversion and alternative strategies, experiments were performed in which the visual pattern associated with the shock was removed in the test session.

3.5.1 Response of fish to CPA paradigm in the absence of visually distinct cues

In this set of experiments fish were introduced to a maze with identical patterns displayed in all arms. The preferred arm was identified at the end of the habituation session as usual. The reason for the preference for any arm could be stochastic, or explained by previously identified biases in

the maze (see Chapter 3.1.3). The conditioning then ran for 60 minutes, followed by a 30-minute test session, in which shocks were not administered (Fig. 38, top left).

The analysis showed that crucial metrics for learning, such as the entry frequency of the shocked arm in conditioning and test sessions, or occupancy of the shocked arm in test session, did not decrease significantly on average (Fig. 38, Table 19). Only the occupancy of the shocked arm during the conditioning session decreased significantly. However, this result can be explained by the increased speed in the shocked arm (see modeling in Chapter 3.3).

Table 19. Arm entry frequency and arm occupancy in the experiments with identical patterns.

Mean \pm s.e.m. b.l.s.t = beyond the limit of the statistical test

	Shocked arm	Safe arm on the left	Safe arm on the right	n	Permutation test <i>p</i> -value
Last 10 minutes of the conditioning session					
Entry freq.	0.28 \pm 0.02	0.38 \pm 0.03	0.32 \pm 0.02	30	0.027
Occupancy	0.12 \pm 0.02	0.34 \pm 0.04	0.30 \pm 0.02	30	b.l.s.t. (0.0)
First 10 minutes of the test session					
Entry freq.	0.35 \pm 0.03	0.32 \pm 0.03	0.33 \pm 0.03	30	0.66
Occupancy	0.23 \pm 0.02	0.30 \pm 0.04	0.26 \pm 0.03	30	0.14

While it cannot be excluded that some fish could use non-visual cues in the CPA paradigm, this finding indicates that, for the majority of the fish, distinct visual cues are necessary for the formation of a short-term memory of the aversive arm. In addition, it shows that non-visual cues, such as odors and any inherent biases in the set-up, were not confounding factors in these experiments, because it was vision that played the major role in learning (see Chapter 3.1.3).

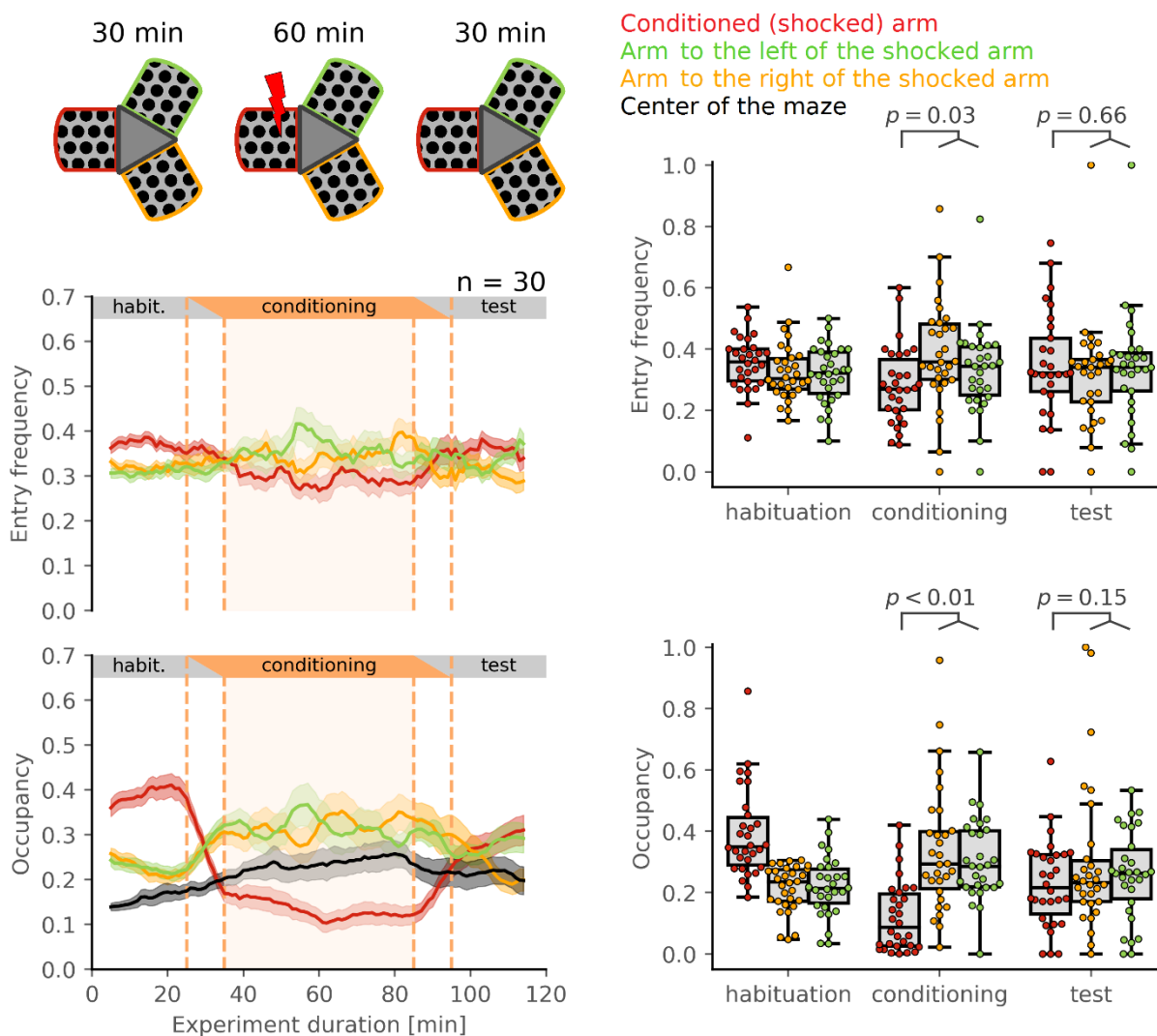


Figure 38. Changes in CPA metrics in experiments with identical visual patterns.

Top left: schematic of the protocol, all patterns are identical in the three sessions. The occupancy of the shocked arm decreased significantly only in the conditioning session; neither occupancy nor entry frequency of the shocked arm decreased significantly in the test session. Sliding window curves are the same as before. Box plots are the same as before. Permutation test for the last 10 minutes of conditioning: entry frequency p -value = 0.027, occupancy p -value = 0.0 (beyond the limit of the statistical test, see Methods); permutation test for the first 10 minutes of test: entry frequency p -value = 0.66, occupancy p -value = 0.14. $n = 30$. Fish age was 22 or 23 dpf.

3.5.2 Decoupling the maze arm and the visual pattern

The experiments consisted of a 30-minute habituation session, a 60-minute conditioning session, then a clockwise (cw) or counterclockwise (ccw) rotation of the patterns, and finally a 30-minute test session. At the moment of rotation, the fish could be located in different parts of the maze, with four possible scenarios:

- (Scenario 1): In the center of the maze;
- (Scenario 2): In the shocked arm: these cases were rare, as the fish usually escaped the shocked arm after receiving electric pulses (unless the conditioning was ineffective (see Chapter 3.4));
- (Scenario 3): In a safe arm, which after the rotation received the previously shocked pattern: the fish found itself in the previously shocked pattern, which was not coupled with shocks at this point, and relearning could begin immediately;
- (Scenario 4): In a safe arm, which after the rotation received another safe pattern.

To exclude possible confounding factors only data from the fish in scenarios one and four were analyzed. Sliding window curves were plotted such that the colors corresponded to the patterns, not the locations, i.e. after the rotation, red indicates the arm with the previously shocked pattern even though the arm changed (Fig. 39, top left). Occupancy and entry frequency of the arm associated with the shocked pattern was significantly lower than for the other two arms even after the rotation (Fig. 39, Table 20).

Table 20. Arm entry frequency and arm occupancy in the experiments with pattern rotation.

Mean \pm s.e.m. b.l.s.t. = beyond the limit of the statistical test

	Shocked arm	Safe arm on the left	Safe arm on the right	n	Permutation test p -value
Last 10 minutes of the conditioning session					
Entry freq.	0.18 \pm 0.01	0.44 \pm 0.04	0.38 \pm 0.04	44	b.l.s.t. (0.0)
Occupancy	0.07 \pm 0.02	0.37 \pm 0.05	0.30 \pm 0.05	44	b.l.s.t. (0.0)

First 10 minutes of the test session

Entry freq.	0.27 ± 0.02	0.34 ± 0.03	0.39 ± 0.03	44	0.004
Occupancy	0.17 ± 0.02	0.26 ± 0.04	0.31 ± 0.04	44	0.002

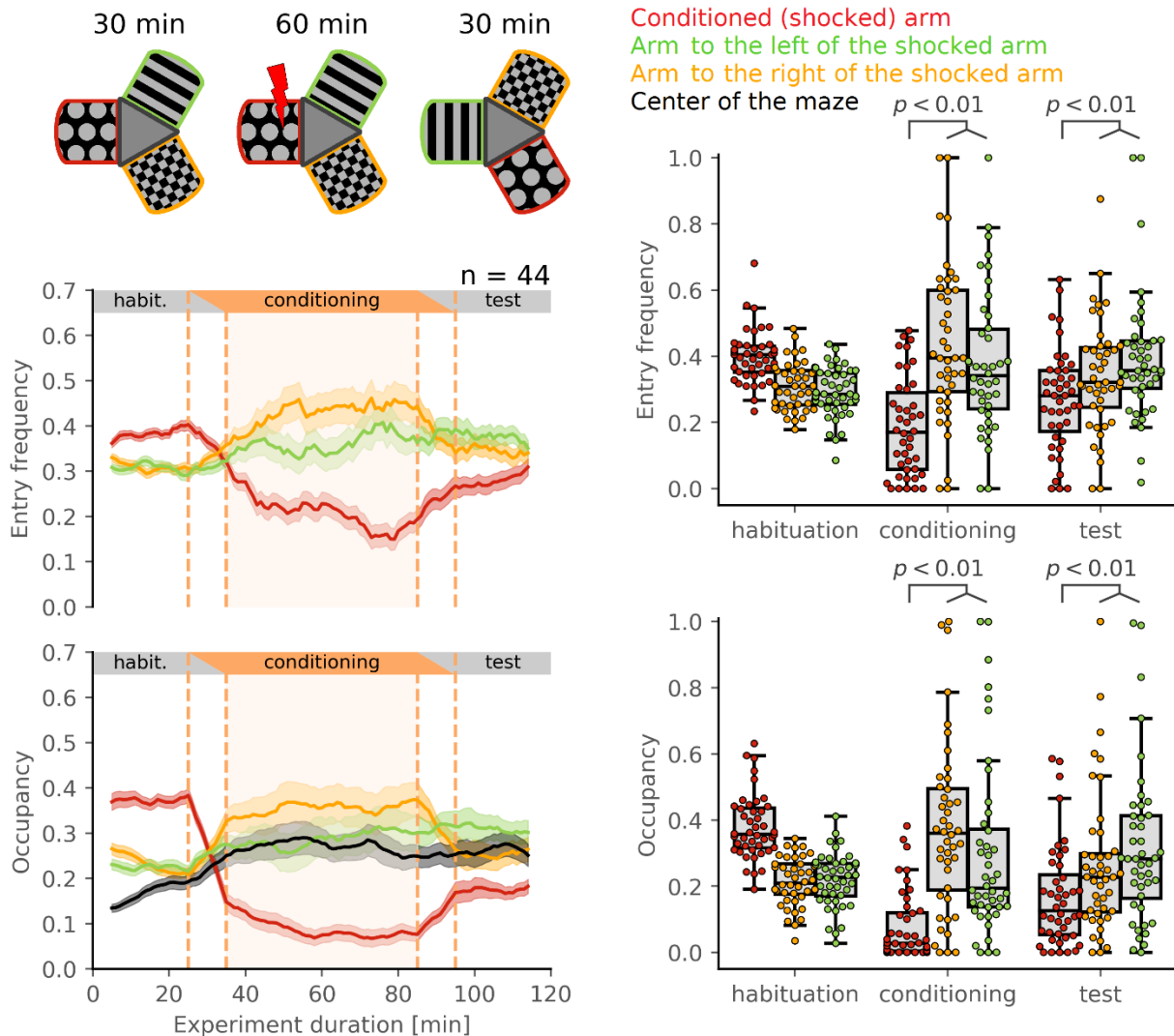


Figure 39. Changes in CPA metrics in experiments with pattern rotation (cw/ccw) in the test session.

Colors indicate patterns, not locations (see schema at the top left). Sliding window curves are the same as before. Box plots are the same as before. Permutation test for the last 10 minutes of conditioning: entry frequency p -value = 0.0 (beyond the limit of the statistical test, see Methods), occupancy p -value = 0.0 (beyond the limit of the statistical test); permutation test for the first 10 minutes of test: entry frequency p -value = 0.004, occupancy p -value = 0.002. $n = 44$. Fish age was between 21 and 23 dpf.

One explanation for this result could be freezing/limited movement of the fish in one of the arms, which would be a stress response and not a visually guided behavior. Alternatively, some fish could use a strategy not guided by the visual patterns. In the latter case, after the rotation, the fish would stay away from the originally shocked arm independently of the pattern rotation. To test this, sliding window curves were replotted so that in the test session the red color corresponded to the originally shocked location (Fig. 40, top left). No significant differences in the entry frequency of the originally shocked arm after the turn and a barely significant effect in the occupancy were observed (Table 21, compare sliding window curves in the test sessions in Fig. 39 and 40). Trajectories of individual fish (Fig. 41) demonstrate examples of how the swimming patterns rotate along with visual patterns.

These results indicate that, after the rotation, avoidance on average was mostly related to visual cues, and not to the location of the shocked arm of the maze.

Table 21. Arm entry frequency and arm occupancy in experiments with pattern rotation (metrics for the test session are calculated in relation to the originally shocked arm).

Mean \pm s.e.m.

	Originally shocked arm	Originally safe arm on the left	Originally safe arm on the right	n	Permutation test <i>p</i> -value
First 10 minutes of the test session					
Entry freq.	0.30 \pm 0.02	0.39 \pm 0.03	0.31 \pm 0.03	44	0.15
Occupancy	0.20 \pm 0.02	0.30 \pm 0.04	0.25 \pm 0.03	44	0.04

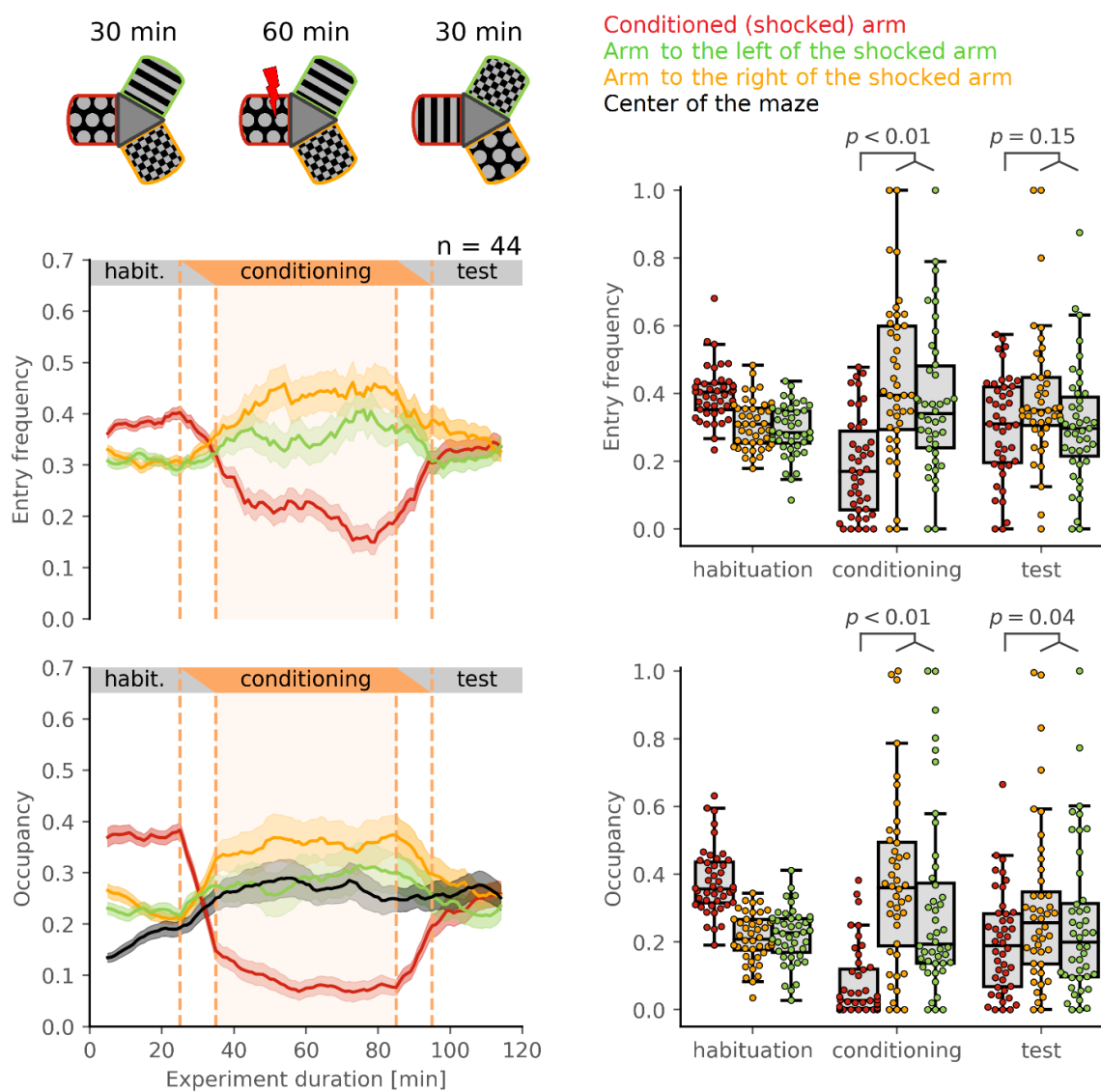


Figure 40. Changes in CPA metrics in experiments with the rotation of patterns (cw/ccw) in the test session (colors correspond to the patterns before the rotation).

Colors correspond to the location of the originally shocked arm, see top left corner. Permutation test for the last 10 minutes of conditioning: entry frequency p -value = 0.0 (beyond the limit of the statistical test, see Methods), occupancy p -value = 0.0 (beyond the limit of the statistical test); permutation test for the first 10 minutes of test: entry frequency p -value = 0.15, occupancy p -value = 0.04. $n = 44$. Fish age was between 21 and 23 dpf.

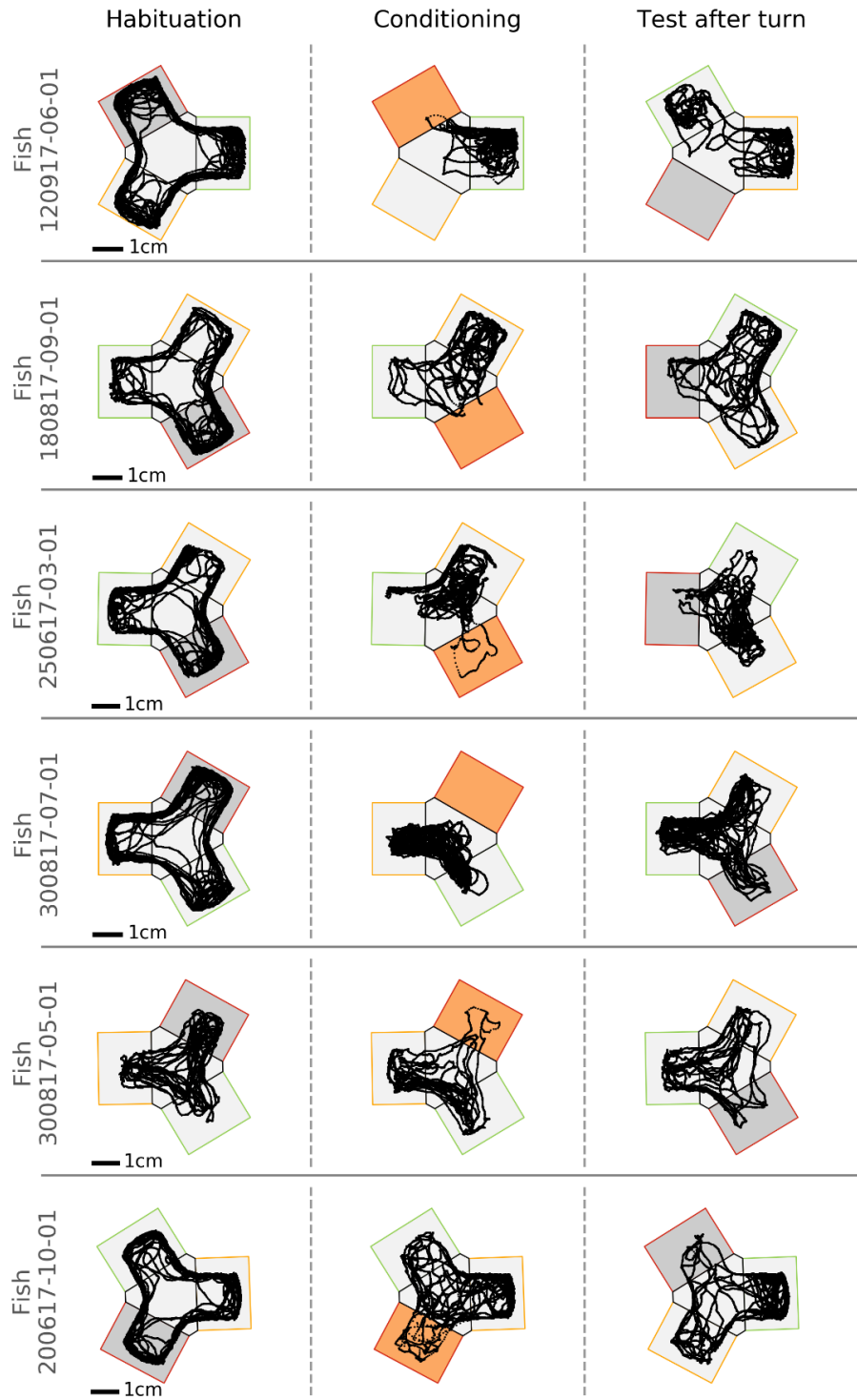


Figure 41. Examples of fish trajectories before and after the rotation.

Each row represents one individual fish.

3.5.3 Alternative strategies to pattern aversion

3.5.3.1 Replacement of the shocked pattern: control experiments

The results presented in the previous paragraphs established the importance of the visual cues in the CPA paradigm. The following paragraphs describe the replacement of the pattern corresponding to the shocked arm of the maze

Before performing the experiments with conditioning, additional control experiments were performed to rule out the possibility that the replacement of the pattern could be aversive in itself. Two scenarios were tested: substitution of the pattern to uniform gray and substitution to a different, previously unseen pattern. In both cases, a habituation session was run for 30 minutes to identify the preferred arm of the fish, followed by a test session for another 30 minutes, in which the patterns in the preferred arm were switched to either gray or a novel pattern. No shocks were applied during these control experiments.

Sliding window curves for the preferred arm show that on average neither occupancy nor entry frequency of the preferred arm changed significantly after pattern replacement (Fig. 42). However, when the pattern was switched to uniform gray some fish responded by avoiding the previously preferred arm after the switch (see individual traces, Fig. 42, left). It seems that for some fish the switch to uniform gray can cause an unwanted aversive reaction, while the switch to a different pattern does not produce such reactions. A possible explanation for this could be that all patterns have high contrast between light and dark elements (stripes, dots, squares), and the switch to uniform gray causes a significant decrease in contrast levels for the fish (despite the average luminance level remaining constant).

To avoid any confounds, switches to a different pattern were used in the subsequent experiments.

3.5.3.2 Replacement of the shocked pattern: conditioning experiments

These experiments consisted of a 30-minute habituation session, a 60-minute conditioning session, and a 30-minute test session, in which shocks were switched off and the pattern in the shocked arm was substituted with a previously unseen one (this neutral pattern had black dots on white background, see schematic in Fig. 43, top left).

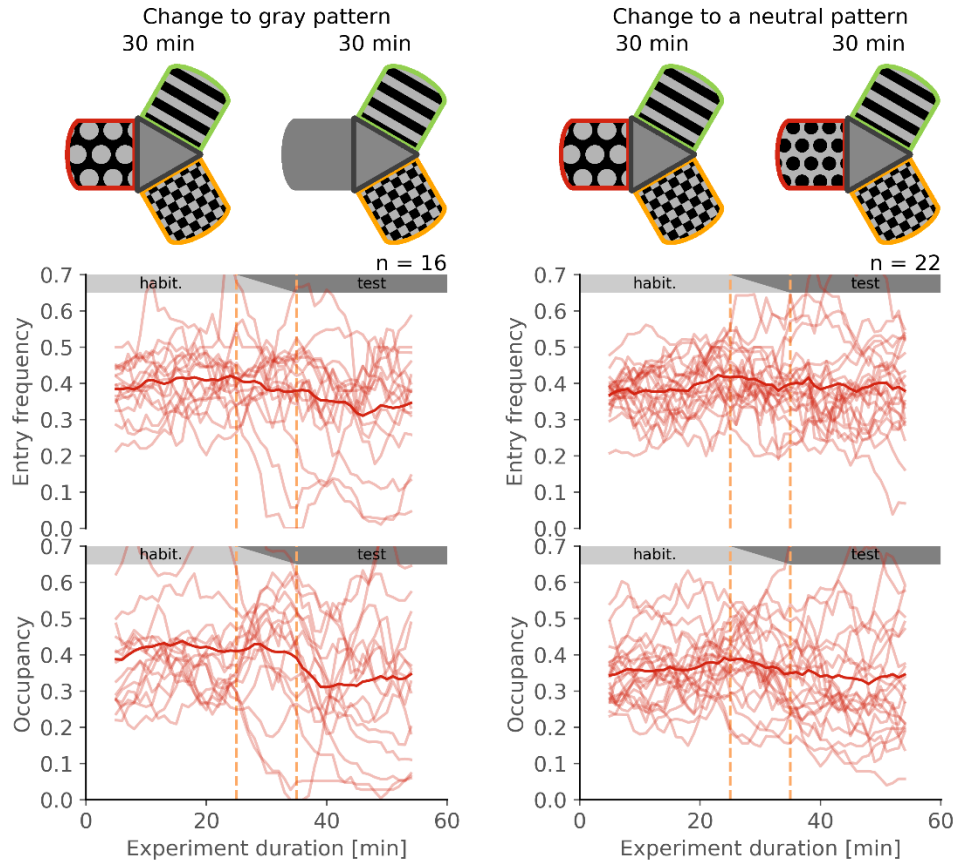


Figure 42. Changes in CPA metrics in control experiments for the replacement of the shocked pattern.

Left: switch of the pattern in the preferred arm to uniform gray. Right: switch of the pattern in the preferred arm to a previously unseen pattern. Only sliding window curves for the preferred arm are shown for clarity of the plot. Transparent red lines in sliding window plots show traces for individual fish; saturated red lines indicate the averages. The preferred arm is shown in red in the schematics on the top. Fish age was between 21 and 23 dpf in both groups.

Results in the test session showed greater variability than in the original experiments with three patterns. However, the occupancy of the shocked arm was still significantly reduced in the beginning of the test session despite the replacement of the shocked pattern (Fig. 43, Table 22).

Individual examples reveal that some fish continued to avoid the conditioned arm even after the substitution of the shocked pattern to a different one (Fig. 44). Moreover, the success in the test session in these examples did not depend on the exact pattern that was associated with the shock

(see the shocked patterns in Fig. 44, right). These fish seemed to be using an alternative strategy to pattern avoidance.

At the same time the performance of the fish decreased on average: entry frequency of the shocked arm returned to chance level after the replacement of the shock-associated pattern. This could be an indication that a subgroup of fish was using the pattern aversion strategy, and lost the aversive response after the pattern was replaced.

Table 22. Arm entry frequency and arm occupancy in the experiments with the replacement of the shocked pattern.

Mean \pm s.e.m. b.l.s.t. = beyond the limit of the statistical test

	Shocked arm	Safe arm on the left	Safe arm on the right	n	Permutation test p -value
Last 10 minutes of the conditioning session					
Entry freq.	0.27 \pm 0.03	0.36 \pm 0.03	0.37 \pm 0.03	40	0.013
Occupancy	0.10 \pm 0.02	0.38 \pm 0.05	0.36 \pm 0.05	40	b.l.s.t. (0.0)
First 10 minutes of the test session					
Entry freq.	0.29 \pm 0.02	0.31 \pm 0.02	0.39 \pm 0.02	40	0.07
Occupancy	0.16 \pm 0.02	0.30 \pm 0.04	0.36 \pm 0.04	40	0.0008

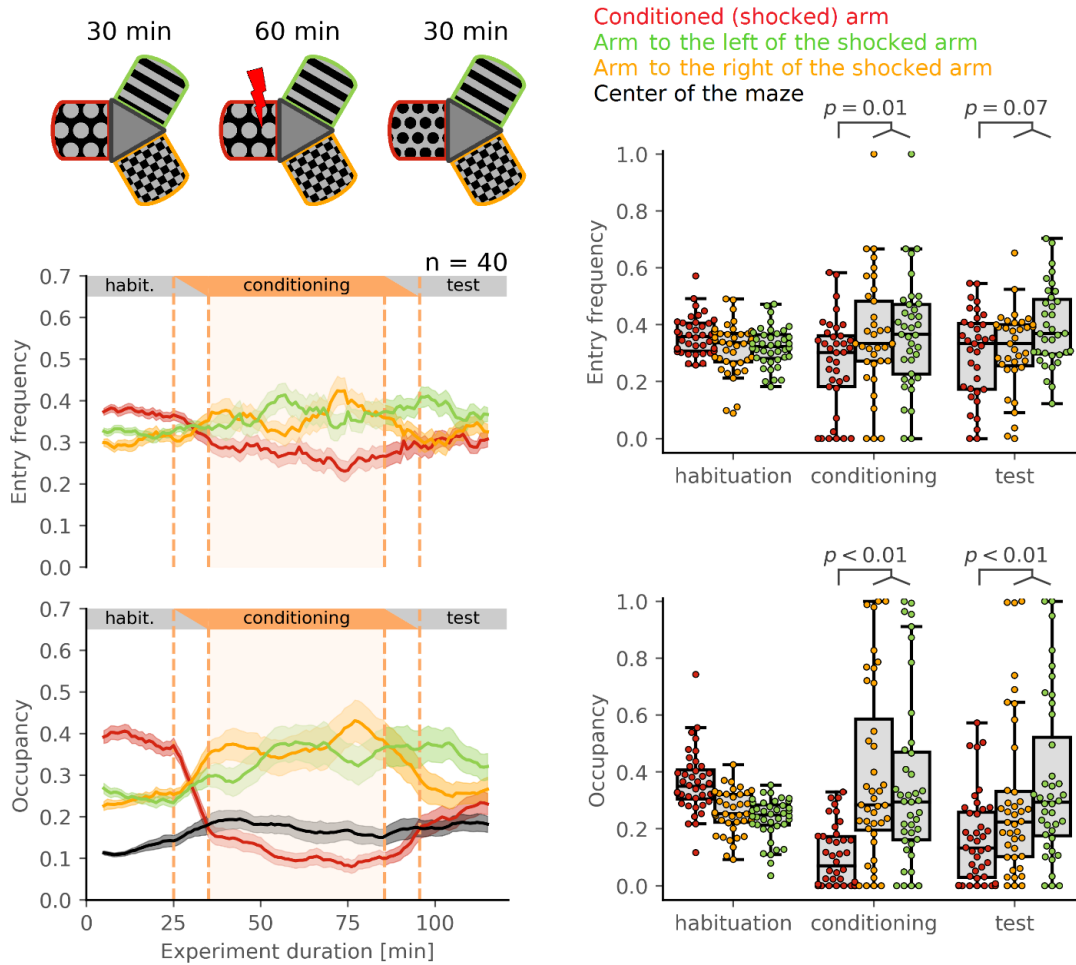


Figure 43. Changes in CPA metrics in experiments in which the shocked pattern was replaced in the test session.

The occupancy of the shocked arm stays significantly reduced even after the replacement of the shocked pattern in the test session. Color scheme and sliding window curves are the same as before. Box plots are the same as before. Permutation test for the last 10 minutes of conditioning: entry frequency p -value = 0.013, occupancy p -value = 0.0 (beyond the limit of the statistical test, see Methods); permutation test for the first 10 minutes of test: entry frequency p -value = 0.07, occupancy p -value = 0.0008. $n = 40$. Fish age was between 20 and 25 dpf.

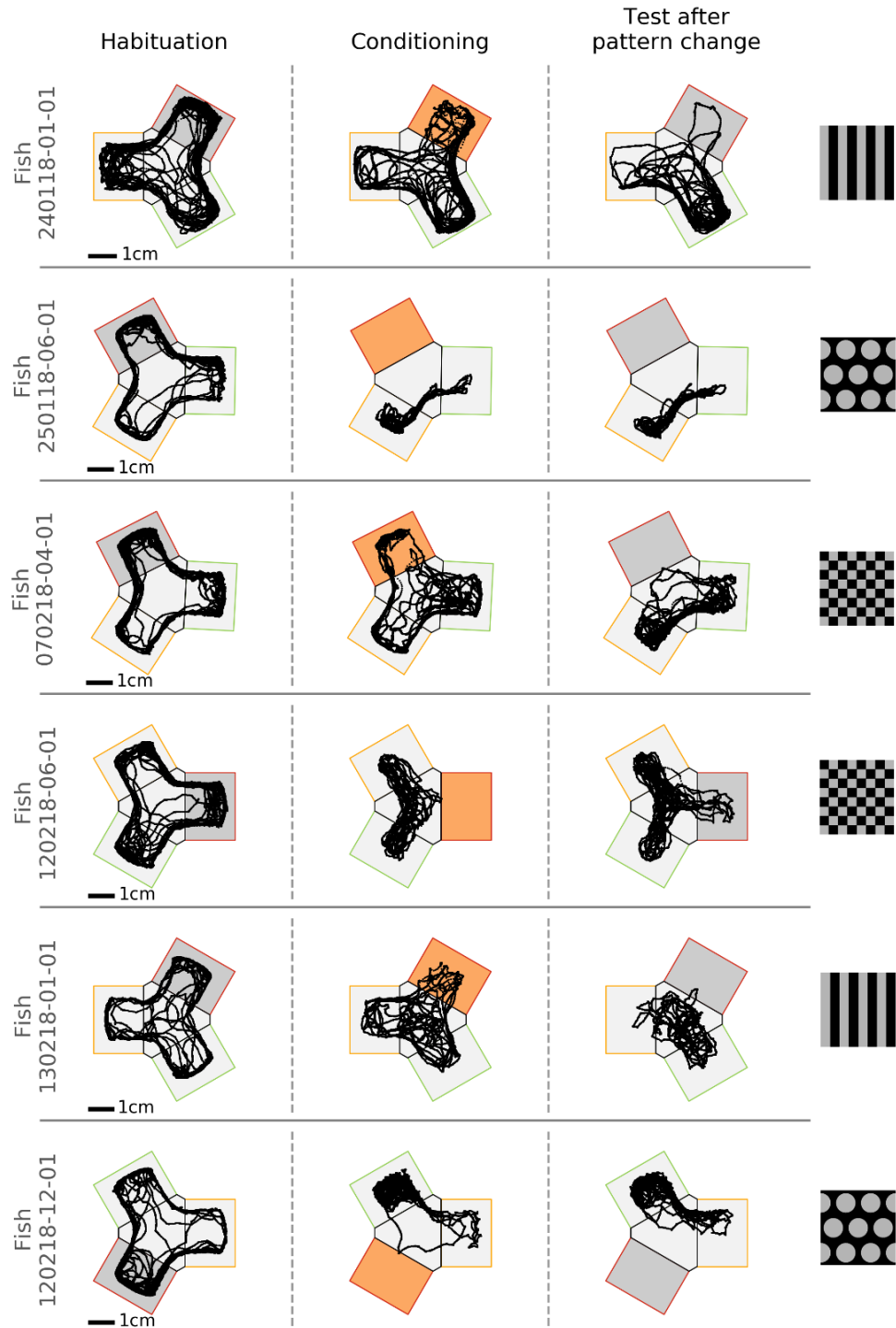


Figure 44. Individual examples of fish trajectories with successful avoidance of the shocked arm after the replacement of the shocked pattern in the test session.

The replaced pattern is shown on the right; its identity did not play a role in successful avoidance after the replacement (data not shown).

Taken together, these experiments reveal that distinct visual cues are necessary for successful aversion of the shocked arm for the majority of fish. Moreover, if visual cues are rotated in the test session, fish continue to avoid the pattern, not the location in the maze. The replacement of the shocked pattern in the test session caused a reduction in the effect of conditioning in the test session, suggesting that there were fish which were relying on pattern aversion. However, some fish kept avoiding the conditioned arm even in the absence of the pattern, directly associated with the shock. This suggests that while some fish could use the shocked pattern as a cue to avoid the shocks, other fish could use alternative strategies, such as learning a safe pattern.

4 Discussion

A new behavioral paradigm, conditioned place avoidance (CPA) in a Y-maze, was developed for investigation of the learning abilities of larval and juvenile zebrafish. At 3 weeks of age the fish successfully responded to the conditioning. This paradigm is a step forward from 2-compartment setups, used previously for larval and juvenile zebrafish. The shape of the Y-maze allows for a straightforward readout of which of the four compartments the animal chooses to swim in (i.e. the three arms and the central, neutral compartment). Manipulation of different cues in the maze revealed that the fish used different strategies to solve the problem, some of which have not been explored previously.

4.1 Onset of learning in the CPA paradigm

Zebrafish showed robust responses to conditioning in the CPA paradigm starting from 3 weeks of age, which agrees with previous observations (Valente et al., 2012) (see Results Chapter 3.2). 1wo fish did not respond to the conditioning, and 2wo fish showed highly variable responses. A possible explanation for this variability is that at this larval stage fish are highly heterogeneous in body size (see Fig. 17 in Results). If brain development correlates with body size, then fish siblings could be at different developmental stages despite being the same age. The group of 2wo fish normally contains a mix of slow- and rapid-developing fish, which could therefore show different capacities for learning. This observation can be used in future experiments to select groups of fish based on their size (i.e. developmental stage) and not chronological age.

A possible explanation as to why 1wo and 2wo zebrafish larvae do not develop conditioned responses is that the brain of the larva is still developing, including the visual system (Branchek & Bremiller, 1984). In particular, at early developmental stages the larva's main life objectives are to feed and to avoid predators, both of which can be achieved by hardwired, innate behaviors (i.e. prey capture and escape responses). Associative learning, which requires the extraction and memorization of salient features from the environment, is a complicated task, which could have secondary ecological importance for a developing larva, given the limited capacity of the larval brain. At later stages of development visual acuity improves, which may contribute to more sophisticated behaviors.

4.2 Dynamics of CPA metrics

The effects of conditioning were assessed with two metrics: arm occupancy and arm entry frequency. These metrics are interrelated (the more frequently the fish enters an arm, the higher the occupancy of that arm), but they can also diverge in an experiment, and therefore reflect different aspects of the conditioning/learning.

Interestingly, some divergence between these metrics can be explained by mechanisms unrelated to learning. Modeling results showed that lowered occupancy of the shocked arm during conditioning can be explained by the fish's reaction to electric shocks (i.e. by increasing speed of swim bouts in the conditioned arm), even in the absence of learning (see Results Chapter 3.2). The occupancy of the shocked arm had to be assessed in the test session following conditioning to confirm that conditioning was successful. At the same time the decrease in the second metric, the entry frequency of the shocked arm, could not be explained by the model. The modeling result is mirrored in the performance of the young larvae, which do not learn in the conditioning paradigm. Their occupancy of the shocked arm decreased during the conditioning as a result of reactions to shocks, but not the entry frequency of the shocked arm.

Crucially, these metrics can change based on the strategies the fish use to avoid electric shocks. Arm occupancy indicates the tendency of the fish to stay **IN** the arm, and arm entry frequency shows how actively the fish visits the arm (i.e. crosses the border **INTO** the arm from the central compartment). If the fish learns to avoid the conditioned arm, both its entry frequency and occupancy should decrease. If alternatively the fish learns to prefer a safe arm or arms, this preference could be manifested in the prolonged duration of each stay in the safe, preferred arm(s). Meanwhile, the entry frequency of all arms might stay the same. Thus, the occupancy of the conditioned arm would decrease, but not its entry frequency. This reasoning could explain why in the experiments with the replacement of the conditioned pattern, the occupancy of the conditioned arm stayed significantly reduced after the pattern replacement, but the entry frequency of the conditioned arm was at chance level (see Results Chapter 3.5.3.2). The replacement of the conditioned pattern should affect only the fish that learned to avoid the conditioned pattern, as the replacement pattern was neutral and not avoided (Results Chapter 3.5.3.1). The fish that instead learned to prefer a safe arm would use the cues of this safe arm, and would not avoid entrance into the conditioned arm.

4.3 Effects of conditioning in the Test session

3wo fish showed a significant decrease in the occupancy and entry frequency of the conditioned arm during the test session (see Results Chapter 3.3.1). The conditioned response persisted for a period of approximately 15 minutes on average across individual fish. The gradual loss of conditioned aversion in the test session can be explained either by passive loss of the response, or by active relearning of the safety of the previously conditioned arm. Active relearning would depend on the presence of the visual cues (given their relevance in the paradigm, see Results Chapter 3.5.1), and would occur when the fish visits the arm with the conditioned pattern and receives no electric shock, thus building a new association of safety with the previously conditioned arm. Passive memory loss should be a function of time, and would happen independently of the presence of the visual cues. Experiments with a delay session before the test, during which all patterns were switched to uniform gray for 5 or 10 minutes, showed that the fish gradually lost the aversion, independent of the presence or absence of the patterns, i.e. the loss was a function of time (Results Chapter 3.3.4). However, the occupancy and the entry frequency of the shocked arm were still significantly reduced in the beginning of the test session even after a 10-minute delay (although the effect was smaller). An additional experiment with a longer delay session (e.g. 15 minutes long) could clarify if the aversive response would be completely gone by the end of the longer delay, or if instead there are more complex underlying kinetics.

These experiments, of course, do not exclude that active relearning could be happening simultaneously with passive loss. A way to test if relearning is happening would be to run reinstatement experiments, in which the fish is reintroduced to the shock in a certain time period after the conditioning. If the formed memory is still there, the reacquisition would have faster kinetics than the first learning episode.

Such rapid memory extinction is in contrast with fear conditioning studies in rodents (Fanselow, 1990). Usually, one electric shock is sufficient for a rodent to establish a very strong aversion to conditioned location. Fish, on the other hand, constantly showed attempts to revisit the conditioned arm of the Y-maze. In the simplest case, such behavior could be an indication of a weak memory or a slower learning curve. Alternatively, this could be a sign of a different behavioral strategy. In particular, when in the wild, two behavioral drives compete against each other in the fish: the need to avoid danger, and the need to forage for food. The result of this competition is defined by

ecological factors within the natural habitat of the animal. Fish live in water, where the position of objects, predators and prey can change very quickly due to water currents and the dimensionality of the environment. Such volatility could foster an increased exploratory behavior, in which fish would revisit previously dangerous places given there is a high probability that the danger is gone, or that food appeared in an otherwise neutral area.

4.4 Variability in responses to shocks and shock response types

The responsiveness to shocks depended on the orientation of the fish in the electric field, a phenomenon that has been observed previously (Tabor et al., 2014). As a consequence, in many cases when the fish was oriented perpendicular to the electric field, the electric pulses did not elicit any response. This suggests that such shocks could be ineffective as noxious stimuli. Given this observation, the experiment could be amended in at least two ways. Electric shocks could be applied only when the fish is oriented towards the electrodes. Alternatively, more electrodes could be added to the setup so that the fish is always facing them, independent of its orientation.

Analysis of individual responses to electric shocks revealed four response types: three low-amplitude types (LA) and one high-amplitude type (HA). LA response types clearly separated into those triggered by shock onset and those triggered by shock offset. Interestingly, this separation was correlated with the orientation of the fish at the moment of the shock, even though orientation was not used as a classification parameter. In particular, swim bouts triggered by shock onset occurred when the fish was oriented towards the anode, while swim bouts triggered by shock offset occurred in fish facing the cathode. Such correlation could be explained by the hypothesis that the direction of the pulse matters for triggering the response. Briefly, two steel-mesh electrodes, such as those used for shock delivery, could act as plates of a capacitor. The capacitor charges during the electric pulse, and discharges after the pulse is switched off, thereby creating a transient current in the opposite direction to the current from the original pulse, hence effectively presenting a pulse in one direction during shock onset and one in the opposite direction during shock offset.

In all response types the distribution of orientation angles was skewed towards 0° value, which corresponded to fish being oriented towards the arm end (looking into the arm). A possible explanation could arise from the fact that delivery of electric shocks always occurred immediately

after the fish entered the arm, when it was looking into the arm. The exit from the arm, which corresponded to the fish oriented towards arm entry (orientation angles close to 180°), did not always coincide with a delivery of the shock. Thus, the probability of a shock reaction in the ‘out-of-arm’ orientation was lower than the probability of shock reaction in the ‘into-the-arm’ orientation.

One LA response type stood out due to its prolonged duration. Individual trajectories for this response type revealed that swim bouts started with a slow forward motion, followed by a stronger escape-like response, while swim bouts associated with other LA response types usually started directly with an escape-like response. Thus, this response type can be explained by the coincidence of a spontaneous swim bout and an escape-like response to shock. Such combination of two swim bouts could account for the increased duration of swim bouts of this type. It also potentially offers clues as to how the response is generated, given that this would mean the shock is able to somehow interrupt an ongoing swim bout.

The most striking response type consisted of HA swim bouts. Swim bouts of this response type were less numerous when compared to the LA response types. Previous studies showed that mild electric pulses directly activate Mauthner cells, bypassing sensory organs (Tabor et al., 2014). Such activation causes the fish to perform a C-bend, resembling the early stage of escape responses – a highly stereotyped tail movement (Liu, Bailey, & Hale, 2012; Temizer et al., 2015). The C-bend resembles the LA response types observed in this study. The HA responses involved a series of powerful swim bouts, and were more variable in dynamics than LA responses. In contrast to LA, HA responses were followed on average by a more aversive response to conditioning (see Results Chapter 3.4.2). One could speculate that the LA responses are triggered by direct activation of the Mauthner cell, as previously described, while HA responses are a result of activation of additional circuits in the neural circuitry. This could include sensory organs (e.g. lateral line, nociceptors), reticulospinal neurons in addition to Mauthner cells (which together could trigger an afferent signal to the brain about an aversive reaction), and direct activation of brain centers for aversive memories (e.g. ventral pallidum – a homologue of mammalian basolateral amygdala, which is required for fear conditioning in mammals (Mueller, Dong, Berberoglu, & Guo, 2011; Poulos et al., 2009)). This observation suggests that electric shocks should be used as aversive

stimuli with caution, as some types of observed LA reactions to shocks might be artifacts of direct activation of the Mauthner cell and might not have any saliency to the animal.

The variability of responses to electric shocks was studied in a cohort of 3wo fish. However, it is not clear if different response types would be observed in younger fish. The intensity of electric pulses was the same for all age groups in age comparison experiments (Results Chapter 3.2). Younger fish are smaller in size and could have different skin resistivity to electric current, and thus they might need a different shock intensity to elicit a proper aversive reaction. It remains to be investigated if the lack of learning in younger animals could partially be explained by the shocks not being ‘aversive’ enough.

Previous studies pointed at brain regions which were responsive to electric shocks. (Duboué, Hong, Eldred, & Halpern, 2017; Randlett et al., 2015; Tabor et al., 2014). Further imaging experiments in zebrafish at different stages of development could elucidate what parts of the brain are activated by electric shocks at different ages, and what types of responses they produce.

4.5 The role of visual cues in the CPA paradigm

Experiments with identical visual patterns revealed that, on average, the absence of distinct visual cues prevents the formation of conditioned responses in the test session (Results Chapter 3.5.1). This was supported by the entry frequency and occupancy of the shocked arm being at chance level in the test sessions. The results of these experiments closely resemble the results of simulations of a “no-learning” model (Results Chapter 3.3.2), i.e. a kinematic model without a learning component in the behavior. This suggests that distinct visual cues are necessary for learning in the CPA paradigm for the majority of the fish. This, however, does not exclude the possibility that a minority of fish (which was not reflected in the sample average) could use non-visual cues to avoid the conditioned arm. Non-visual cues could include odors in the water, unobserved in-maze cues, or a magnetic field (Myklatun et al., 2018).

4.6 Fish strategies in the CPA paradigm

Fish reacted to conditioning with different strategies. A subgroup of fish learned to stay in the central compartment of the maze, thus avoiding all of the arms (Results Chapter 3.3). This strategy was effectively the most optimal 'safe haven', and did not require differentiation between the patterns. In this strategy, the fish could use the contrast between patterns in the arms and grey color of the central compartment as a cue for arm aversion; alternatively, the fish could use pattern-independent perception of the central area as a part of the maze most removed from the walls (a more open space).

Another subgroup seemed to be using a strategy of pattern aversion. This group was revealed by experiments where the shock pattern was removed (Results Chapter 3.5.3). Here, the performance of the fish in the test session without the conditioned pattern worsened compared to experiments with the conditioned pattern present. In particular, the entry frequency of the shocked arm was not significantly decreased after the replacement of the conditioned pattern. These experiments suggest that a subgroup of animals were not able to avoid the conditioned arm after the replacement of the conditioned pattern, thus implicating a pattern aversion strategy.

Interestingly, the occupancy of the conditioned arm after the replacement of the shocked pattern was still significantly reduced. This means that some fish could avoid the conditioned arm even in the absence of the shocked pattern. In this group, two groups of strategies could be mixed: fish that learned a safe pattern, and fish that used non-visual cues. However, previous experiments showed that visual cues were dominant in the learning of the conditioned response. This serves as a strong indication that the majority of fish were learning a safe pattern rather than utilizing non-visual cues.

This repertoire of strategies is interesting from an ecological point of view. The strategy of picking the safe center is the easiest, but it limits the area of exploration the most. Fish that avoid the shocked pattern have the advantage of exploring all other arms, which helps with foraging. The strategy of finding a safe arm could be interpreted as finding a shelter, and could be more beneficial for the animal in the long-term. Further experiments are necessary to investigate whether the same fish can use different strategies at different time points, or whether the strategy of choice is intrinsic to each individual.

5 Outlook

5.1 Further behavioral experiments

All experiments described in this work contained only a single conditioning session. A next step could be to introduce multiple conditioning sessions for each animal. These experiments could reveal if repeated conditioning strengthens the aversive memory. The robustness of the memory could also be tested in relation to the duration of the conditioning sessions.

The conducted experiments revealed several strategies that fish use to avoid a location in the Y-maze. The pattern avoidance strategy was inferred from the reduction in performance after the replacement of the shocked pattern. Stronger corroboration for the pattern avoidance hypothesis could be obtained with an experiment in which the shocked pattern is removed for a brief period, and then shown again. The fish utilizing the pattern avoidance strategy would lose the avoidance of the arm after the pattern removal, and regain it once the shocked pattern is back.

As speculated above, the ‘safe haven’ strategy could be useful for the fish to learn shelter/safety areas. To test this hypothesis, the fish could be introduced to an alternative aversive stimulus after conditioning with electric shocks (e.g. a looming disc). If the fish learns the safety property of an arm, then it would perform a directional escape into the learned safe arm after seeing a threatening stimulus (a strategy used by escaping rodents (Vale, Evans, & Branco, 2017)).

The conditioning stimulus in all experiments was coupled with a pattern of the maze. In such conditions, most fish learned to rely on the visual cues in order to avoid the shocks. An alternative conditioning paradigm could involve pairing the shocks with a specific movement of the fish (e.g. apply shocks every time the fish enters an arm to its right). These experiments would probe the capacity of the zebrafish to use an egocentric navigation strategy.

5.2 Imaging of a behaving juvenile zebrafish in a Y-maze

One of the advantages of studying learning in zebrafish is the possibility of whole-brain imaging in a behaving animal.

Neural correlates of fear learning in the mammalian brain, including the amygdala, are located deep in the mammalian brain, and present an accessibility challenge for neural recordings. The amygdala is positioned as such during the developmental process of evagination of the neural tube, a hallmark step of mammalian brain folding. At the same time, the brain of teleost fish (including zebrafish) folds in a different way, called eversion (Wullimann & Mueller, 2004). During eversion, the homologue areas of the hippocampus and amygdala, located in the telencephalon, stay on the surface of the brain, making them easily accessible for imaging.

However, several challenges stand in the way of imaging in the juvenile zebrafish.

One of these is the immobilization of the animal for imaging. Embedding fish in agarose is the standard procedure used for larval zebrafish live imaging. In this procedure, the fish is placed into a drop of low-melting point agarose, which prevents the animal from moving during the recordings, but keeps them alive and awake. The still developing larval zebrafish do not use their gills for breathing; instead they obtain oxygen through skin diffusion (Rombough, 2002). However, oxygen diffusion is possible only over very small distances. Once the fish grow to the juvenile stage, diffusion is not sufficient to supply the animal with enough oxygen. At this stage, the fish start using the gills. When juvenile zebrafish are embedded in agarose, the gills are blocked, and the fish suffocate. Luckily, several techniques have been developed to prolong the survival of embedded juvenile zebrafish. One option is to place the fish into highly oxygenated water to increase the efficiency of diffusion. A second alternative is to remove the agarose from around the gills and the mouth, and concomitantly pump water through the mouth to aerate the gills. A combination of these techniques proved successful and kept juvenile fish alive for up to 3 hours during imaging (Bergmann et al., 2018; Matsuda et al., 2017; Vendrell-Llopis & Yaksi, 2016).

Imaging of the behaving animals presents another challenge. The only behavioral readout available during the imaging in a head-restrained animal is the tail flicks of the fish, or the corresponding activity of some motor neurons in the spinal cord. Algorithms for inferring the intended swimming direction of the animal from the tail flicks have been used to create closed-loop virtual reality systems (Ahrens, Huang, Narayan, Mensh, & Engert, 2013; Jouary, Haudrechy, Candelier, & Sumbre, 2016; Trivedi & Bollmann, 2013). Larval zebrafish have been shown to swim

successfully in simple virtual environments. This technique still needs to be adapted for the juvenile zebrafish.

An alternative to imaging of the embedded juvenile zebrafish is to develop techniques for cellular resolution imaging in free-swimming fish (Kim et al., 2017). Here imaging is performed on a freely moving animal, as the microscope objective moves along the trajectory of the animal and keeps the brain in the field of view and in focus. The movement of the objective is calculated using a predictive model of fish motion. However, this technology has only been tested on larval zebrafish, and still needs to be adapted for the imaging of juveniles.

6 Conclusion

This dissertation describes a new conditioned place avoidance paradigm in a Y-maze chamber for juvenile zebrafish. This paradigm has the advantages of using a small chamber with an easily controlled set of parameters. It builds on existing 2-compartment chamber paradigms, previously used for studying operant conditioning in juvenile zebrafish, allowing for more potential manipulations of presented cues.

3-week-old larvae were identified as the earliest age group to respond robustly to conditioning. Fish predominantly relied on visual cues in this paradigm. Moreover, several strategies behind the conditioned place aversion were revealed. However, the limited number of compartments and cues in the maze presents a challenge for studying more sophisticated forms of learning, such as allocentric navigation or path integration. This study sets the groundwork for this type of paradigm, and in the future it can be gradually extended by including more cues and compartments to the maze. One can also make use of newly developed virtual reality set-ups for freely swimming zebrafish, although it is not yet clear to what extent immersion in the virtual environment can be achieved (Stowers et al., 2017). An exciting prospect would be to study how the behavior of the fish becomes more sophisticated based on the amount of information available to it.

7 Appendix

7.1 Abbreviations

a.u.	arbitrary units
b.l.s.t	beyond limit of the statistical test
cw/ccw	clockwise/counterclockwise
CPA	conditioned place avoidance
CS	conditioned stimulus
CV	coefficient of variation
FIR	finite impulse response
fps	frames per second
HA	high amplitude
IR	infrared
dpf	days post fertilization
LA	low amplitude
ns	not significant
OMR	optomotor response
OKR	optokinetic response
SD	standard deviation
s.e.m.	standard error of the mean
US	unconditioned stimulus
wo	weeks old

7.2 Number of animals used in experiments

Table with fish numbers used in each experiment. “Overstayers” group was excluded from the analysis due to fish staying in the shocked arm for longer than 1 minute (see Methods). “Center” group was excluded from the analysis due to fish staying in the center of the maze for longer than 40 minutes in the conditioning session (see Methods for the heuristics used for excluding fish).

Experiment	Used in analysis	Excluded: overstayers*	Excluded: center*	Total	Experiment duration [min]
Age comparison: 1 week	14	4	0	18	30+60 = 90
Age comparison: 2 weeks	10	7	0	17	30+60 = 90
Age comparison: 3 weeks	23	7	1	23	30+60 = 90
Control	24	0	0	24	120
Three patterns + test	42	13	8	63	30+60+30 = 120
Three patterns + delay 5 min + test	25	9	6	40	30+60+5+30 = 125
Three patterns + delay 10 min + test	22	4	7	31	30+60+10+30 = 130
Identical patterns	30	18	6	54	30+60+10 = 120
Replacement of the shocked pattern	40	21	7	67	30+60+10 = 120
Control: pattern change to gray	16	0	0	16	30+30 = 60
Control: pattern change to neutral	22	0	0	22	30+30 = 60
Turn**	44 (77)	16 (29)	15 (17)	74 (121)	30+60+30 = 120

* These sets can overlap

** Only fish for which rotation happened in the center/safe arm (total number in brackets, see explanation in Results Chapter 3.5.2)

Bibliography

- Ahrens, M. B., Huang, K. H., Narayan, S., Mensh, B. D., & Engert, F. (2013). Two-photon calcium imaging during fictive navigation in virtual environments. *Frontiers in Neural Circuits*, *7*, 104. <https://doi.org/10.3389/fncir.2013.00104>
- Aizenberg, M., & Schuman, E. M. (2011). Cerebellar-dependent learning in larval zebrafish. *The Journal of Neuroscience : The Official Journal of the Society for Neuroscience*, *31*(24), 8708–8712. <https://doi.org/10.1523/JNEUROSCI.6565-10.2011>
- Aoki, R., Tsuboi, T., & Okamoto, H. (2015). Y-maze avoidance: An automated and rapid associative learning paradigm in zebrafish. *Neuroscience Research*, *91*, 69–72. <https://doi.org/10.1016/J.NEURES.2014.10.012>
- Bauer, E. P. (2015). Serotonin in fear conditioning processes. *Behavioural Brain Research*, *277*, 68–77. <https://doi.org/10.1016/J.BBR.2014.07.028>
- Bergmann, K., Meza Santoscoy, P., Lygdas, K., Nikolaeva, Y., MacDonald, R., Cunliffe, V., & Nikolaev, A. (2018). Imaging Neuronal Activity in the Optic Tectum of Late Stage Larval Zebrafish. *Journal of Developmental Biology*, *6*(1), 6. <https://doi.org/10.3390/jdb6010006>
- Bianco, I. H., Kampff, A. R., & Engert, F. (2011). Prey Capture Behavior Evoked by Simple Visual Stimuli in Larval Zebrafish. *Frontiers in Systems Neuroscience*, *5*, 101. <https://doi.org/10.3389/fnsys.2011.00101>
- Branchek, T., & Bremiller, R. (1984). The Development of Photoreceptors in the Zebrafish, *Brachydanio rerio*. I. Structure. *THE JOURNAL OF COMPARATIVE NEUROLOGY*, 224–107. Retrieved from <https://onlinelibrary.wiley.com/doi/pdf/10.1002/cne.902240109>
- Burgess, H. A., & Granato, M. (2007). Modulation of locomotor activity in larval zebrafish during light adaptation. *The Journal of Experimental Biology*, *210*(Pt 14), 2526–2539. <https://doi.org/10.1242/jeb.003939>
- Burgess, H. A., Schoch, H., & Granato, M. (2010). Distinct Retinal Pathways Drive Spatial Orientation Behaviors in Zebrafish Navigation. *Current Biology*, *20*(4), 381–386. <https://doi.org/10.1016/J.CUB.2010.01.022>

- Chen, T.-W., Wardill, T. J., Sun, Y., Pulver, S. R., Renninger, S. L., Baohan, A., ... Kim, D. S. (2013). Ultrasensitive fluorescent proteins for imaging neuronal activity. *Nature*, *499*(7458), 295–300. <https://doi.org/10.1038/nature12354>
- Chen, X., & Engert, F. (2014). Navigational strategies underlying phototaxis in larval zebrafish. *Frontiers in Systems Neuroscience*, *8*, 39. <https://doi.org/10.3389/fnsys.2014.00039>
- dal Maschio, M., Donovan, J. C., Helmbrecht, T. O., & Baier, H. (2017). Linking Neurons to Network Function and Behavior by Two-Photon Holographic Optogenetics and Volumetric Imaging. *Neuron*, *94*(4), 774–789.e5. <https://doi.org/10.1016/J.NEURON.2017.04.034>
- Dreosti, E., Lopes, G., Kampff, A. R., & Wilson, S. W. (2015). Development of social behavior in young zebrafish. *Frontiers in Neural Circuits*, *9*, 39. <https://doi.org/10.3389/fncir.2015.00039>
- Duboué, E. R., Hong, E., Eldred, K. C., & Halpern, M. E. (2017). Left Habenular Activity Attenuates Fear Responses in Larval Zebrafish. *Current Biology*, *27*(14), 2154–2162.e3. <https://doi.org/10.1016/J.CUB.2017.06.017>
- Dunn, T. W., Gebhardt, C., Naumann, E. A., Riegler, C., Ahrens, M. B., Engert, F., & Del Bene, F. (2016). Neural Circuits Underlying Visually Evoked Escapes in Larval Zebrafish. *Neuron*, *89*(3), 613–628. <https://doi.org/10.1016/J.NEURON.2015.12.021>
- Duvarci, S., & Pare, D. (2014). Amygdala Microcircuits Controlling Learned Fear. *Neuron*, *82*(5), 966–980. <https://doi.org/10.1016/J.NEURON.2014.04.042>
- Easter, S. S., & Nicola, G. N. (1996). The Development of Vision in the Zebrafish (*Danio rerio*). *Developmental Biology*, *180*(2), 646–663. <https://doi.org/10.1006/dbio.1996.0335>
- Easter, S. S., & Nicola, G. N. (1997). The development of eye movements in the zebrafish (*Danio rerio*). *Developmental Psychobiology*, *31*(4), 267–276. [https://doi.org/10.1002/\(SICI\)1098-2302\(199712\)31:4<267::AID-DEV4>3.0.CO;2-P](https://doi.org/10.1002/(SICI)1098-2302(199712)31:4<267::AID-DEV4>3.0.CO;2-P)
- Fanselow, M. S. (1990). Factors governing one-trial contextual conditioning. *Animal Learning & Behavior*, *18*(3), 264–270. Retrieved from <https://link.springer.com/content/pdf/10.3758%2FBF03205285.pdf>

- Freeman, J. H. (2015). Cerebellar learning mechanisms. *Brain Research*, *1621*, 260–269. <https://doi.org/10.1016/J.BRAINRES.2014.09.062>
- Giustino, T. F., & Maren, S. (2015). The Role of the Medial Prefrontal Cortex in the Conditioning and Extinction of Fear. *Frontiers in Behavioral Neuroscience*, *9*, 298. <https://doi.org/10.3389/fnbeh.2015.00298>
- Guggiana-Nilo, D. A., & Engert, F. (2016). Properties of the Visible Light Phototaxis and UV Avoidance Behaviors in the Larval Zebrafish. *Frontiers in Behavioral Neuroscience*, *10*, 160. <https://doi.org/10.3389/fnbeh.2016.00160>
- Hinz, R. C., & de Polavieja, G. G. (2017). Ontogeny of collective behavior reveals a simple attraction rule. *Proceedings of the National Academy of Sciences of the United States of America*, *114*(9), 2295–2300. <https://doi.org/10.1073/pnas.1616926114>
- Jouary, A., Haudrechy, M., Candelier, R., & Sumbre, G. (2016). A 2D virtual reality system for visual goal-driven navigation in zebrafish larvae. *Scientific Reports*, *6*(1), 34015. <https://doi.org/10.1038/srep34015>
- Jouary, A., & Sumbre, G. (2016). Automatic classification of behavior in zebrafish larvae. *BioRxiv*, 052324. <https://doi.org/10.1101/052324>
- Jun, J. J., Steinmetz, N. A., Siegle, J. H., Denman, D. J., Bauza, M., Barbarits, B., ... Harris, T. D. (2017). Fully integrated silicon probes for high-density recording of neural activity. *Nature*, *551*(7679), 232–236. <https://doi.org/10.1038/nature24636>
- Kalueff, A. V., Gebhardt, M., Stewart, A. M., Cachat, J. M., Brimmer, M., Chawla, J. S., ... Zebrafish Neuroscience Research Consortium. (2013). Towards a comprehensive catalog of zebrafish behavior 1.0 and beyond. *Zebrafish*, *10*(1), 70–86. <https://doi.org/10.1089/zeb.2012.0861>
- Kenney, J. W., Scott, I. C., Josselyn, S. A., & Frankland, P. W. (2017). Contextual fear conditioning in zebrafish. *Learning & Memory (Cold Spring Harbor, N.Y.)*, *24*(10), 516–523. <https://doi.org/10.1101/lm.045690.117>
- Kim, D. H., Kim, J., Marques, J. C., Grama, A., Hildebrand, D. G. C., Gu, W., ... Robson, D. N. (2017). Pan-neuronal calcium imaging with cellular resolution in freely swimming zebrafish.

- Nature Methods*, 14(11), 1107–1114. <https://doi.org/10.1038/nmeth.4429>
- Kimmel, C. B., Ballard, W. W., Kimmel, S. R., Ullmann, B., & Schilling, T. F. (1995). Stages of embryonic development of the zebrafish. *Developmental Dynamics*, 203(3), 253–310. <https://doi.org/10.1002/aja.1002030302>
- Kubo, F., Hablitzel, B., Dal Maschio, M., Driever, W., Baier, H., & Arrenberg, A. B. (2014). Functional Architecture of an Optic Flow-Responsive Area that Drives Horizontal Eye Movements in Zebrafish. *Neuron*, 81(6), 1344–1359. <https://doi.org/10.1016/J.NEURON.2014.02.043>
- Liu, Y.-C., Bailey, I., & Hale, M. E. (2012). Alternative startle motor patterns and behaviors in the larval zebrafish (*Danio rerio*). *Journal of Comparative Physiology A*, 198(1), 11–24. <https://doi.org/10.1007/s00359-011-0682-1>
- Lopez, J. C., Bingman, V. P., Rodriguez, F., Gomez, Y., & Salas, C. (2000). Dissociation of Place and Cue Learning by Telencephalic Ablation in Goldfish. *Behavioral Neuroscience Nadel Schacter & Tulving*, 114(4), 687–699. <https://doi.org/10.1037//0735-7044.114.4.687>
- Low, R. J., Gu, Y., & Tank, D. W. (2014). Cellular resolution optical access to brain regions in fissures: imaging medial prefrontal cortex and grid cells in entorhinal cortex. *Proceedings of the National Academy of Sciences of the United States of America*, 111(52), 18739–18744. <https://doi.org/10.1073/pnas.1421753111>
- Marques, J. C., Lackner, S., Félix, R., & Orger, M. B. (2018). Structure of the Zebrafish Locomotor Repertoire Revealed with Unsupervised Behavioral Clustering. *Current Biology*, 28(2), 181–195.e5. <https://doi.org/10.1016/J.CUB.2017.12.002>
- Matsuda, K., Yoshida, M., Kawakami, K., Hibi, M., & Shimizu, T. (2017). Granule cells control recovery from classical conditioned fear responses in the zebrafish cerebellum. *Scientific Reports*, 7(1), 11865. <https://doi.org/10.1038/s41598-017-10794-0>
- McClellan, J. H., & Parks, T. W. (1973). A unified approach to the design of optimum FIR linear phase digital filters. *IEEE Transactions on Circuit Theory*, 20(6), 697–701. <https://doi.org/10.1109/TCT.1973.1083764>
- Miller, N., & Gerlai, R. (2012). From Schooling to Shoaling: Patterns of Collective Motion in

- Zebrafish (Danio rerio). *PLoS ONE*, 7(11), e48865.
<https://doi.org/10.1371/journal.pone.0048865>
- Mirat, O., Sternberg, J. R., Severi, K. E., & Wyart, C. (2013). ZebraZoom: an automated program for high-throughput behavioral analysis and categorization. *Frontiers in Neural Circuits*, 7, 107. <https://doi.org/10.3389/fncir.2013.00107>
- Mitra, S. K. (2001). *Digital Signal Processing: : A Computer-Based Approach with DSP Laboratory Using MATLAB* (2nd ed.). McGraw-Hill Higher Education.
- Moore, B. R. (2004). The evolution of learning. *Biological Reviews*, 79(2), 301–335.
<https://doi.org/10.1017/S1464793103006225>
- Mucha, R. F., Van Der Kooy, D., O’Shaughnessy, M., & Buceniaks, P. (1982). Drug reinforcement studied by the use of place conditioning in rat. *Brain Research*, 243(1), 91–105.
[https://doi.org/10.1016/0006-8993\(82\)91123-4](https://doi.org/10.1016/0006-8993(82)91123-4)
- Mueller, T., Dong, Z., Berberoglu, M. A., & Guo, S. (2011). The dorsal pallium in zebrafish, *Danio rerio* (Cyprinidae, Teleostei). *Brain Research*, 1381, 95–105.
<https://doi.org/10.1016/J.BRAINRES.2010.12.089>
- Myklatun, A., Lauri, A., Eder, S. H. K., Cappetta, M., Shcherbakov, D., Wurst, W., ... Westmeyer, G. G. (2018). Zebrafish and medaka offer insights into the neurobehavioral correlates of vertebrate magnetoreception. *Nature Communications*, 9(1), 802.
<https://doi.org/10.1038/s41467-018-03090-6>
- Olton, D. S. (1979). Mazes, Maps, and Memory. *American Psychologist*, 34(7), 583–596.
Retrieved from <http://psycnet.apa.org/fulltext/1979-30319-001.pdf>
- Orger, M. B., Smear, M. C., Anstis, S. M., & Baier, H. (2000). Perception of Fourier and non-Fourier motion by larval zebrafish. *Nature Neuroscience*, 3(11), 1128–1133.
<https://doi.org/10.1038/80649>
- Parichy, D. M., Elizondo, M. R., Mills, M. G., Gordon, T. N., & Engeszer, R. E. (2009). Normal table of postembryonic zebrafish development: Staging by externally visible anatomy of the living fish. *Developmental Dynamics*, 238(12), 2975–3015.
<https://doi.org/10.1002/dvdy.22113>

- Patterson, B. W., Abraham, A. O., MacIver, M. A., & McLean, D. L. (2013). Visually guided gradation of prey capture movements in larval zebrafish. *The Journal of Experimental Biology*, 216(Pt 16), 3071–3083. <https://doi.org/10.1242/jeb.087742>
- Pavlov, I. P., Gantt, W. H., Volborth, G., & Cannon, W. B. (1928). *Lectures on Conditioned Reflexes Twenty-five Years of Objective Study of the Higher Nervous Activity (Behaviour) of Animals*. Retrieved from <http://digitalcommons.hsc.unt.edu/hmedbks/35>
- Poulos, A. M., Li, V., Sterlace, S. S., Tokushige, F., Ponnusamy, R., Fanselow, M. S., & Thompson, R. F. (2009). Persistence of fear memory across time requires the basolateral amygdala complex. *Proceedings of the National Academy of Sciences of the United States of America*, 106(28), 11737–11741. Retrieved from <http://www.pnas.org/content/pnas/106/28/11737.full.pdf>
- Randlett, O., Wee, C. L., Naumann, E. A., Nnaemeka, O., Schoppik, D., Fitzgerald, J. E., ... Schier, A. F. (2015). Whole-brain activity mapping onto a zebrafish brain atlas. *Nature Methods*, 12(11), 1039–1046. <https://doi.org/10.1038/nmeth.3581>
- Roberts, A. C., Bill, B. R., & Glanzman, D. L. (2013). Learning and memory in zebrafish larvae. *Frontiers in Neural Circuits*, 7, 126. <https://doi.org/10.3389/fncir.2013.00126>
- Roberts, A. C., Reichl, J., Song, M. Y., Dearing, A. D., Moridzadeh, N., Lu, E. D., ... Glanzman, D. L. (2011). Habituation of the C-Start Response in Larval Zebrafish Exhibits Several Distinct Phases and Sensitivity to NMDA Receptor Blockade. *PLoS ONE*, 6(12), e29132. <https://doi.org/10.1371/journal.pone.0029132>
- Rombough, P. (2002). Gills are needed for ionoregulation before they are needed for O₂ uptake in developing zebrafish, *Danio rerio*. *The Journal of Experimental Biology*. Retrieved from <http://jeb.biologists.org/content/jexbio/205/12/1787.full.pdf>
- Schultz, W., Dayan, P., & Montague, P. R. (1997). A neural substrate of prediction and reward. *Science (New York, N.Y.)*, 275(5306), 1593–1599. <https://doi.org/10.1126/SCIENCE.275.5306.1593>
- Semmelhack, J. L., Donovan, J. C., Thiele, T. R., Kuehn, E., Laurell, E., & Baier, H. (2014). A dedicated visual pathway for prey detection in larval zebrafish. *ELife*, 3, e04878.

<https://doi.org/10.7554/eLife.04878>

- Skinner, B. F. (1938). *The behavior of organisms*. Retrieved from [http://s-f-walker.org.uk/pubsebooks/pdfs/The Behavior of Organisms - BF Skinner.pdf](http://s-f-walker.org.uk/pubsebooks/pdfs/The%20Behavior%20of%20Organisms%20-%20BF%20Skinner.pdf)
- Skinner, B. F. (1948). "Superstition" in the pigeon. *Journal of Experimental Psychology*, 38(2), 168–172. Retrieved from <http://psycnet.apa.org/fulltext/1948-04299-001.pdf>
- Stowers, J. R., Hofbauer, M., Bastien, R., Griessner, J., Higgins, P., Farooqui, S., ... Straw, A. D. (2017). Virtual reality for freely moving animals. *Nature Methods*, 14(10), 995–1002. <https://doi.org/10.1038/nmeth.4399>
- Tabor, K. M., Bergeron, S. A., Horstick, E. J., Jordan, D. C., Aho, V., Porkka-Heiskanen, T., ... Burgess, H. A. (2014). Direct activation of the Mauthner cell by electric field pulses drives ultrarapid escape responses. *Journal of Neurophysiology*, 112(4), 834–844. <https://doi.org/10.1152/jn.00228.2014>
- Temizer, I., Donovan, J. C., Baier, H., & Semmelhack, J. L. (2015). A Visual Pathway for Looming-Evoked Escape in Larval Zebrafish. *Current Biology*, 25(14), 1823–1834. <https://doi.org/10.1016/J.CUB.2015.06.002>
- Todd, T. P., Vurbic, D., & Bouton, M. E. (2014). Behavioral and neurobiological mechanisms of extinction in Pavlovian and instrumental learning. *Neurobiology of Learning and Memory*, 108, 52–64. <https://doi.org/10.1016/j.nlm.2013.08.012>
- Trivedi, C. A., & Bollmann, J. H. (2013). Visually driven chaining of elementary swim patterns into a goal-directed motor sequence: a virtual reality study of zebrafish prey capture. *Frontiers in Neural Circuits*, 7, 86. <https://doi.org/10.3389/fncir.2013.00086>
- Tully, T., & Quinn, W. G. (1985). Classical conditioning and retention in normal and mutant *Drosophila melanogaster*. *Journal of Comparative Physiology*, 157, 263–277. Retrieved from <https://link.springer.com/content/pdf/10.1007/BF01350033.pdf>
- Vale, R., Evans, D. A., & Branco, T. (2017). Rapid Spatial Learning Controls Instinctive Defensive Behavior in Mice. *Current Biology: CB*, 27(9), 1342–1349. <https://doi.org/10.1016/j.cub.2017.03.031>

-
- Valente, A., Huang, K.-H., Portugues, R., & Engert, F. (2012). Ontogeny of classical and operant learning behaviors in zebrafish. *Learning & Memory (Cold Spring Harbor, N.Y.)*, *19*(4), 170–177. <https://doi.org/10.1101/lm.025668.112>
- Vendrell-Llopis, N., & Yaksi, E. (2016). Evolutionary conserved brainstem circuits encode category, concentration and mixtures of taste. *Scientific Reports*, *5*(1), 17825. <https://doi.org/10.1038/srep17825>
- Vladimirov, N., Mu, Y., Kawashima, T., Bennett, D. V., Yang, C.-T., Looger, L. L., ... Ahrens, M. B. (2014). Light-sheet functional imaging in fictively behaving zebrafish. *Nature Methods*, *11*(9), 883–884. <https://doi.org/10.1038/nmeth.3040>
- Wolman, M. A., Jain, R. A., Liss, L., & Granato, M. (2011). Chemical modulation of memory formation in larval zebrafish. *Proceedings of the National Academy of Sciences of the United States of America*, *108*(37). <https://doi.org/10.1073/pnas.1107156108>
- Wullimann, M. F., & Mueller, T. (2004). Teleostean and mammalian forebrains contrasted: Evidence from genes to behavior. *The Journal of Comparative Neurology*, *475*(2), 143–162. <https://doi.org/10.1002/cne.20183>



Acknowledgements

When I was applying for a PhD position, I was guided by a wish to have a challenge. The time of my PhD indeed turned out to be one. There were moments of doubt, dead ends and exhaustion. Pushing through those moments would not be possible without many people, and I owe deep gratitude to them.

First of all, I would like to thank my supervisors Herwig Baier and Andreas Herz. Herwig taught me to be an independent researcher and offered me freedom and time to explore my ideas. I thank him for his always fair judgement and excellent scientific advice; I should have listened to it more often than I did. Andreas was always supportive during hard times, and helpful with new analysis and modeling ideas for my experimental results. I also thank him for the support of my participation in the ACCN, it was one of the highlights of my PhD time, where I met wonderful people and learned so much. I also thank Andreas and Alex Loebel for introducing me to the neuroscience community of Munich in the distant 2012 during my times as an Amgen scholar. I also thank Ruben Portugues, for his support at TAC meetings and for his sharp and mindful questions.

I want to say a big thank you to Álvaro Tejero-Cantero, who taught me how to organize my data and structure my thoughts. His rejection of superficial approaches and passion for finding the answers to the core of a problem many times inspired me and hopefully made me a better researcher.

My gratitude goes to Joe Donovan, an excellent office mate and a fellow Python enthusiast. I could always count on his positive attitude, creative insights and helpful ideas, especially at the low points. I thank Duncan Mearns, Alison Barker, and Thomas Helmbrecht for discussions during day hours and late nights in the lab about science and what it takes to be a scientist. I thank Karin Finger-Baier for her indispensable help and time during the application for the animal license. Thank you to all members of Baier lab, for exciting scientific atmosphere, readiness to help and fun trips to Oktoberfest and Ringberg.

Drago, Alison, Alex, Joe and Veronika provided excellent (and quick) comments for this monograph, thank you!

I thank the GSN team, which supports the students scientifically and organizes wonderful retreats and events where I could share my research findings, learn and have fun at the same time.

Dear Fluffable (who said that?!): thank you for fantastic jams, gigs, laughs and chilling, Joe, Dominique, Joel, Michi D, Drago.

Tough moments were sweetened and happy moments were made unforgettable by the Partnachplatz gang, old and new. Thank you Judi, Veronika, Anna, Sara, Martin, Drago, Alex. Vilim and Elena, thank you for classical music experiences and critical discussions on politics, art, life, universe and everything.

Anna, thank you for dancing enthusiasm and wonderful company. Obrigada pela Liliana, minha amiga maravilhosa, com quem pude compartilhar o meu amor por Portugal. Martin, Jaimito and Uri, man's not hot!

Drago, thank you for your kindness, advice scientific and not, and for always being there. You joined in late, but caught up quickly.

Veronika and Judi, already mentioned earlier, have to appear again, as I cannot imagine my Munich experience without you. Thank you for fantastic trips, legendary nights, spontaneous and planned adventures, generosity and patience. You made Munich a second home for me.

Finally, I want to say thank you to my parents and sister, for their support and infinite trust in me.

Curriculum Vitae

Ksenia Yashina

yashina@neuro.mpg.de

Am Klopferspitz 18,

82152 Martinsried

Education:

2013 – now

PhD

Graduate School of Systemic Neurosciences at Ludwig-Maximilians
Universität München.

2008 – 2013

Diploma with Honors, major in Bioinformatics, Lomonosov Moscow State
University, Russia

“Development of novel inhibitors of human poly(ADP-ribose)polymerase
with the use of virtual screening”

Supervisors Prof. Dr. Vitas Švedas and Dr. Dmitry Nilov

Fellowships, courses and research experience:

2015

Advanced Scientific Programming in Python, Munich

2015

Advanced Course in Computational Neuroscience, Champalimaud Centre
for the Unknown, Portugal

2012

Amgen Scholars Program Scholarship and Summer Internship, LMU,
Germany

Project “Enhancement of vesicle release but not vesicle recovery explains non-monotonic short-term dynamics of synaptic transmission”, supervisors Dr. Alex Loebel and Prof. Dr. Andreas Herz

2011 Bioinformatics summer internship, Leids Universitair Medisch Centrum, the Netherlands

Project “Integration of MS-GFDB in peptide/protein identification workflows”, supervisor Dr. Magnus Palmblad

Conferences and publications:

In preparation Ksenia Yashina, Álvaro Tejero-Cantero, Andreas Herz and Herwig Baier. “A novel conditioned place avoidance paradigm reveals a repertoire of learning strategies in a juvenile zebrafish”, in preparation for submission to eLife

2015 Poster “Exploring navigational abilities of zebrafish larvae in real and virtual mazes” in proceedings of <interact> Life Science Symposium for Young Scientists, Munich, Germany

2013 Poster “Enhancement of vesicle release but not recovery explains non-monotonic short-term dynamics of synaptic transmission” in proceedings of British Conference of Undergraduate Research, Plymouth, UK

2012 Poster “De novo repeat identification in genomes based on occurrences of pairs of short words at different distances” in proceedings of XVIII International Student, postgraduate and young scientist conference “Lomonosov”, Moscow, Russia

Author contributions

The study was designed by Ksenia Yashina, Andreas Herz and Herwig Baier.

Setup was designed and built by Ksenia Yashina.

All experiments were performed by Ksenia Yashina.

Analysis was performed by Ksenia Yashina and Álvaro Tejero-Cantero.

First Author: Ksenia Yashina _____

First Supervisor: Herwig Baier _____

Eidesstattliche Versicherung / Affidavit

Hiermit versichere ich an Eides statt, dass ich die vorliegende Dissertation “**Learning In A Small Vertebrate: A Novel Paradigm For Juvenile Zebrafish To Study Conditioned Place Avoidance**” selbstständig angefertigt habe, mich außer der angegebenen keiner weiteren Hilfsmittel bedient und alle Erkenntnisse, die aus dem Schrifttum ganz oder annähernd übernommen sind, als solche kenntlich gemacht und nach ihrer Herkunft unter Bezeichnung der Fundstelle einzeln nachgewiesen habe.

I hereby confirm that the dissertation “**Learning In A Small Vertebrate: A Novel Paradigm For Juvenile Zebrafish To Study Conditioned Place Avoidance**” is the result of my own work and that I have only used sources or materials listed and specified in the dissertation.

München, den

Ksenia Yashina, August 1st, 2018

Munich, date

Unterschrift signature